Agreement Q2396019

Reconnecting Winter Run to Their Ancestral Waters: Monitoring Reintroduction Success on the McCloud

Final Data Collection Report prepared for the California Department of Fish and Wildlife

March 2026

UC Santa Cruz Co-PIs: Cyril Michel, Miles Daniels, Jeremy Notch, Ann-Marie Osterback

UC Davis Co-PIs: Carson Jeffres, Amelie Segarra

NOAA Co-PIs: Diana Baetscher, Rachel Johnson

MBARI Co-PI: James Birch

Executive Summary

Over the past three years, this project has generated substantial learning across three interconnected domains: (1) aligning scientific priorities with the Winnemem Wintu Tribe in ways that uphold and center Tribal values and Traditional Ecological Knowledge; (2) innovating or adapting monitoring methods to ensure cultural appropriateness while maintaining scientific rigor; and (3) deepening our understanding of salmon life history, behavior, and survival upon their return to ancestral waters. Taken together, this project has demonstrated what is possible when Tribal sovereignty, culturally grounded methods, and adaptive scientific inquiry are brought into intentional partnership.

Working collaboratively with the Winnemem Wintu Tribe required continual adaptation of our scientific priorities to better reflect Tribal concerns and ecological knowledge. Early in the project, we learned that many of the questions we initially posed were ones for which the Tribe already held deep generational knowledge. Guided by Chief Caleen Sisk, we shifted our approach to presenting scientific options, listening to Tribal leaders' priorities, and co-developing monitoring strategies and scientific questions. This iterative process led to new lines of inquiry each year. For example, we expanded from initial observations of upstream fish presence to asking how far upstream juveniles dispersed, which tributaries they entered, and what habitats they used throughout the year. The Tribe also encouraged an expanded pathogen assessment above the reservoir and pushed us to further investigate predation on Nur around the in-river traps.

These adaptations came with important learning curves in how to respectfully integrate Indigenous knowledge alongside Western scientific frameworks, but doing so strengthened the scientific process and deepened shared understanding. We found particular value in meeting in place on the river, where decision-making was grounded in context. To support real-time coordination across the Tribe, agencies, and scientists, we relied on multiple communication pathways, including monthly monitoring meetings, a special session at the Bay-Delta Science Conference, and ultimately an in-season data dashboard that delivered rapid summaries and visualization of emerging results. These experiences underscore that diverse communication formats and shared spaces are essential for successful collaborative science.

A central component of aligning scientific practice with Tribal values was the deliberate shift toward non-invasive, culturally grounded monitoring methods. These approaches aimed to minimize stress to fish, avoid removing mucus or scales, and keep equipment out of the river wherever possible. This challenged many standard Western fisheries techniques, such as handling fish on measuring boards, and required the team to innovate alongside Tribal members or leverage existing technologies that met these

cultural criteria. Many of these approaches ultimately enhanced, rather than limited, scientific insight and opened new possibilities for fisheries monitoring.

One major outcome was the development of the fish viewer, a tool conceptualized by Chief Caleen Sisk and Marine Sisk of the Winnemem Wintu Tribe, built by the UC Davis team, then iterated upon by the Tribal field crew members. By keeping fish fully submerged and using advanced algorithms to estimate length, weight, and condition from images of the fish in the viewer, the fish viewer reduces handling time and stress, respects Tribal values, and generates richer biological data than traditional methods. It has already gained interest from monitoring agencies across the Central Valley.

Similarly, non-invasive environmental DNA (eDNA) sampling provided an effective way to understand fish distribution, habitat use, and seasonal movement in areas where trapping was not feasible. Simple water-collection methods, paired with laboratory extraction of DNA and RNA, enabled broad spatial and temporal sampling, including in remote locations. Advanced tools such as the MBARI autosamplers further increased temporal resolution while reducing the need for human presence. Although initially deployed for pathogen detection and Chinook presence, this technology can support future monitoring of fish communities, including predator movements, and invasive species.

Parentage-based tagging (PBT) likewise proved to be a powerful genetic tool for linking individual fish to their parents and tracking reintroduced McCloud fish across their life cycle. While full PBT results remain pending, the method already identified two returning adults in 2025 and inspired a Master's research project from a Tribal member exploring whether fish genotype can be detected directly from water surrounding fish, such as in the fish viewer or a bucket, potentially eliminating the need for only using mortalities. These examples illustrate how Tribal-led values catalyzed scientific innovation throughout the project.

With shared scientific priorities and culturally attuned methods in place, the project yielded key insights into the life history of reintroduced winter-run Chinook Salmon. Across multiple field seasons, we collectively observed that salmon use the river in diverse ways across the annual cycle. Notably, some individuals exhibited extended in-river rearing - a "yearling" strategy - likely rearing through the winter and outmigrating in spring. Fish accessed a variety of habitats, including upstream of their incubation site, with the extent of the upstream rearing still to be determined. We also documented increasing variation in size and timing of outmigration across the field seasons, reflecting a flexible life-history portfolio and emphasizing the ecological importance of volitional passage in the Tribal-led Nur Nature Base design. Meanwhile,

macroinvertebrate sampling showed that the benthic food community is dynamic across years yet appears to support salmon feeding during critical growth windows.

The knowledge gained over four years of reintroduction efforts and three years of coordinated science and monitoring provides a strong foundation for the future of McCloud River salmon restoration. These findings offer baseline data to evaluate success, demonstrate that reintroduced fish can survive and thrive in their ancestral watershed, and point to numerous opportunities for continued research. Equally important, the project has generated a suite of culturally aligned, non-invasive monitoring tools and collaborative practices that can be applied not only in the McCloud River but across watersheds throughout California. Together, these advancements strengthen the scientific, cultural, and practical pathways needed to support long-term recovery of winter-run Chinook Salmon.

Task 2: Reintroduction Quality

To assess the quality of the McCloud River reintroduction, we eventually want to look at a few interrelated dimensions: fish passage estimates, egg-to-juvenile survival, fish released below Shasta dam and their return rate, and then compare these metrics to conditions below Shasta Dam, particularly during drought years. A central requirement of this framework is estimating how many fish pass through the river and are captured at in-river traps, which we focused on for this project. Since 2022, we have conducted trap efficiency trials for the CDFW and PSMFC-operated traps using simple mark–recapture designs. In these trials, winter-run Chinook from Livingston Stone National Fish Hatchery (LSNFH) of similar developmental stages to McCloud-reared juveniles were marked using caudal fin clips, Bismarck Brown dye, and, in one case, VIE tags. Known numbers of marked fish were released two habitat units upstream of the traps, and subsequent recaptures were enumerated to estimate trap efficiency. Over four field seasons, we conducted 18 efficiency trials, yielding in-season feedback that informed trap modifications and location adjustments to improve catch performance, while also providing the basis for expanding raw catches into passage estimates, which are still to be calculated. In this report and the associated data files, we include trapping data for all traps (including the DWR-operated JSCS) and efficiency trial results for all trials conducted at all traps.

Trap catch and efficiency

In 2022, efficiency trials were conducted for each trap configuration, but multiple traps operating concurrently complicated interpretation. We applied a simple efficiency expansion to daily catches to generate preliminary estimates of total fish passage during the trapping season; however, there were significant caveats. In particular, simple expansions cannot separate trap efficiency from survival to the trap, and spatial variation in fish movement across the channel may mean that not all traps had equal opportunity to intercept fish. These uncertainties likely skew trap-specific efficiency estimates and propagate into passage calculations, thus we did not include them in the final data.

In 2023, with the implementation of the JSCS, we were able to expand this framework by conducting “paired-release” trials in addition to standard single-release efficiency trials. In these paired releases, fish with one type of mark were released above the upstream trap of interest (IPT or RST), while fish with a different mark were released downstream, such that all fish could be captured at the JSCS but only the upstream release group could be captured at the first trap. This design allows separate estimation of survival to the first trap and trap efficiency by fitting a Cormack–Jolly–Seber–type model. We collaborated with Russ Perry (USGS) to analyze these data within a

Bayesian framework, producing a more robust passage estimate and uncertainty bounds for 2023 than could be obtained from simple efficiency expansions alone (Table 2.1; Figure 2.1).

Table 2.1. Posterior summary of total abundance of winter-run Chinook salmon during the 2023 trapping period.

Mean	Standard Deviation	Median	2.5th - 97.5th percentile
16141	2149	15878	12726-21278

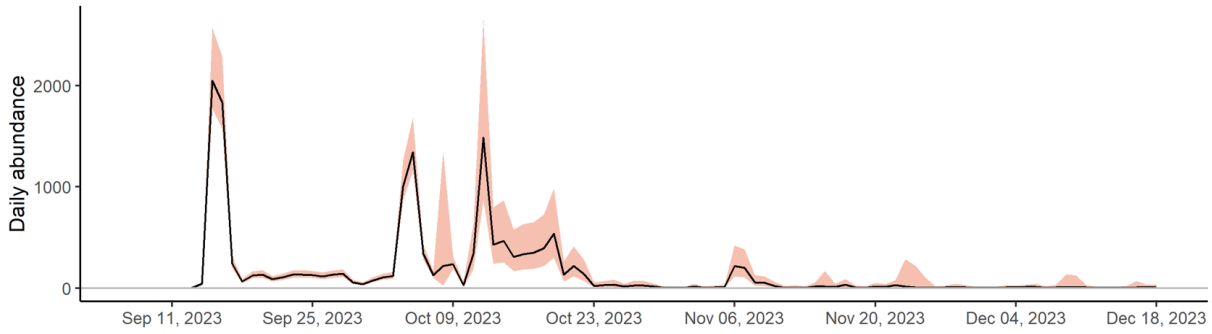

Figure 2.1. Daily abundance estimate with 95% credible interval for juvenile winter run Chinook salmon passing McCloud River incline plane and rotary screw traps in 2023.

In 2024, we aimed to build on the 2023 paired-release design to further refine estimates of true trap efficiency. However, poor performance of the JSCS head-of-reservoir trap limited our ability to execute the full paired-release program. Instead, we conducted single-release trials that informed trap configurations and locations and allowed for crude efficiency-based catch expansions. In 2025, we again planned paired-release trials and successfully implemented three such trials before weather interruptions. We also conducted two early-season single-release trials for the IPT. Passage estimates for 2024 and 2025 have not yet been compiled but will be analyzed in future work.

Given the limitations of simple efficiency expansions and the complexities of fish movement in this system, we have planned a more extensive modeling effort, funded by NOAA and led by Cyril Michel. This analysis will incorporate uncertainty and survival estimates into a unified framework to produce more robust passage estimates and lower-bound egg-to-juvenile survival rates. Importantly, both eDNA and angler catch observations indicate extended in-river residence of salmon in the McCloud River, meaning that fish outmigrating during non-trapping periods remain unaccounted for in passage estimates. As a result, any survival estimates are likely conservative (underestimates) and biased toward fish that outmigrate during trap operation windows.

Variation in outmigration timing from trap data

Despite these limitations, trapping data from 2022–2025 allow us to begin examining patterns in outmigration timing (Figure 2.2). While differences in trap operation periods and configurations across years constrain direct comparisons, we observe more evenly distributed outmigration timing in 2024 and 2025, coinciding with increased egg inputs to the Nur Nature Base and the availability of volitional passage. This contrasts with sharper spikes in 2022 and 2023, when fish from the RSI were released en masse. The increasingly diversified outmigration timing suggests that fish are making decisions about when to leave, potentially holding territories in the river and delaying emigration until fall, and that this diversification may help “spread risk” across time. Fish that migrate at different times encounter different environmental conditions and predator communities in the McCloud and, subsequently, in the Sacramento River and Delta. These patterns indicate that reintroduced winter-run Chinook in the McCloud are expressing more naturalistic, variable outmigration behaviors over time, a key indicator of improving reintroduction quality.

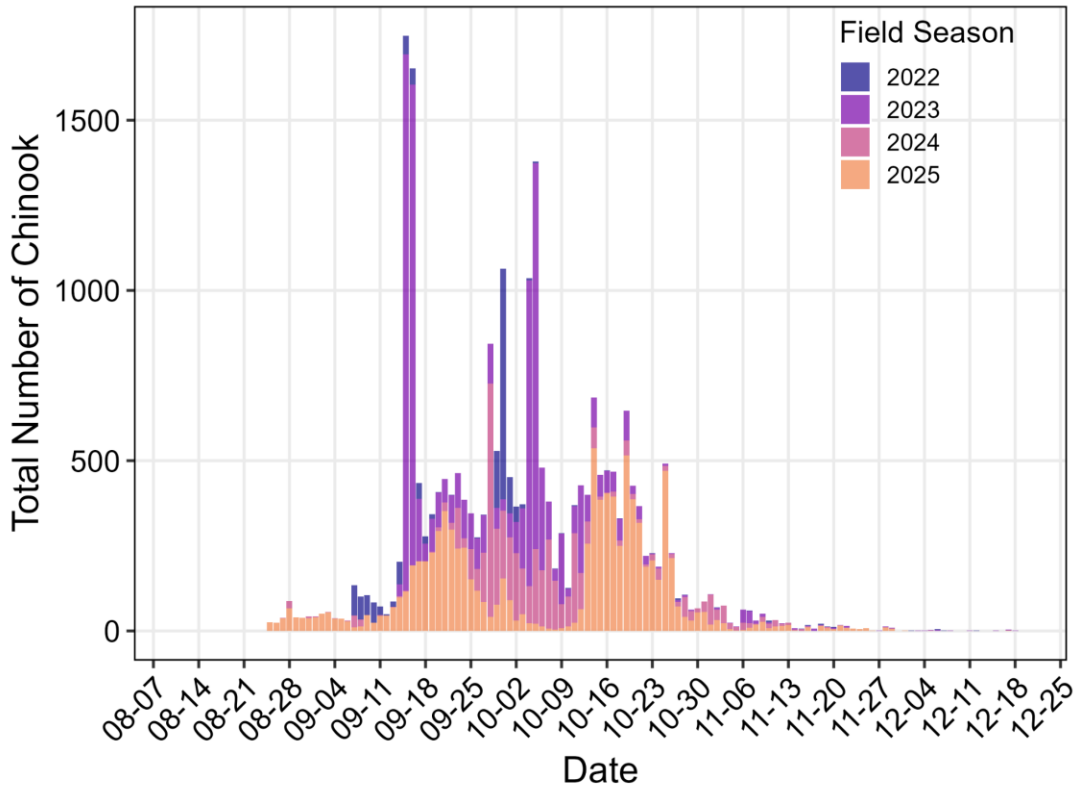

Figure 2.2. Trap catch of winter-run Chinook salmon across four field seasons, encompassing all in-river and head-of-reservoir traps.

Task 3: Growth and Foodscape

For salmon reintroduced into the McCloud River to be successful, the river's food web must provide sufficient foraging opportunities to support growth and survival. To evaluate this "foodscape," we paired macroinvertebrate sampling in the benthos and drift with monitoring of juvenile size at in-river traps. For 2024 and 2025, length and weight data used in these analyses come primarily from the fish viewer, representing a major innovation and collaboration between the Winnemem Wintu Tribe and UC Davis. Measuring fish length with standard Western methods - such as placing fish on a measuring board - as done in 2022 and 2023 were inconsistent with Tribal values of keeping fish submerged and preserving their protective mucus. Through multiple iterations in the 2024 field season, we developed and implemented a "fish viewer," in which live fish remain in water while being photographed. UC Davis mathematics PhD Brian Knight developed an algorithm to estimate length and weight from these images, building on previous work from Eric Holmes and Carson Jeffres, and the approach was piloted and refined in 2024. The system was further validated with fall-run Chinook reared at UC Davis, and by fall 2025 both the fish viewer hardware and the automated length–weight extraction software were fully operational, with only minor in-season adjustments.

Macroinvertebrate community

To characterize invertebrate prey availability, we collected kick-net samples at a fixed location near The Nature Conservancy Kerry-Landreth Preserve, downstream of the incubation site at AhDiNa Campground, from 2022–2025. Sampling occurred monthly, with the window of sampling shifting each year as we adapted to weather conditions and sought to incorporate more seasonality. This sampling provided a multi-year, seasonal record of benthic invertebrate abundance and composition. For kick net sampling, we randomly selected three locations along the river at our sample site for three transects. For each transect, the kick net (area = 0.279 m^2) was placed on river right, river left, and in the center of the river, where depth and substrate were appropriate, on the river bottom and held while one crew member scrubbed the rocks within the area for 45 seconds, before kicking the substrate for another 15 seconds. In 2022 and again in September and October 2025, each transect was collected, stored, and sorted separately; thus, for these sample dates we use the averages across transects in the figures discussed below, and show the standard deviation of the samples. In 2023, 2024, and early 2025, all three transects were combined into a single composite sample per sample date.

In 2024–2025, we supplemented these benthic samples with drift-net collections at AhDiNa, near the incubation site, to better characterize the prey field encountered by

actively foraging juvenile salmon, whose primary feeding mode is in the drift. Kick net sampling focuses on stirring up the benthos, collecting some invertebrates in the drift but giving a more holistic picture of the river invertebrate community; in contrast, drift sampling is a passive method of sampling where a drift net is installed in the current to collect any invertebrates moving downstream in the water column.

In general, across the four years of kicknet sampling, invertebrate density increased in the fall months of September and October (Figure 3.1). Seasonal shifts in taxonomic composition (Figure 3.2) and functional feeding groups (Figure 3.3) are evident from spring through fall, though not obviously consistent between years. Density in 2025 was highest compared to other sample years, due to in part a large increase in oligochaetes found in the samples; when removing oligochaetes from the data, benthic density in 2024 and 2025 are similar, peaking in September at just over 1500 individuals per square meter. Notably, the density of Ephemeroptera, Plecoptera, and Trichoptera ("EPT") organisms tended to peak and stay high between August to November, with peaks in the percent abundance of EPT taxa tending to occur in October (Figure 3.4). The exception is 2023, which showed the inverse relationship where the percent EPT was lowest during this period. These three Orders that make up the EPT group are notable as they are highly sensitive to water quality and require clean, well-oxygenated waters that salmon also thrive in. Additionally, they provide a high quality food source for salmonids.

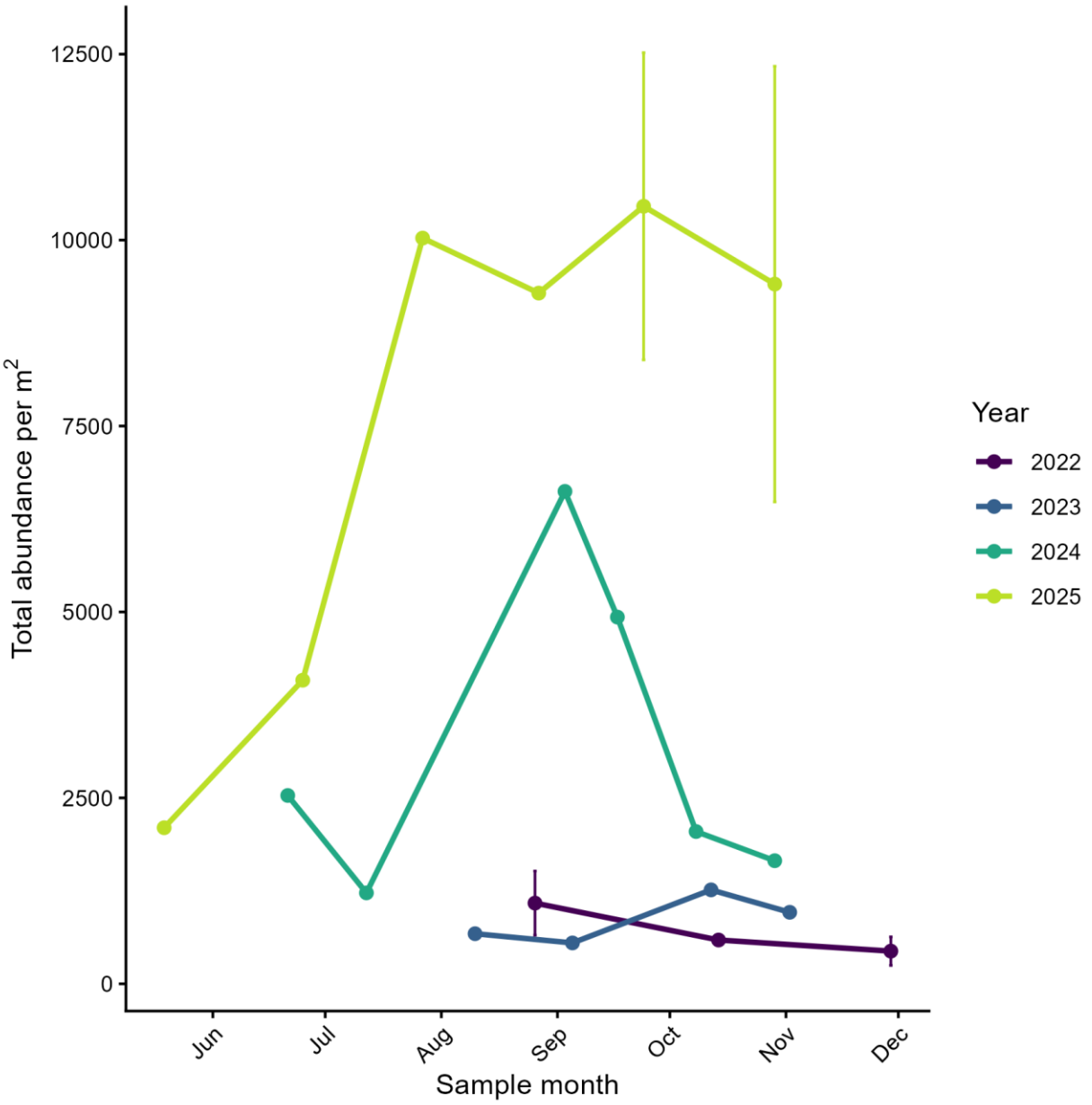

Figure 3.1. Density of benthic macroinvertebrates across the spring to fall seasons for each sampling year (2022-2025) on the McCloud River at The Nature Conservancy Kerry-Landreth Preserve. Macroinvertebrates were collected using a kicknet method along a river transect. For dates where three separate transects were collected, we averaged the density across all three samples (e.g., 2022 samples, September and October 2025 samples) and error bars show ± standard deviation.

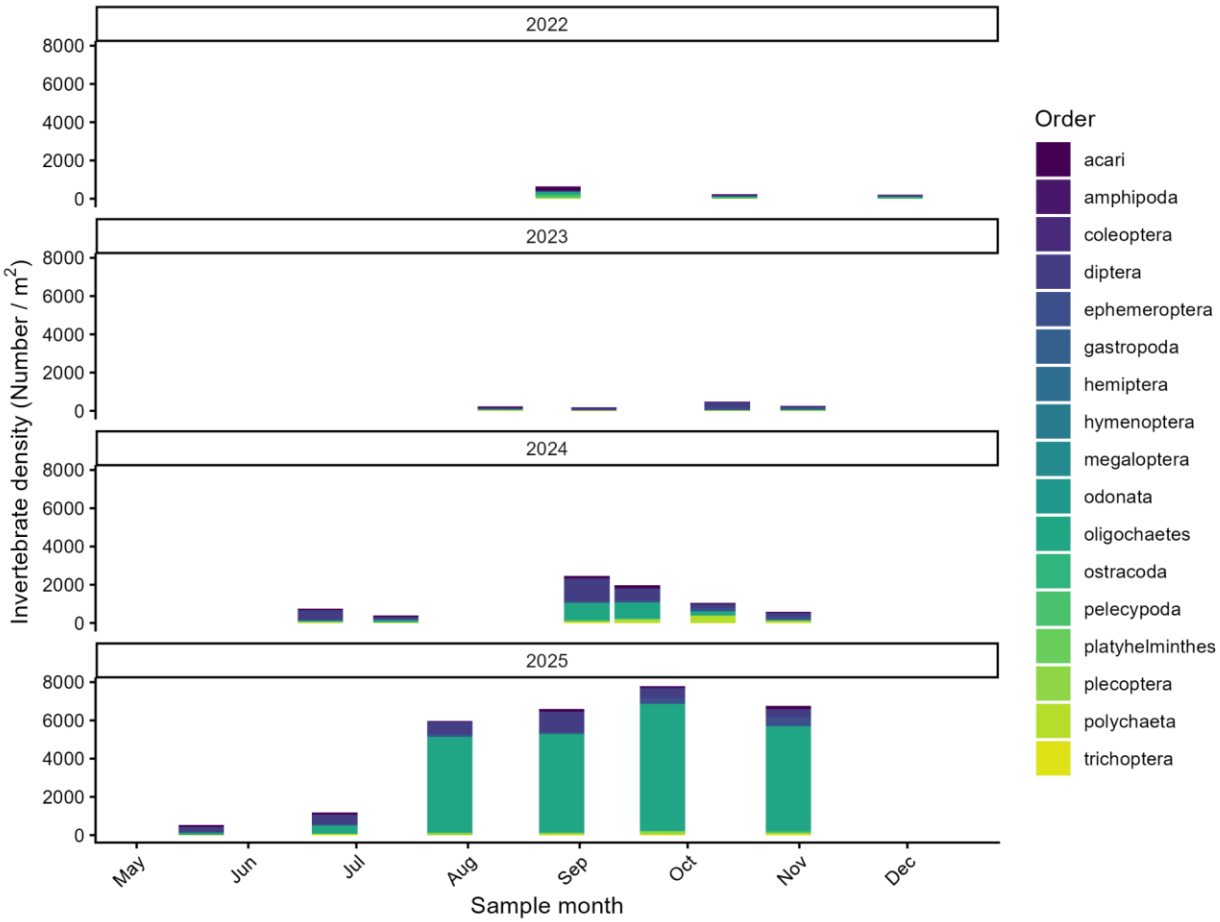

Figure 3.2. Density of benthic macroinvertebrates across the spring to fall seasons for each sampling year (2022-2025) on the McCloud River at The Nature Conservancy Kerry-Landreth Preserve, according to Order. For invertebrates not classified at the Order level (e.g., acari, oligochaetes, ostracoda, polychaeta, platyhelminthes, gastropoda, pelecypoda), the Phylum, Class, or Subclass was used in place of Order. Macroinvertebrates were collected using a kicknet method along a river transect. For dates where three separate transects were collected, we averaged the density of each Order across all three samples (e.g., 2022 samples, September and October 2025 samples).

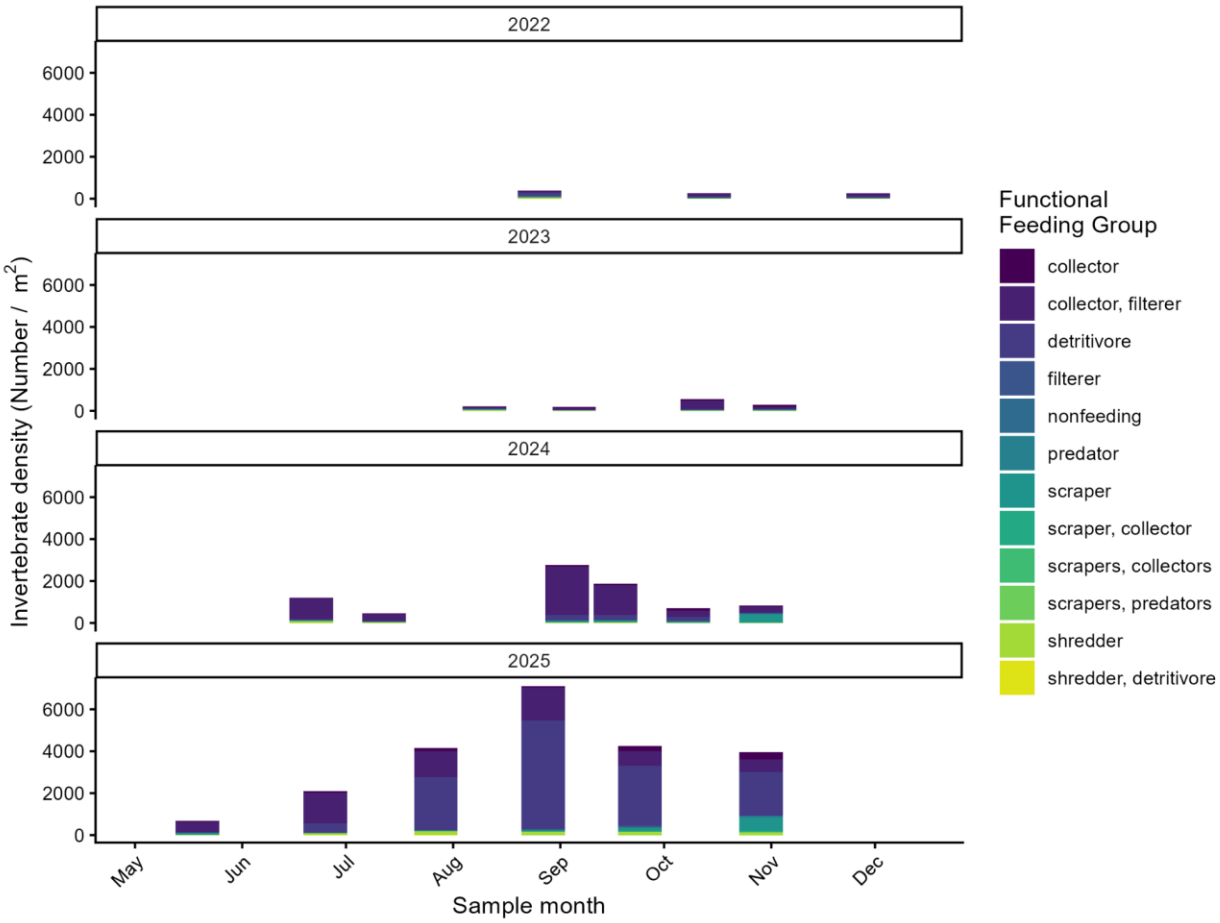

Figure 3.3. Density of benthic macroinvertebrates across the spring to fall seasons for each sampling year (2022-2025) on the McCloud River at The Nature Conservancy Kerry-Landreth Preserve, according to their functional feeding group. Macroinvertebrates were collected using a kicknet method along a river transect. For dates where three separate transects were collected, we averaged the density of each functional feeding group across all three samples (e.g., 2022 samples, September and October 2025 samples).

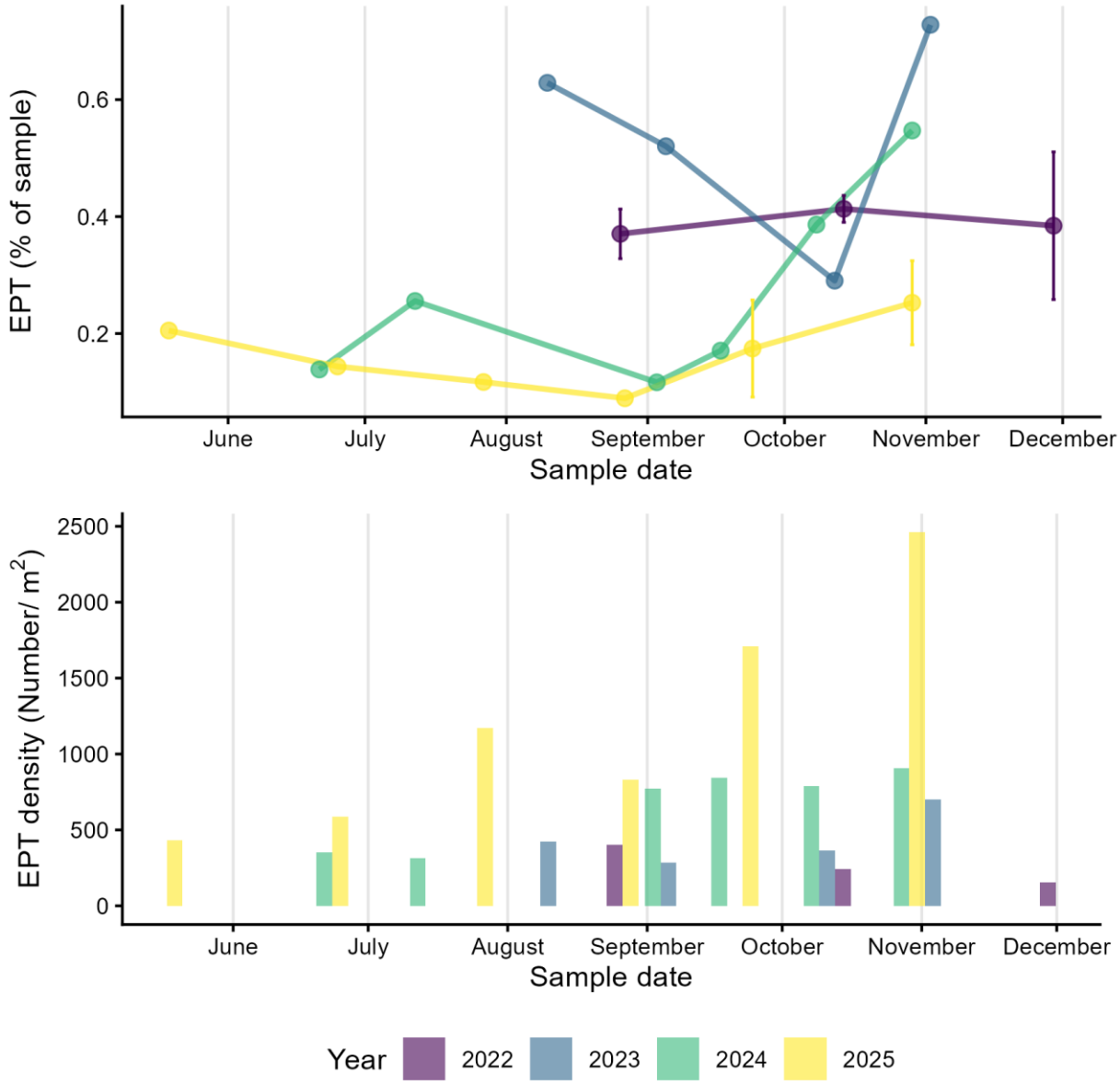

Figure 3.4. Benthic macroinvertebrates of the Orders Ephemeroptera, Plecoptera, Trichoptera ("EPT") collected across the spring to fall seasons for each sampling year (2022-2025) on the McCloud River at The Nature Conservancy Kerry-Landreth Preserve. (Top) Percent of total sample that were EPT taxa, by abundance. For dates that consisted of three separate transects, we show the mean percent EPT across the three samples and ± standard deviation. (Bottom) Density in number per meter squared of EPT in samples. Macroinvertebrates were collected using a kicknet method along a river transect. For dates with three transect collections, we show the mean of the three samples.

The pattern of increase in overall invertebrate density in the fall months is also found in the drift during 2024 and 2025 sampling (Figure 3.5, Figure 3.6). We found the number

of invertebrates per cubic meter of river was highest in September and October, as well as the rate at which invertebrates were delivered; this would mean that drift foraging salmon would have the highest density of food around them, delivered at the fastest rate, in the fall. While EPT density was highest in September and October, the percent of the total drift sample showed no clear pattern of increase, but did drop in late October to early November in both years, when individuals from the Order Diptera and oligochaetes experienced a large increase in density. Diptera, especially the Family Chironomidae, dominated drift samples in general and are another common food source for salmon. Similar to kick net samples, densities in 2025 were modestly higher, likely pointing to some favorable change in environmental conditions in 2025. Overall, our macroinvertebrate sampling revealed that density of invertebrates peaks in the fall at a similar time when Nur are emerging from the gravel and starting to exogenously feed, consistent with a phenology adapted for the McCloud River.

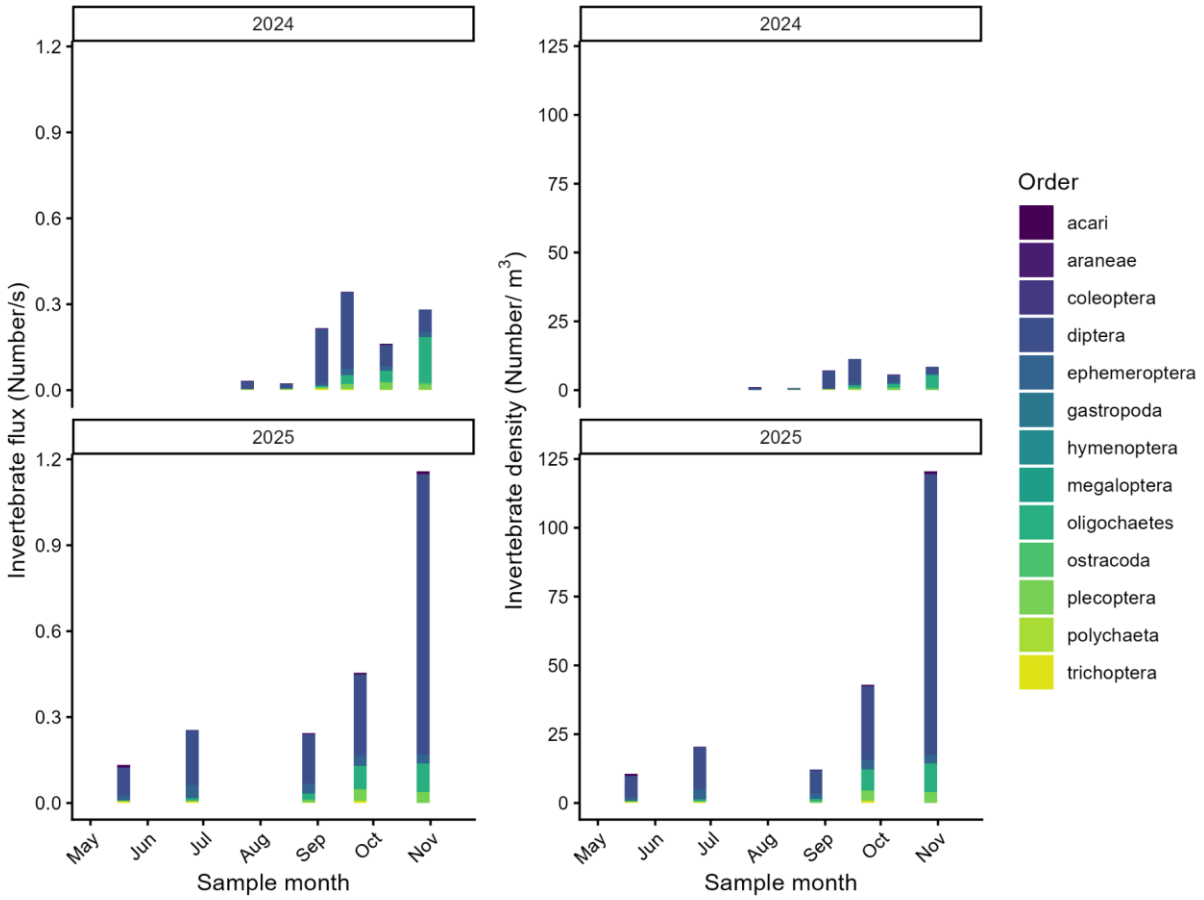

Figure 3.5. Composition of drift samples by Order for 2024 (top) and 2025 (bottom) across the spring to fall seasons on the McCloud River at AhDiNa Campground. (Left) Flux, in number per second, of macroinvertebrates. (Right) Density, in number per cubic meter, of macroinvertebrates. For invertebrates not classified at the Order level (e.g., acari, oligochaetes), the Subclass was used in place of Order. Samples were collected using a drift net set for thirty minutes before dusk.

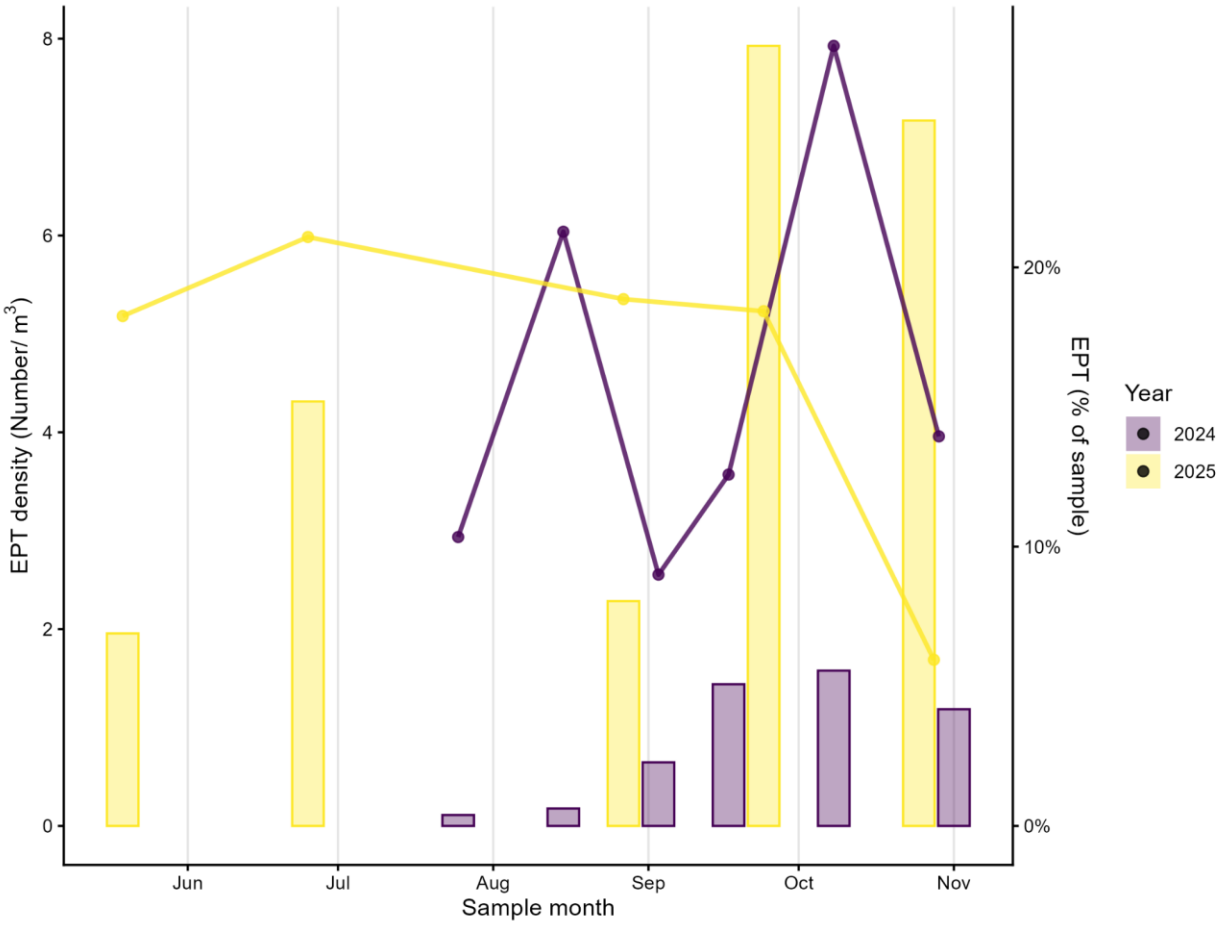

Figure 3.6. Density and percent of sample by abundance of macroinvertebrates of the Orders Ephemeroptera, Plecoptera, Trichoptera ("EPT"), captured in the drift across the spring to fall seasons in 2024 (purple) and 2025 (yellow) on the McCloud River at AhDiNa Campground. Samples were collected using a drift net set for thirty minutes before dusk.

In 2022 and 2023, we initially attempted to directly measure in-river growth by placing fish from streamside incubation tanks into cages in the McCloud River and monitoring changes in size over weekly intervals. However, these cage experiments proved logistically challenging and were ultimately not aligned with Tribal values; caged fish appeared stressed and did not grow well. As a result, the approach was discontinued

after 2023, and the project shifted toward more hands-off methods (but see data file included with report). Instead, we now focus on “apparent growth” inferred from trap data - i.e., comparing sizes of fish at the traps across seasons and years. Preliminary observations suggest that apparent growth at the traps may be increasing over field seasons, potentially reflecting higher egg inputs into the Nur Nature Base and the availability of volitional passage (e.g., 2024), which allows juveniles to leave natal structures when ready, occupy territories in the river, and grow before outmigrating (Figure 3.7). Data in 2025 showed even greater variation in fork length at capture, but apparent growth appeared slower. Unfortunately, our ability to interpret this data is limited as size data is highly dependent on when traps were fishing, leading to gaps in the record and size-selectivity of different gear. As PBT results become available, we will be able to extend these analyses from apparent growth to absolute growth by linking fish size at capture to known spawn dates and rearing histories.

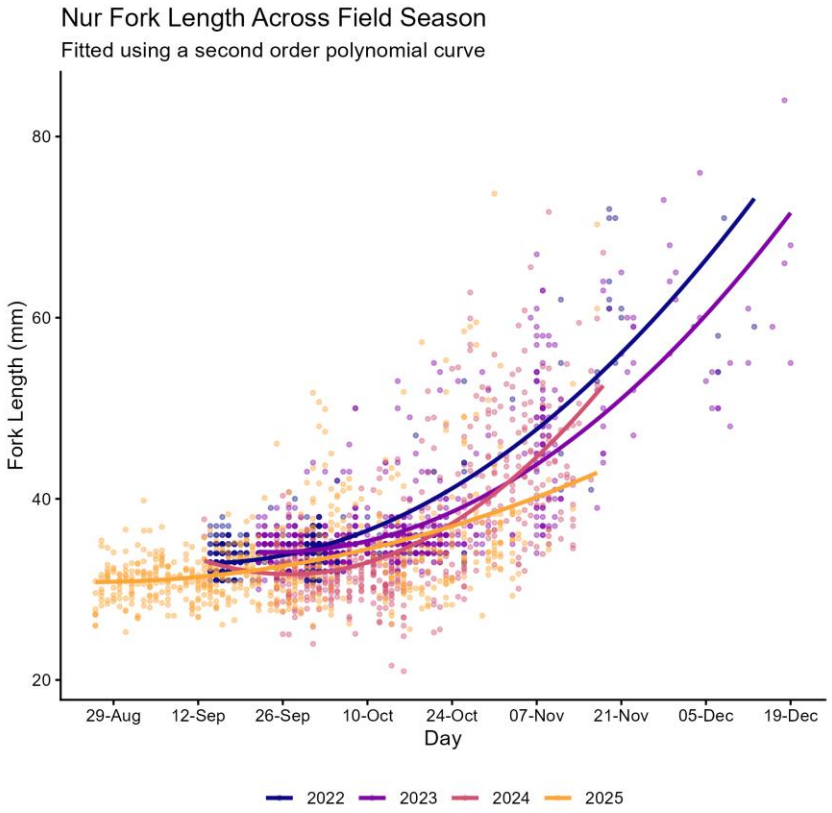

Figure 3.7. Fork length of winter-run Chinook salmon captured at in-river traps on the McCloud River by day, for four field seasons, with yearly apparent growth curve.

Task 4: Survival

Introduction

Acoustic telemetry has become a widely used tool in California's Central Valley to estimate movement and survival rates of outmigrating juvenile salmon. In the McCloud River, we applied this technology within a focused reach spanning the lower river and reservoir interface to evaluate success of trapping operations and to estimate the proportion of tagged fish that survive throughout the reach and ultimately enter Lake Shasta. The primary purpose was to help resource managers identify locations where fish may rear for extended periods, reaches with low apparent survival, and locations of potential predator hot spots. In addition, acoustically tagged salmon provided a secondary, independent, method of estimating trap efficiency of the JSCS, and monitored how tagged salmon interacted with the JSCS upon arriving at the location. Finally, acoustic telemetry provided estimates of residence time in the McCloud River prior to downstream migration towards the trap and reservoir.

Methods

Survival and movement

Acoustic telemetry studies were conducted in the fall of 2023, 2024 and 2025 by UC Santa Cruz staff. Juvenile Salmon Acoustic Telemetry System (JSATS) technology was used to tag and track late-fall Chinook salmon smolts sourced from Coleman National Fish Hatchery (CNFH). JSATS technology is ideal for estimating survival and movement rates of juvenile salmon due to the small size of the acoustic tag (0.22 grams), allowing researchers to tag fish as small as 5 grams and 80mm fork length. During the 2024 season, UC Santa Cruz collaborated with the United States Geologic Survey (USGS - Columbia River Research Laboratory, Cook, WA), who were separately funded by CDFW to also conduct a telemetry project in Shasta Reservoir. Acoustic tags, receivers, and staff resources were pooled together to ensure that releases of acoustic-tagged Chinook salmon occurred periodically throughout the outmigration season, and to increase the overall receiver network.

During each study week, approximately 100 late-fall Chinook salmon smolts were tagged at CNFH and held overnight prior to transport to the release location. Fish were transported from CNFH to the lower McCloud River in 120 quart coolers equipped with multiple aerators, for a travel time of approximately one hour. Prior to release, water temperature was measured in the cooler and in the McCloud River, with gradual water tempering occurring if the temperature difference was greater than 2°C between the two sources. In 2023 the release groups were placed in buckets, carried up the riverbank,

and placed in mesh enclosures at the release location just upstream of McCloud Bridge (and the CDFW incline plane trap) until release. In 2024 and 2025 the release site was approximately 200 meters downstream of the McCloud Bridge, three meters downstream from the CDFW incline plane trap, and ranging from 0.4 to 2.68 river kilometers upstream of the JSCS (the JSCS location changed within and among years). UCSC completed two releases of ~100 smolts on 9/27/2023 (n=102) and 10/10/2023 (n=98) in 2023, seven releases of ~100 smolts in 2024 over four weeks (table 4.1), and one release of 58 smolts on 11/20/2025 in 2025, for a total of 200 fish released in 2023, 656 fish released in 2024, and 58 fish released in 2025.

In order to track the tagged fish, Acoustic Telemetry Systems (ATS) model SR3017 and Lotek model WHS4350 acoustic receivers were deployed in multiple arrays at key locations within the study area (Fig. 4.1). In 2023 ATS hydrophones were mounted to a steel rod secured to a 45lb weight plate to ensure minimal movement underwater and improve detection efficiency. That year, the most upstream line of receivers was deployed just upstream of the JSCS, where five receivers were deployed in the shape of a large “X” with consistent spacing between them to estimate 2-dimensional movements of study fish as they approached the JSCS. Immediately downstream of the JSCS, another five receivers were deployed in a similar configuration to estimate the approximate location where fish may be escaping the JSCS trap. Further downstream in the McCloud arm of Shasta Reservoir (near the Nosoni Creek arm), a dual line of receivers was deployed to ensure that survival to the JSCS was identifiable (using a CJS mark-recapture model), and to estimate the total number of fish entering the reservoir. These receivers were moored to Vemco VR2AR acoustic release receivers as means of retrieving them in the deep channel within the reservoir.

In 2024 ATS hydrophones were again deployed in a large “X” shape for 2-dimensional fish tracking, with two receivers in each “arm” above and below the trap, and one receiver centered directly in front of the trap box of the JSCS (Fig 4.1, Fig 4.2). These were suspended in water roughly a meter from the riverbed, secured between a float and 45lb weight plate. When the JCSC was repositioned downstream, the 2-dimensional array was not re-deployed, but two ATS hydrophones were deployed off the back (downstream side) of the JSCS to detect fish moving past the trap. Two dual lines (moored to Vemco acoustic releases) were deployed downstream the McCloud River arm. USGS deployed additional receivers in Shasta Reservoir, including at Shasta Dam, to evaluate salmon passage time and success through the reservoir. We do not report on detections from these receivers, those findings will be included in USGS reports. Finally, additional receivers were deployed downstream of Shasta Reservoir in the lower Sacramento River to detect fish captured in the JSCS and transported downstream to a release location in Redding, or fish that passed through the Shasta Dam infrastructure.

In 2025 three Lotek hydrophones were deployed on the JSCS trap. Due to the redesign of the JSCS in 2025 and the shallow and noisy environment in which it was installed, the receivers had a limited range (Fig 4.1), and 2-dimensional tracking was not attempted. Two dual lines moored to Vemco acoustic releases were again deployed downstream the McCloud River arm.

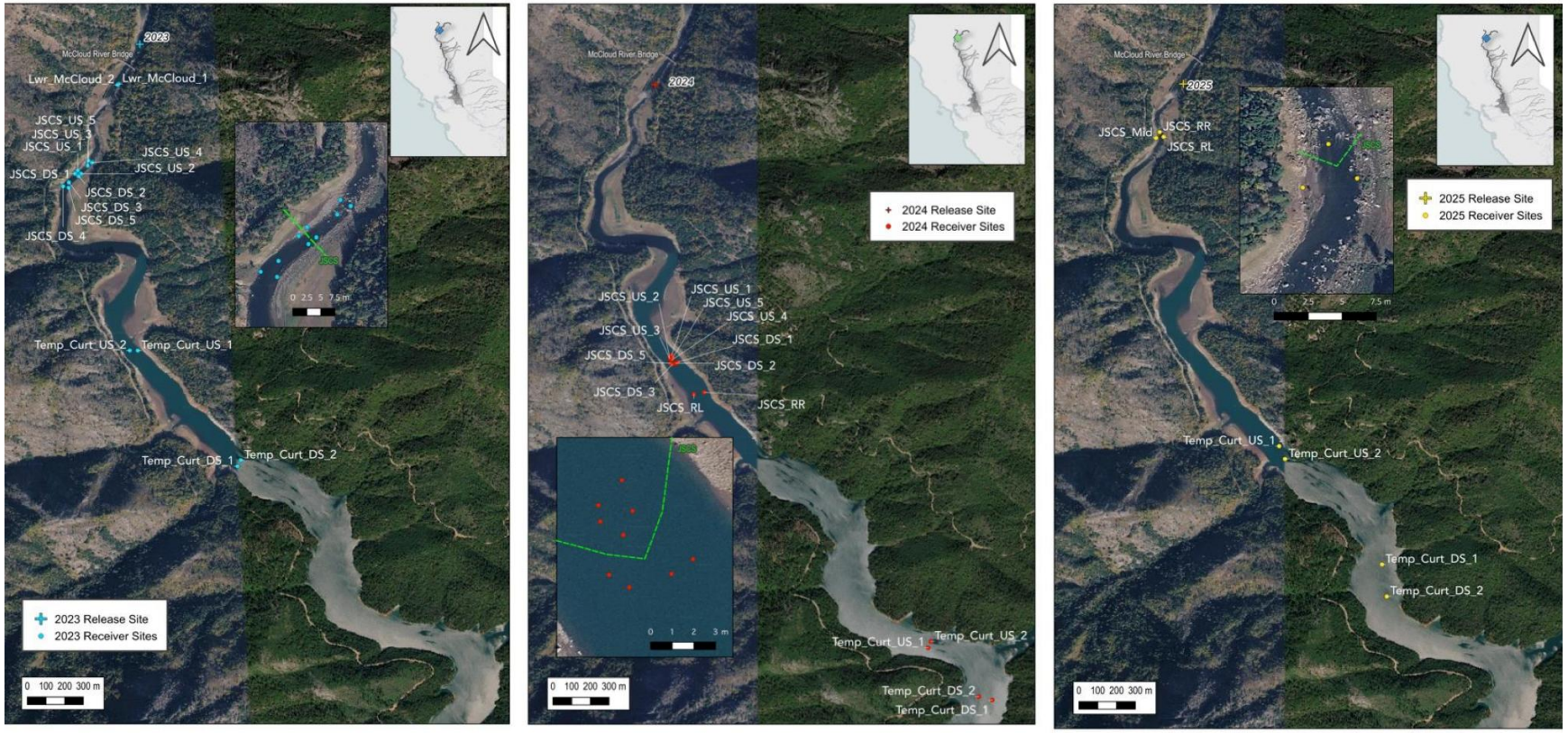

Figure 4.1. Locations of fish release sites and acoustic receiver sites for the three study years. Background imagery from Google taken 11/72023. Approximate locations of the JSCS relative to receivers are in green.

To extract valid detections of tagged fish, raw receiver files were filtered to remove false detections by requiring a minimum of four detections occurring within a time window consistent with the programmed tag pulse rate interval (PRI; typically 5sec). Following this filtering protocol, encounter histories were created and analyzed using a spatial form of the Cormack-Jolly-Seber (CJS) model for live recaptures (Cormack 1964; Jolly 1965; Seber 1982) using program MARK (White and Burnham 1999) within the RMark package (Laake 2013) in R statistical software, version 3.3.0 (R Core Team 2016). The CJS framework is well suited for juvenile salmon which exhibit an obligate downstream movement behavior after release. We modeled survival by year, reach, and release group, allowing for yearly comparisons in relatively small reaches around the JSCS and into Shasta Reservoir.

Two-dimensional positions relative to the JSCS

So as to identify where juvenile winter-run Chinook salmon may be evading capture at the JSCS, acoustic-tagged late-fall-run Chinook salmon were used as surrogates to evaluate 2-dimensional (latitude and longitude) movements with respect to the JSCS trap. A pilot effort was attempted in the 2023 season, but a technological issue made it impossible to accurately resolve 2-dimensional (2D) positions of acoustic-tagged fish that year. A more comprehensive effort was conducted during the 2024 season.

During the 2024 season, a total of 17 acoustic receivers and 10 beacon tags were deployed just upstream and downstream of the JSCS at its first deployment location (Fig. 4.2). A total of three groups of acoustic-tagged late-fall-run Chinook salmon were released upstream of the JSCS before it was relocated starting on October 28th, 2024, resulting in an estimated 256 fish available for 2D tracking (Fig. 4.6). The 2D tracking array was removed on October 28th, and was not redeployed at the second JSCS location that year.

Resolving 2D positions in 2024 was a collaborative effort between UC Santa Cruz and Pacific Northwest National Laboratories (PNNL, P.I. Dr. Daniel Deng). Briefly, acoustic tag detections were downloaded from all 17 acoustic receivers, then false positives were removed from the detection data using filtering algorithms. Using beacon tag detections (which are meant to be heard by multiple receivers simultaneously), receiver clocks were synchronized post-hoc so as to allow for accurate triangulation. Then, using the clock-corrected fish detections, 2D positions were resolved for each tag transmission that was heard by a minimum of 4 receivers. Three different positioning solvers (i.e., triangulation algorithms) were assessed, including two proprietary PNNL solvers (the Neural Network and Neural Network Plus solvers, hereafter NN and NN+ respectively) and one open-source solver (Yet Another Positioning Solver, hereafter YAPS, Baktoft et al. 2017). The positioning accuracy of the different solvers and the

overall 2D tracking array was assessed by drifting five live acoustic tags attached to a buoy and GPS logger through the array on September 17th, 2024. The known GPS locations of the tags during each drift can be assessed against the triangulated positions from the solvers.

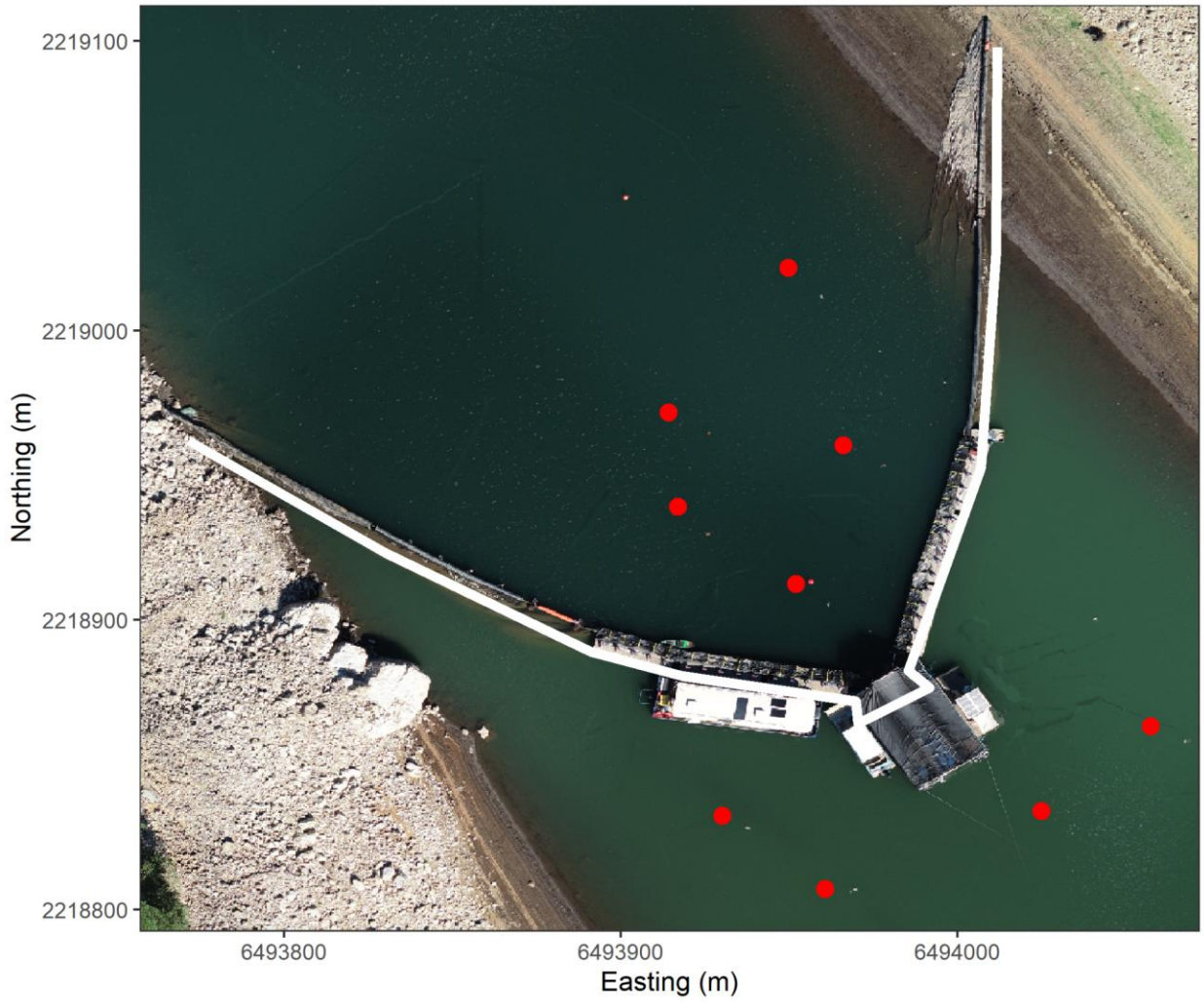

Figure 4.2. Position of receivers (red points) with respect to the JSCS trap in 2024. These receivers were successfully used to resolve two-dimensional positions of acoustic-tagged late-fall-run Chinook salmon.

Results

In total, 912 late-fall yearling Chinook salmon were acoustically tagged and released across three study years (2023-2025). Annual sample sizes varied, with 200 fish released in 2023, 654 fish in 2024, and 58 fish in 2025 (Table 4.1). Release timing and the number of release groups also differed among years. Release locations were also

slightly different, with fish released ~50 meters upstream of McCloud Bridge in 2023, and fish released just downstream of the bridge and CDFW incline plane trap in 2024-2025. Tagged fish size varied among years. Mean fork length and weight were 94 mm and 11.0 g in 2023, 133 mm and 27.9 g in 2024, and 130 mm and 28.2 g in 2025.

Table 4.1. Number of tagged fish released and detected at each receiver location in 2024. Note that each receiver location includes two or more acoustic receivers to ensure redundancy and full coverage of the channel width.

Detection location (ordered from upstream to downstream)	**9/24 release group**	**10/15 release group**	**10/22 (USGS release group)**	**10/29 release group**	**11/5 release group**	**11/19 (USGS release group)**	**12/03 (USGS/ CDFW release group)**
Release	65	100	100	104	106	102	77
JSCS Location 1 (trap relocated starting 10/29, but receivers stayed put)	26	93	88	*84*	*96*	*8*	*77*
Physically captured in JSCS trap and trucked	0	2	0	*NA* (trap being relocated from location 1 to 2)	0	0	0
Shasta Reservoir @ Nosoni Creek - Upstream	41	56	65	84	97	97	64
Shasta Reservoir @ Nosoni Creek - Downstream	39	43	58	78	78	91	56

Detected in Keswick Reservoir or anywhere downstream	0	1 (trucked downstream capture in the JSCS)	0	1	2	4	1

Survival and movement

Survival for tagged fish varied by year and release group. In 2023, survival from release upstream of the McCloud Bridge to just upstream of the CDFW trap was 90% for the 9/27 group and 85% for the 10/10 release group, respectively (Fig. 4.3). That was the only year during which survival estimates from above McCloud Bridge to the CDFW trap were available. Fish were released just downstream of the CDFW trap in 2024 and 2025. Survival from the CDFW trap to the JSCS ranged from 70 to 76% in 2023, 98 to 100% in 2024, and 98% in 2025 (Fig. 4.3). Survival from the JSCS to the head of the McCloud Arm at Nosoni Creek ranged from 50 to 66% in 2023, from 58 to 95% in 2024, and 100% in 2025. Cumulative (total) survival from release to the head of the McCloud Arm in at Nosoni Creek was 46% in 2023, 78% in 2024, and 98% in 2025 (Fig 4.4).

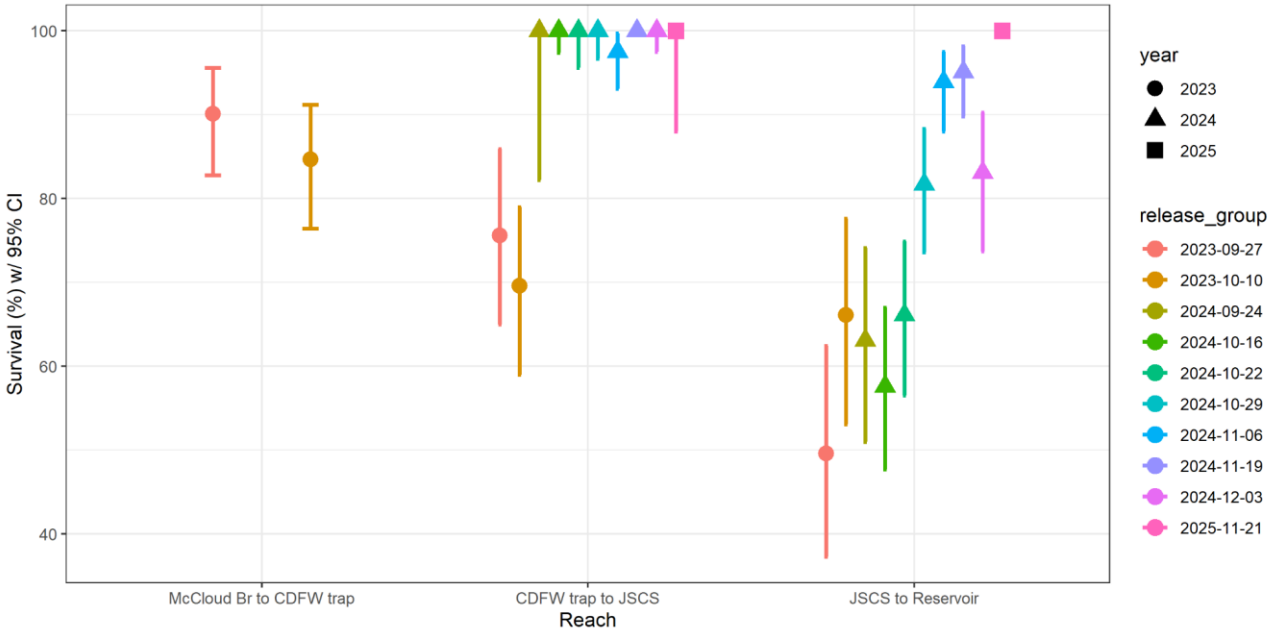

Figure 4.3. Survival estimates for acoustic-tagged late-fall-run Chinook salmon in all years for three consecutive river reaches (left to right): Release upstream of McCloud Bridge to CDFW trap, CDFW trap to JSCS, and JSCS to Nosoni Creek in the McCloud Arm or Shasta Reservoir. Note that the JSCS and the reservoir receivers changed locations year to year, and therefore inter-annual survival comparisons should be for discussion purposes only.

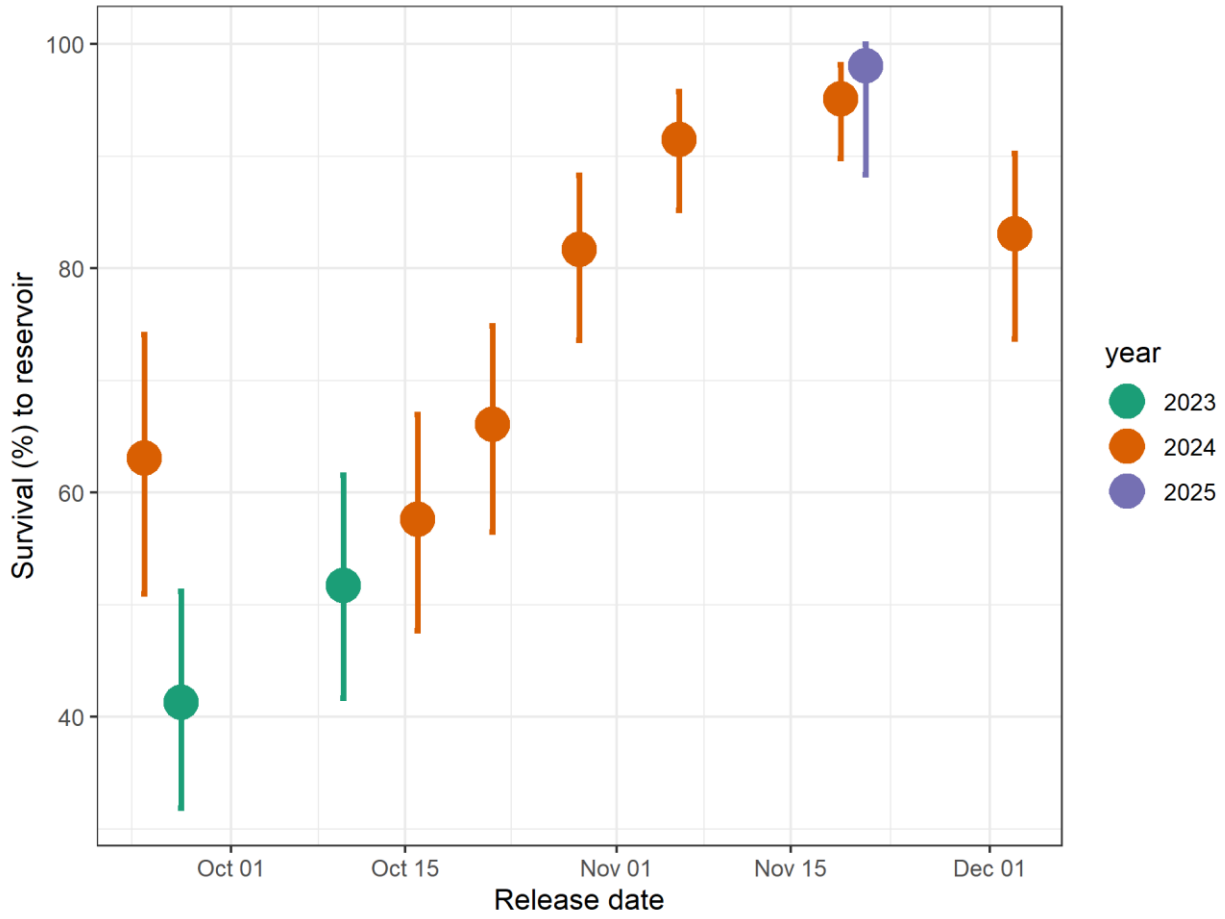

Figure 4.4. Survival from release site (immediately downstream of inclined plane trap) to Nosoni Creek for acoustic-tagged Late-fall-run Chinook salmon in 2023-2025.

Fish movement rates were generally rapid, with a median migration time to the head of Shasta Reservoir of 1.8 days across the three years, ranging from 0.2 to 74.7 days. However, some fish remained in the system for long periods of time, and only finally moved downstream with late season flow events associated with storms (Figs 4.5, 4.6, 4.7). A small number of fish were detected downstream of Shasta Dam in 2023 and 2024, either by receivers deployed into Keswick reservoir or Redding (only available in 2024), or by the larger real-time telemetry array found in the Central Valley (available all three years). In 2023, two fish were detected downstream of Shasta Dam, specifically at

the Below Salt Creek receiver site near Red Bluff. These were both fish captured in the JSCS and trucked to Redding for release (Figure 4.5). In 2024, a total of 9 fish were detected downstream of Shasta Dam (Table 4.1), 1 of which were captured in the JSCS and trucked to Redding for release (Figure 4.6). The remaining 8 fish are presumed to have gone through the Shasta Dam infrastructure. Three of these 8 fish successfully outmigrated to the most downstream receiver location at Benicia Bridge, 525 river kilometers downstream of their release site on the McCloud River. No fish were detected downstream of Shasta Dam in 2025.

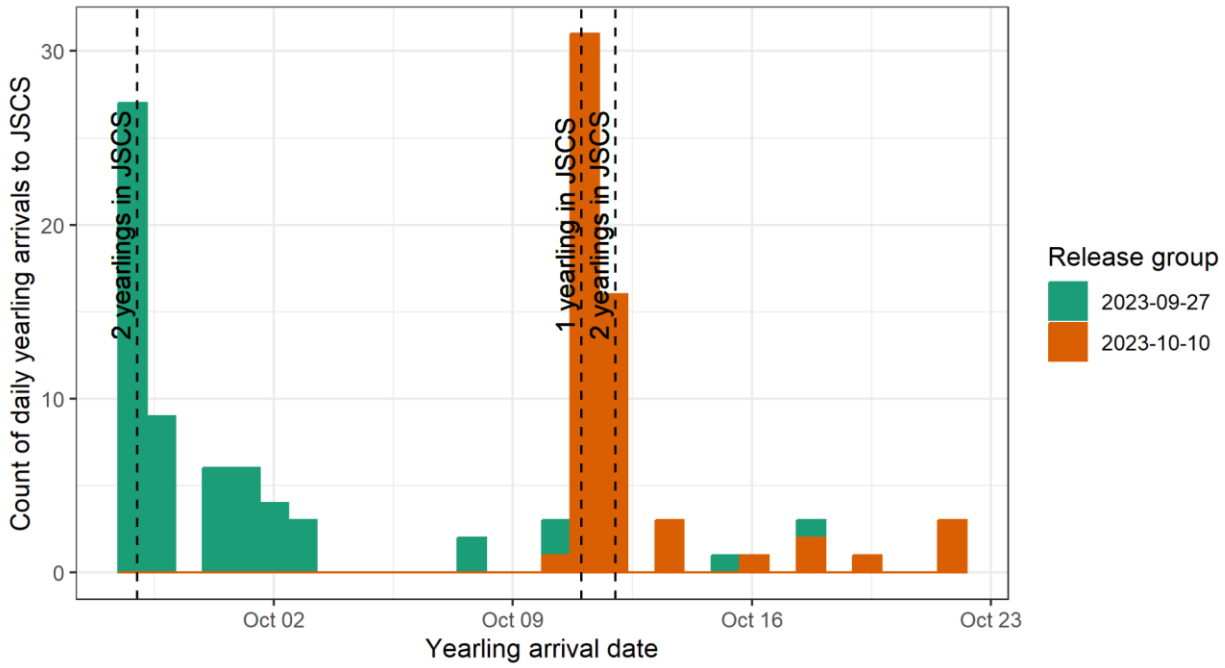

Figure 4.5. Histogram of arrivals of acoustic-tagged late-fall-run Chinook salmon yearlings to the first location of the JSCS in 2023, color coded by release group. Note the JSCS was relocated to a more downstream site starting on 10/25/2023.

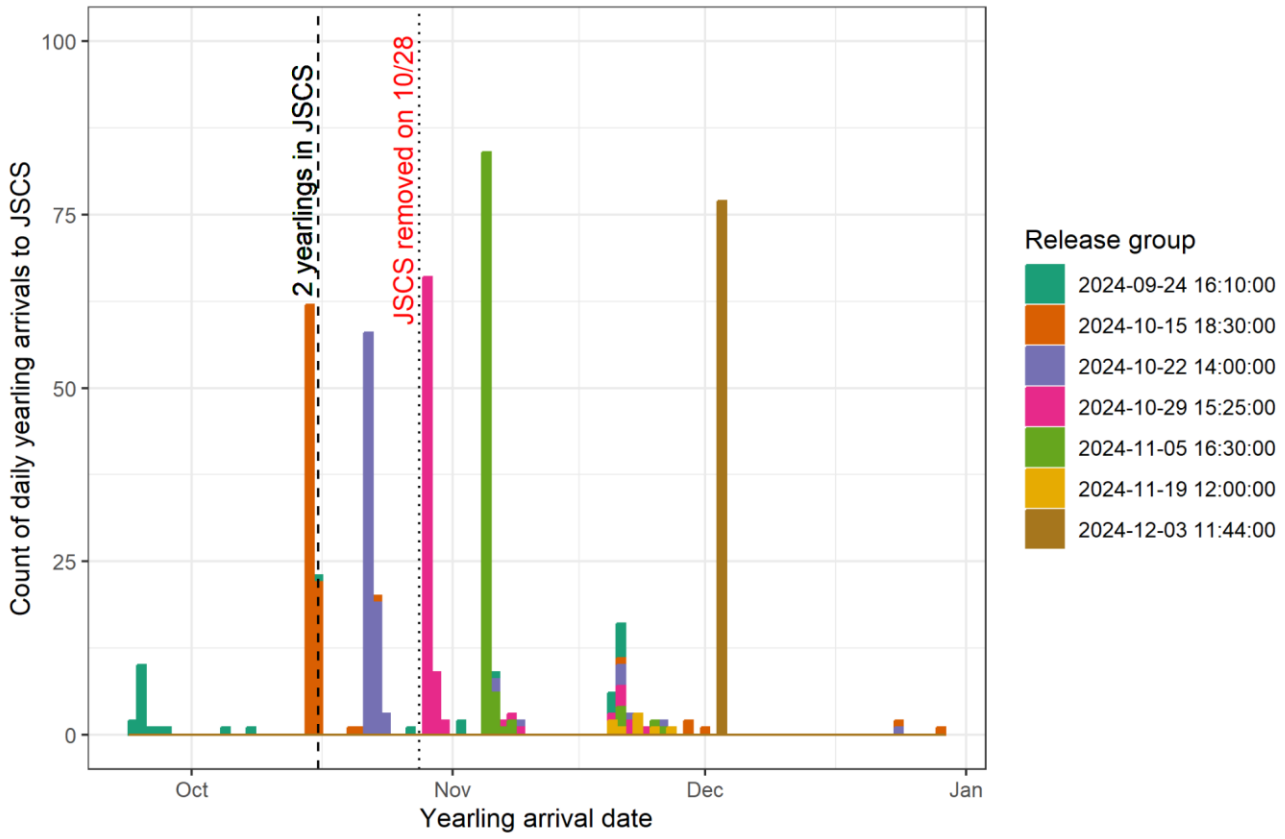

Figure 4.6. Histogram of arrivals of acoustic-tagged late-fall-run Chinook salmon yearlings to the first location of the JSCS in 2024, color coded by release group. Note the JSCS was relocated to a more downstream site starting on 10/28/2024.

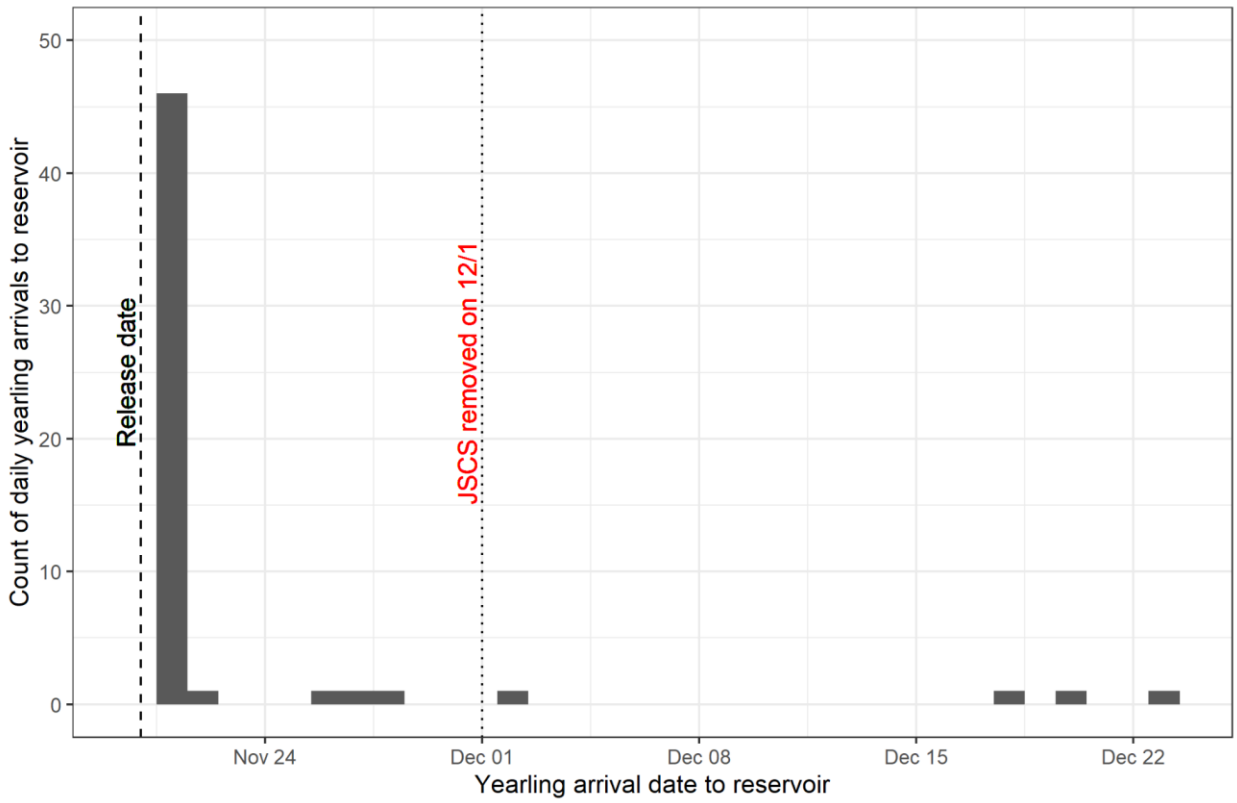

Figure 4.7. Histogram of arrivals of acoustic-tagged late-fall-run Chinook salmon yearlings to the reservoir in 2025. Note the JSCS was removed on 12/1/2025.

Telemetry data can be used to estimate how many fish arrived to the JSCS locations each year (during the trapping season), and therefore should have been available to catch in the trap. The estimated number of fish available to catch varied between 56 and 105 per release group (Fig. 4.8). Furthermore, we can use the number actually caught in the trap to estimate trap efficiency. Trap catches of these large yearling acoustic-tagged late-fall-run Chinook salmon were low; only 7 were ever captured, 2 from the 9/27/2023 release group, 3 from the 10/10/2023 group, and 2 from the 10/15/2024 release group. Using a multi-state mark recapture model (with the 2 states being captured in trap and not captured in trap), we were able to estimate trap efficiency for the two release groups in 2023: 4.8% for the 9/27/2023 release group, and 5.8% for the 10/10/2023 group. A multi-state model was not run for the one release group with trap captured in 2024, but with near perfect detection efficiency, the capture probability is approximated to be 2% (2 captured out of 100 available for capture). For all other release groups, capture probability is 0%.

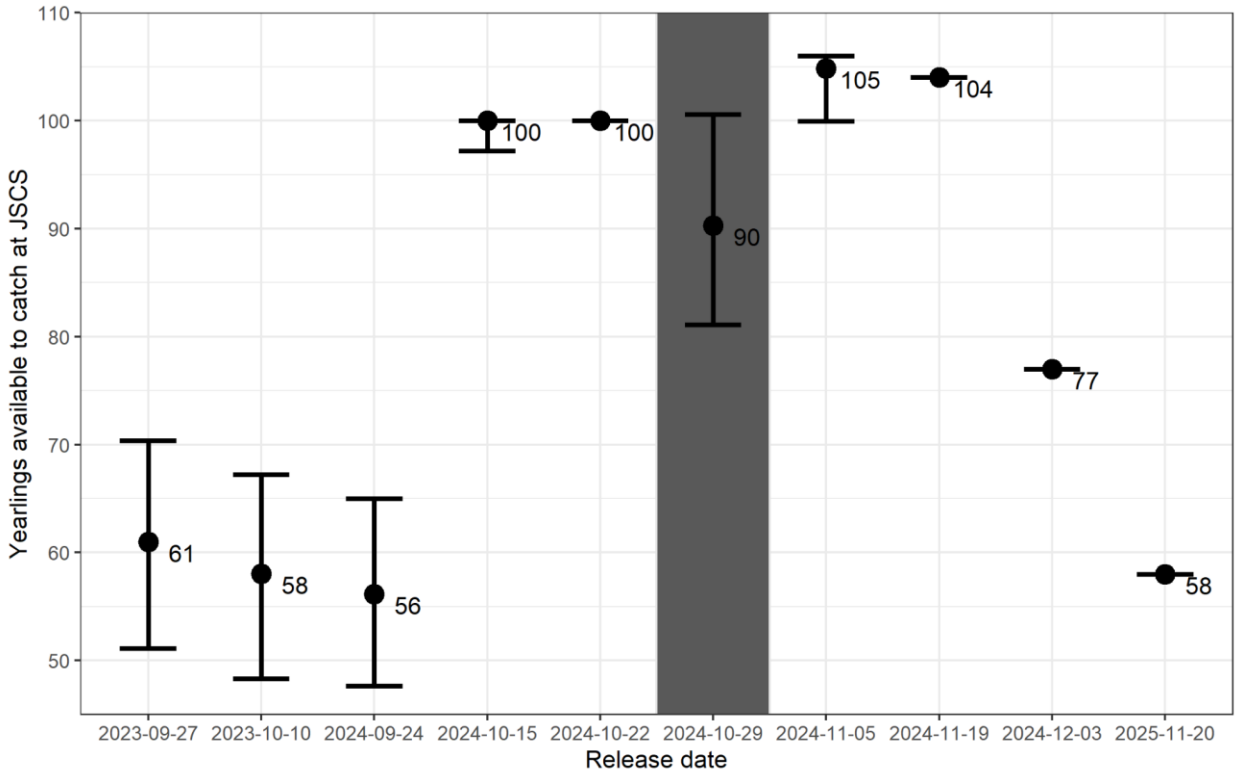

Figure 4.8. The number of acoustic-tagged yearling late-fall-run Chinook salmon available to be caught at JSCS locations in all three years according to acoustic telemetry. Note that the 10/29/2024 release group (within gray box) occurred when the trap was being moved and therefore few of these fish would be expected to be captured. Only 7 acoustic-tagged late-fall-run Chinook salmon were ever captured, 2 from the 9/27/2023 group, 3 from the 10/10/2023 group, and 2 from the 10/15/2024 release group.

Two-dimensional positions relative to the JSCS

All three solvers resulted in a relatively high degree of 2D positioning accuracy as assessed using the tag drifts. Specifically, for all five of the drifted live acoustic tags, across all 3 of the solvers, the median easting and northing error (in meters) was less than 2 and 1 meter, respectively. A visual comparison between the known GPS locations and the three solvers shows high solver accuracy (Fig. 4.9), but ultimately the NN+ solver had the lowest 2D range error and was selected for all fish 2D positioning.

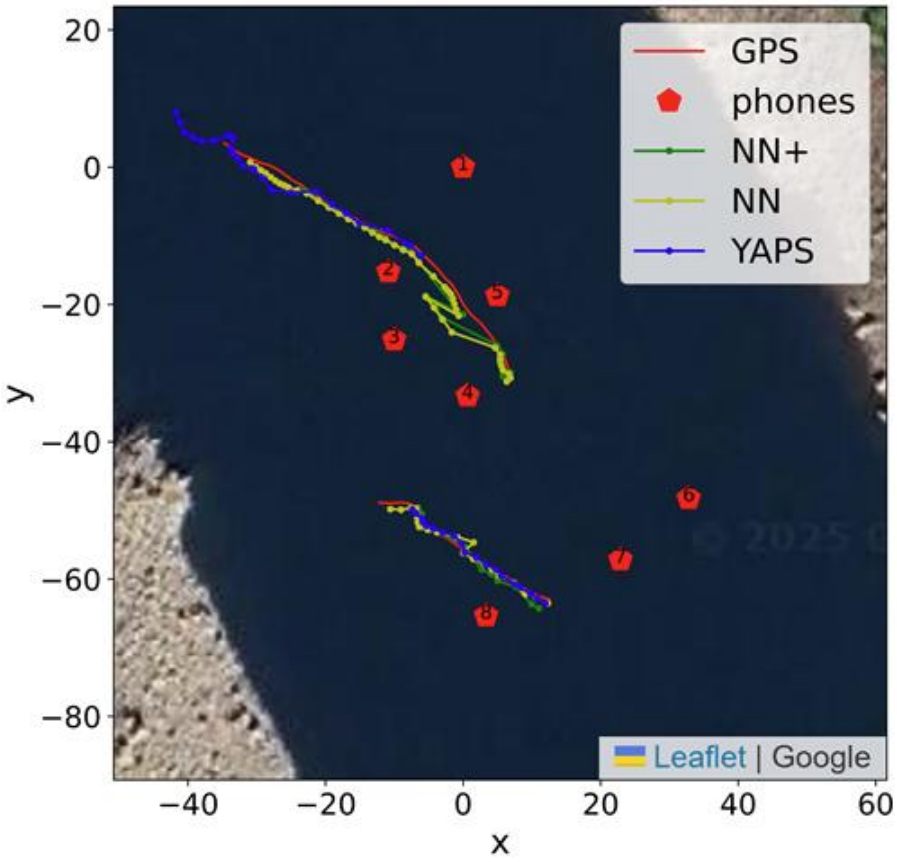

Figure 4.9. Two-dimensional positions of both the known GPS track of a live acoustic tag (red lines), and the triangulated tracks form the positioning solvers (green, yellow, and blue lines). Red pentagon icons depict the location of acoustic receivers.

In total, the NN+ solver was able to resolve some portion of fish tracks near the JSCS for 183 unique fish. Unique fish tracks varied in length, with some fish having as few as 4000 positions while others had up to 100,000 positions. The length of fish tracks were both a function of the performance of the 2D array during the time a fish approached the JSCS, but also, a function of the fish's behavior. Some fish exhibit relatively rapid and direct movement to and through the JSCS (e.g. Fig 4.10. right panel), while others exhibited a milling behavior on the upstream side of the JSCS (e.g. Fig. 4.10. left panel).

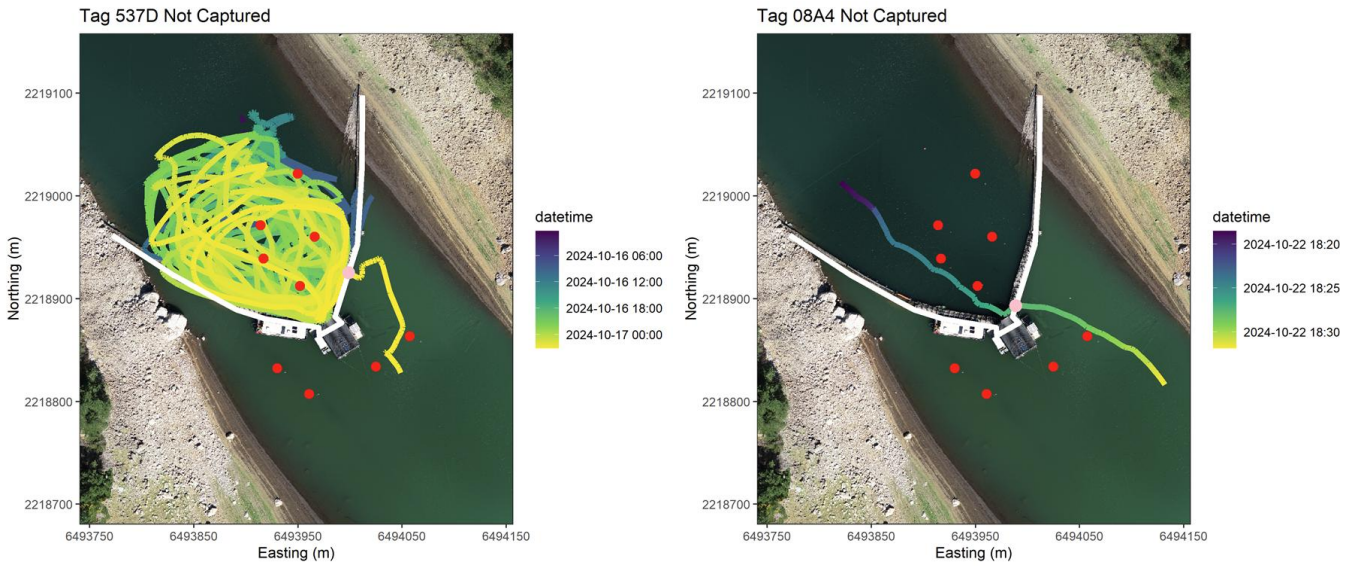

Figure 4.10. Two unique two-dimensional fish tracks in proximity to the JSCS during mid-October, 2024.

Ultimately, out of the 183 2D fish tracks, we were able to assign the approximate location of where fish escaped capture by the JSCS for 166 fish. A density heatmap of these locations indicated that the majority of fish escaped through the eastern wing of the trap, near the trapbox itself (Fig. 4.11). While the depth at which these fish were located when they escaped through the trap could not be resolved with sufficient accuracy, anecdotal observations would indicate that the fish were passing through a gap between the trap wing and the riverbottom.

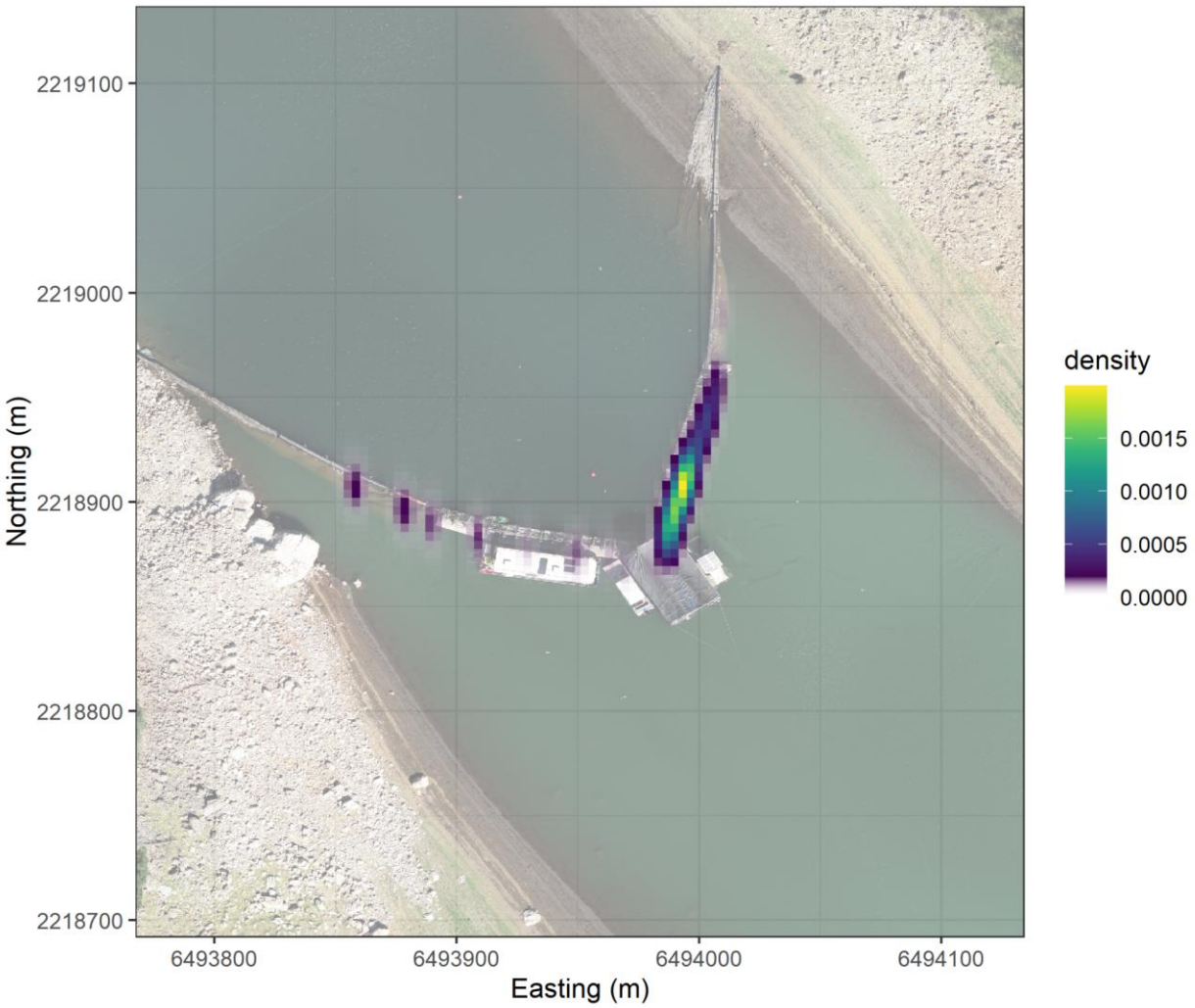

Figure 4.11. Density heatmap of where fish were evading capture along the JSCS in 2024.

Discussion

The acoustic telemetry results provide the first estimates of juvenile salmon survival in the lower McCloud River and entrance into Shasta Reservoir. Overall, survival to the head of Shasta Reservoir was relatively low for fish released earlier in the fall (September–October) but increased for fish released later in the year (November–December; Fig. 4.4). Survival was generally higher in the McCloud River between the release location and the JSCS and lower in the final reach from the JSCS to the head of Shasta Reservoir. Tagged fish typically migrated downstream quickly after release, but many fish appeared to reside in the lower McCloud River for extended periods, which may have influenced the survival estimates reported here, as tag battery life was approximately 70 days. Although late-fall Chinook salmon smolts are known to migrate downstream rapidly in the Sacramento River (Michel et al. 2015), it appears that many

individuals reared for extended periods in the lower McCloud River before migrating downstream into Shasta Reservoir.

Differences in tagged fish survival across the fall and winter season may be due to changing environmental conditions in the lower McCloud River and Shasta Reservoir. Tagged fish released earlier in the season (September-October), often experienced warmer water temperatures in the lower river and reservoir, as well as lower flows, which typically lead to lower survival in juvenile salmon. Water temperatures generally decreased later in the season, and more frequent flow events occurred which likely improved survival conditions for later release groups. In addition, some of the earlier release groups may have been infected with columnaris (*F. columnare*) and were potentially moribund after release, which could have been a factor in the low survival estimates we observed. Fish appeared to be in better health after water temperatures cooled at CNFH for the remaining release groups.

Overall, very few tagged fish were captured by the JSCS, with only five and two individuals known to be collected in 2023 and 2024, respectively. Most tagged fish appeared to pass through the structure at a single area of the trap (Fig. 4.11). The JSCS was redesigned and relocated upstream into the riverine section of the McCloud River in 2025. No acoustically tagged fish were captured in the new configuration, however, the number of tagged fish available for capture in 2025 was relatively small compared to previous years.

The results of this tagging study are most representative of yearling Chinook salmon smolts, as the only surrogates available during this study period were late-fall-run Chinook salmon obtained from CNFH. Survival for the more typical fry-sized juvenile winter-run Chinook salmon may be lower than the estimates reported here, as larger fish generally exhibit higher survival rates than smaller fish (Sogard, 1997). However, observations from many anglers indicate that yearling winter-run Chinook salmon exist in the lower McCloud River. These survival estimates are likely most representative of the small proportion of juveniles that rear in the river for a year (or more) prior to outmigration. As acoustic tags continue to become smaller, more representatively sized fish should be tagged and released to obtain more accurate information on movement and survival rates of the focused study population.

References

Baktoft, H., Gjelland, K. Ø., Økland, F., & Thygesen, U. H. (2017). Positioning of aquatic animals based on time-of-arrival and random walk models using YAPS (Yet Another Positioning Solver). Scientific Reports, 7(1), 1429

Cormack, R. M. 1964. Estimates of Survival from the Sighting of Marked Animals. Biometrika 51:429-438.

Jolly, G. M. 1965. Explicit Estimates from Capture-Recapture Data with Both Death and Immigration-Stochastic Model. Biometrika 52:225-247.

Laake, J.L. 2013. RMark: An R Interface for Analysis of Capture-Recapture Data with MARK. AFSC Processed Rep 2013-01, 25p. Alaska Fish. Sci. Cent., NOAA, Natl. Mar. Fish. Serv., 600 Sand Point Way NE, Seattle WA 98115.

Michel, C. J., A. J. Ammann, S. T. Lindley, P. T. Sandstrom, E. D. Chapman, M. J. Thomas, G. P. Singer, A. P. Klimley, and R. B. MacFarlane. 2015. Chinook salmon outmigration survival in wet and dry years in California's Sacramento River. Canadian Journal of Fisheries and Aquatic Sciences 72:1749-1759.

Seber, G. A. F. 1965. A Note on the Multiple-Recapture Census. Biometrika 52:249-259.

Sogard, S. M. 1997. Size-selective mortality in the juvenile stage of teleost fishes:A review. Bulletin of Marine Science, 60(3), 1129–1157.

White, G. C., and K. P. Burnham. 1999. Program MARK: survival estimation from populations of marked animals. Bird Study 46:120 - 139.

Task 5: Pathogens

The central objective of this task was to develop a baseline and shared understanding of how pathogens (i.e., disease-causing organisms) relate to the reintroduction potential of winter-run Chinook salmon on the McCloud River (Winnemem Waywaket). Infectious diseases are increasingly recognized as important factors when managing wildlife health and conservation (Preece et al. 2017, Pacioni et al. 2015, Altizer et al. 2011) and in Pacific Northwest watersheds, salmon population health has been documented to be affected by disease impacts (Chapman et al. 2020, Fujiwara et al. 2011, Foott et al. 2017). To what extent pathogens will impact reintroduced winter run and to what extent the introduction of winter run will impact the presence and distribution of pathogens and how this may change over space and time is not currently well known. However, understanding what types of pathogens are present and where and in what abundances they are distributed in the McCloud River is an important first step to building a more holistic picture of how winter-run, pathogens, and the environment interact. Therefore, our overarching question for this task is: **What is the current distribution of salmon pathogens in the McCloud River?**

We addressed this question and identified the connections between reintroduction potential and pathogens through environmental monitoring. Specifically, we employed two main study types that each provided connected but different information around pathogens and salmon health. The first approach took the form of a surveillance study, where environmental surface water samples were collected at routine locations and at routine intervals (primarily an upstream (AhDiNa) and downstream (Bollibokka) site at weekly to monthly intervals). By collecting and screening water samples for pathogens, we surveyed the environment and therefore were able to assess which pathogens were in the environment and therefore had the potential to infect salmon. These water samples consisted of 1L samples in triplicate that were screened for pathogen presence and abundance using molecular approaches and able to identify 47 different pathogens (i.e., bacteria, viruses, parasites, and a fluke) known to be infectious to salmon (Miller et al., 2016).

The second approach took the form of monitoring tissues (e.g., gill, kidney, and intestine) of fish associated with sentinel exposure studies and from those fish captured as a part of other tasks for this project (i.e., hook-line sampling for Rainbow and Brown Trout for predation studies). By screening fish tissues for pathogens and combining this information with that provided from the water samples, we combined multiple lines of evidence and more confidently identified pathogens that are both in the environment and infecting hosts. The sentinel studies took the form of exposure studies, where a population of fish that are assumed to be free of pathogens were deployed in the river at

a location (AhDiNa) that was paired to the environmental water sampling. After exposing fish, we sampled the population and screened tissues for pathogens using the same molecular approaches applied to the water samples. Tissue samples collected from fishing efforts to assess Chinook predation from Rainbow and Brown Trout (Task 7 - Predation Risk) that were captured via hook-line were processed using the same approach as the sentinel fish in addition to culture and histology based approaches to identify live “culturable” pathogens and disease states of fish (note: culture and histology results are not shown here). A main difference between the sentinel fish and the hook-line samples was that wild fish caught via hook-line have been exposed to ambient conditions for an unknown period of time. These hook-line samples therefore represented a method to identify pathogens that may not have been present at the sentinel exposure sites and or required a higher duration or concentration of exposure than occurred during sentinel events.

Results from this section are outlined in three primary sub-sections: 1) Water Samples, 2) Sentinel Studies, and 3) Hook-Line Studies. Each section consists of a brief summary of the methods followed by results. Each section is structured in a similar progression that goes from prevalence to abundance data and where appropriate section specific topics. The section ends with a discussion around how each of these three sections when combined together leads to an improved understanding of pathogens exposure and disease impacts on the McCloud River.

Water Samples

Water sampling occurred over two years in 2023 and 2024 with a focus on quantifying the prevalence and abundance of pathogens present in the environment. In both years, samples that were collected from July to October, to cover the primary incubation and rearing time period of winter-run Chinook, were prioritized for analysis. Samples were screened using molecular methods that detect both the presence (yes/no outcome) and abundance (quantitative outcome) of pathogen DNA and/or RNA. Overall, we screened for a total of 47 different pathogens, of which 21 were parasites, 14 were bacteria, 11 were viruses, and 1 was a fluke (Table 5.1). During this period water sampling occurred primarily at two field sites at weekly to monthly intervals. The upstream site was AhDiNa and the downstream site was Bollibokka. Samples were also collected at sites just downstream of AhDiNa as a part of Task 6- Outmigration Phenology.

At each site, water samples were collected in triplicate (1L x3) with field and lab blanks ran at each sampling event for quality control and assurance purposes. Samples were collected as hand grab samples just below the surface of the water and placed on ice until further processing. To isolate pathogen DNA/RNA from water, samples were vacuum filtered through 0.22-µm pore size filter membranes. Following filtration, the

volume of water filtered through each membrane (target of 500 mL) was recorded. Membranes were then placed in 2 mL centrifuge tubes with RNALater (QIAGEN Sciences, Germantown, MD, U.S.A.) and held at -80°C until DNA/RNA extraction and qPCR analysis using established protocols (Miller et al. 2016).

Overall, a total of 277 water samples were screened. Of those, 88% (244/277) were positive for at least one pathogen. The distribution of the number of different pathogens detected in a water sample is shown in Table 5.2 and ranged from zero to as many as eight pathogens detected in a single water sample. Prevalence of detection for each of the 47 pathogens screened for across all sites and separated by pathogen type (i.e. bacteria, parasite, virus, and fluke) are summarized in Figure 5.1. For this report we are using a prevalence threshold of 10% to separate pathogens that are considered to be common (>= 10%) or rare (<10%). By pathogen type, four bacterial pathogens and two parasites had a prevalence of above 10%, while the prevalence of viruses and the fluke were all less than 5%. *Rickettsia-like-organism* was the most prevalent bacterial pathogen (48%), *Ichthyophthirius multifiliis* was the most prevalent parasite (57%), while viruses that were detected and the fluke had a prevalence of ~1%.

Table 5.1. List of 47 pathogens screened

Microbe Full Name	Assay Name	Type
1. *Aeromonas hydrophila*	Ae_hyd	Bacterium
2. *Aeromonas salmonicida*	Ae_sal	Bacterium
3. *Candidatus Branchiomonas cisticola (CBc)*	CB_cys	Bacterium
4. *Flavobacterium psychrophilum (Fp)*	Fl_psy	Bacterium
5. *Gill chlamydia*	Sch	Bacterium
6. *Moritella viscosa*	Mo_vis	Bacterium
7. *Piscichlamydia salmonis*	Pch_sal	Bacterium
8. *Piscirickettsia salmonis*	Pisck_sal	Bacterium
9. *Renibacterium salmoninarum (Rs)*	Re_sal	Bacterium
10. *Rickettsia-like organism (RLO)*	RLO	Bacterium
11. *Tenacibaculum maritimum*	Te_mar	Bacterium
12. *Vibrio anguillarum*	Vi_ang	Bacterium
13. *Vibrio salmonicida*	Vi_sal	Bacterium
14. *Yersinia ruckeri (Yr)*	Ye_ruc	Bacterium
15. *Nanophyetus salmincola*	Na_sal	Fluke
16. *Ceratonova shasta (Cs)*	Ce_sha	Parasite
17. *Cryptobia salmositica*	Cr_sal	Parasite
18. *Dermocystidium salmonis (Ds)*	De_sal	Parasite
19. *Facilispora margolisi*	Fa_mar	Parasite
20. *Gyrodactylus salaris*	Gy_sal	Parasite
21. *Ichthyophonus hoferi*	Ic_hof	Parasite
22. *Ichthyophthirius multifiliis (Im)*	Ic_mul	Parasite
23. *Kudoa thyrsites*	Ku_thy	Parasite
24. *Loma salmonae*	Lo_sal	Parasite
25. *Myxobolus arcticus*	My_arc	Parasite
26. *Myxobolus cerebralis (Mc)*	My_cer	Parasite
27. *Myxobolus insidiosus*	My_ins	Parasite
28. *Neoparamoeba perurans*	Ne_per	Parasite
29. *Nucleospora salmonis*	Nu_sal	Parasite
30. *Paranucleospora theridion (syn. Desmozoon lepeophtherii)*	Pa_ther	Parasite
31. *Parvicapsula kabatai*	Pa_kab	Parasite
32. *Parvicapsula minibicornis (Pm)*	Pa_min	Parasite
33. *Parvicapsula pseudobranchicola*	Pa_pse	Parasite
34. *Sphaerothecum destructuens*	Sp_des	Parasite
35. *Spironucleus salmonicida*	Sp_sal	Parasite
36. *Tetracapsuloides bryosalmonae*	Te_bry	Parasite
37. *Atlantic salmon paramyxovirus*	ASPV	Virus
38. *Infectious hematopoietic necrosis virus*	IHNV	Virus
39. *Infectious salmon anemia virus*	snow7	Virus
40. *Infectious salmon anemia virus*	ISAV8	Virus
41. *Piscine myocarditis virus*	PMCV1	Virus
42. *Piscine reovirus*	PRV	Virus
43. *Salmon alphavirus 1, 2, and 3*	SAV	Virus
44. *Salmonid herpesvirus/Oncorhynchus masou herpes virus (OMV)*	OMV	Virus
45. *Viral encephalopathy and retinopathy virus*	VER	Virus
46. *Viral erythrocytic necrosis virus*	VEN	Virus
47. *Flavivirus salmonis*	Fl_sal	Virus

Table 5.2. Frequency of different pathogens detected in water samples.

Pathogen count	0	1	2	3	4	5	6	7	8
Number of samples	33	60	54	36	29	27	30	4	4
Percent	11.91	21.66	19.49	13.00	10.47	9.75	10.83	1.44	1.44

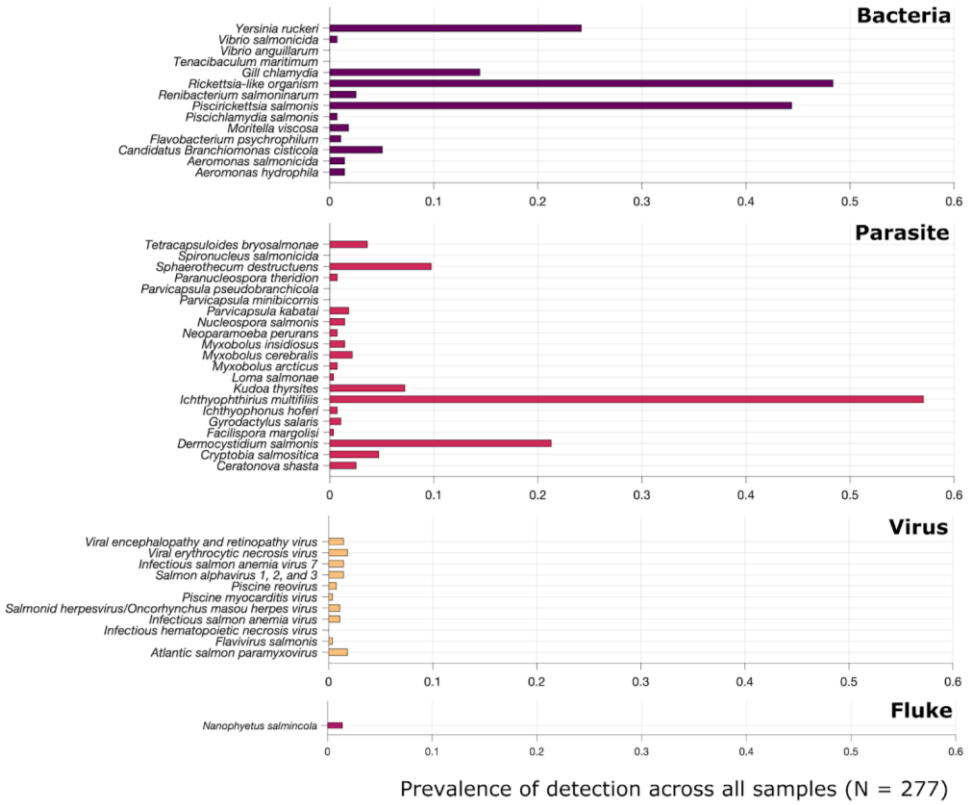

Figure 5.1. **Pathogen Detection Frequency in McCloud River Water Samples.** Distribution of prevalence across four taxonomic groups (Bacteria, Parasite, Virus, and Fluke) screening for 47 total targets. Data represents the detection frequency (n/N) where N = 277. High prevalence was observed in *Ichthyophthirius multifiliis* (>0.5) and *Rickettsia-like organisms* (~ 0.48).

Focusing on the two sites that were most consistently sampled (AhDiNA and Bollibokka), we see a similar pattern of prevalence of detection as shown in Figure 5.2. Specifically, *Rickettsia-like-organism* and *Ichthyophthirius multifiliis* were frequently detected, in addition to nine other pathogens that had a prevalence of detection above 10% across both sites (*Piscirickettsia salmonis*, *Yersinia ruckeri*, *Dermocystidium salmonis*, *Gill chlamydia, Sphaerothecum destructuens, Kudoa thyrsites, Candidatus*

Branchiomonas cisticola, Cryptobia salmositica, Tetracapsuloides bryosalmonae). Differences in prevalence between groups (e.g., AhDiNa vs. Bollibokka) were evaluated using a Pearson's Chi-Squared Test of Independence (χ^2). This test determines whether the observed frequency of pathogen detection significantly deviates from the expected frequency under the null hypothesis of no difference between groups. All statistical tests were two-tailed, and a significance threshold of alpha = 0.05 was applied. When comparing if the prevalence varied between sites, *Ichthyophthirius multifiliis* was statistically more prevalent at AhDiNa (82% vs. 50%), while *Yersinia ruckeri* and *Dermocystidium salmonis* were more prevalent at Bollibokka, (89% vs. 49%) and (89% vs. 30%) respectively.

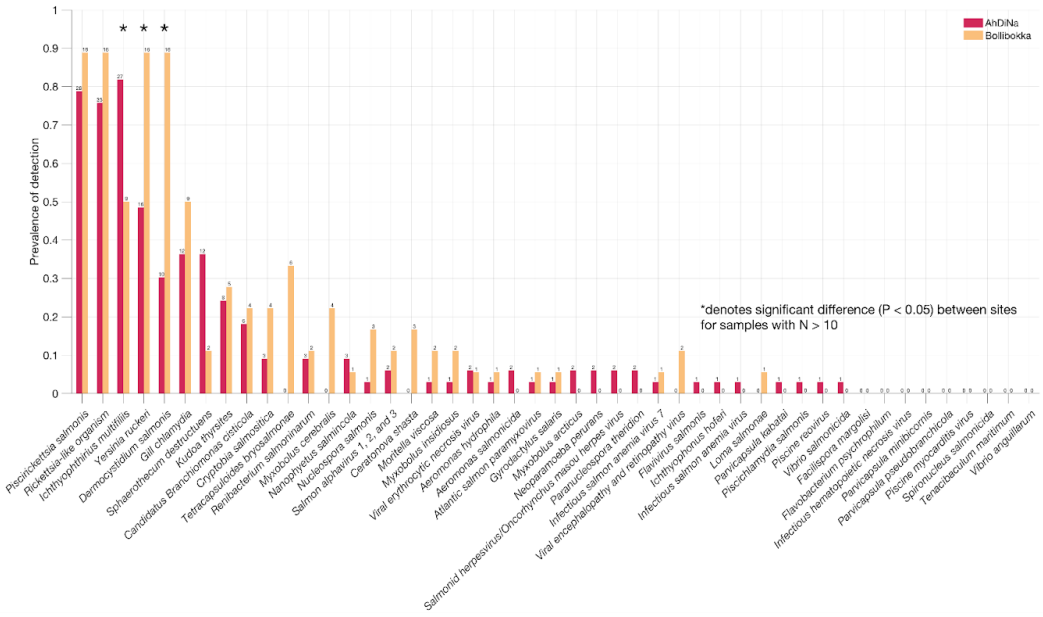

Figure 5.2. **Comparative Prevalence of Pathogens at Upstream and Downstream McCloud River Sites.** Bars represent the frequency of detection for 47 pathogens at AhDiNa (upstream) and Bollibokka (downstream). Asterisks (*) denote statistically significant differences (P < 0.05) between sites for pathogens with N > 10 with a Chi-Squared test. Numbers above bars represent the number of positive samples.

To further explore differences in pathogens across sites, pathogen abundance (Log_{10} Copy# L^{-1}) for both AhDiNa and Bollobokka in 2023 and 2024 are summarized in Figure 5.3. The abundance is shown as a heatmap, where individual sample dates are shown on the x-axis and pathogens on the y-axis. Visually, Figure 5.3 shows that some pathogens are consistently detected at greater abundances (i.e., cells that are darkblue) over time at both sites, such as *Ichthyophthirius multifiliis*, while other pathogens are detected are lower abundances (i.e., cells that are light blue), such as *Yersinia ruckeri.* Note, however, that when comparing abundance data, it is most

appropriate to compare similar pathogen types, such as parasites, to each other as parasites that are multicellular are expected to inherently have a great DNA abundance compared to unicellular bacteria. Additionally, even different parasites have different sizes and so a single *Ichthyophthirius multifiliis* would have a different abundance compared to a single *Dermocystidium salmonis.* Therefore, hereafter, our statistical analysis is based on comparing the trends for the same species of pathogen.

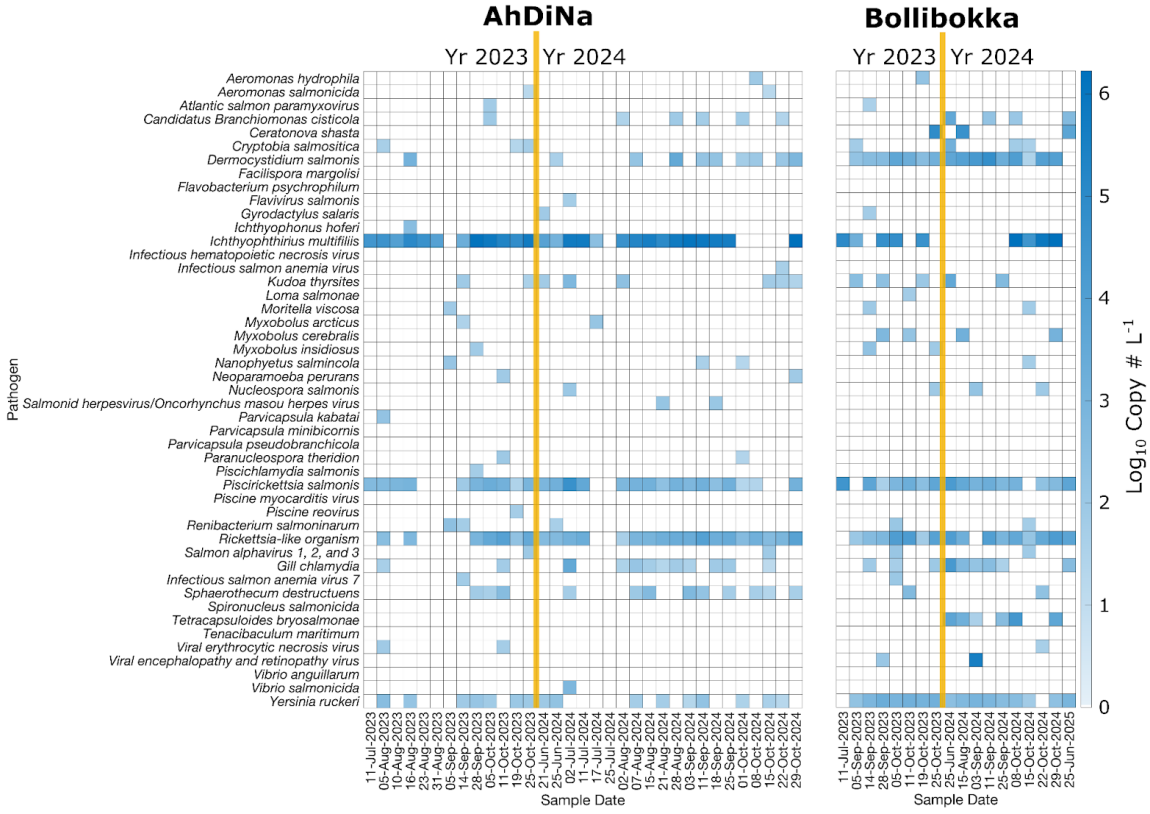

Figure 5.3. **Spatiotemporal Distribution and Relative Abundance of Pathogens in the McCloud River.** Heat map illustrating the detection and abundance of 47 pathogens at the upstream AhDiNa and downstream Bollibokka routine monitoring sites across 2023 and 2024. Cell color density represents the relative abundance of pathogen genetic material, measured as Log_{10} Copy# L^{-1}. The y-axis lists individual pathogen species, while the x-axis denotes discrete sample dates. Pathogens such as *Ichthyophthirius multifiliis* and *Piscirickettsia salmonis* demonstrate persistent, high-abundance signals across both years and locations, whereas others show seasonal or site-specific pulses.

Isolating abundance data for AhDiNa and Bollibokka and displaying the distribution of abundance values is shown in Figure 5.4. To aid in visualization, box-plots are displayed when either site had more than 10 positive detection. To quantify differences in pathogen loads between sites (e.g., AhDiNa vs. Bollibokka), we analyzed

the **abundance of genetic material**, measured as the log-transformed copy number (Log_{10} Copy# L^{-1}). Differences in mean abundance between two independent groups were evaluated using an Independent Samples t-Test. This parametric test assesses whether the average pathogen load at one site is statistically distinct from the other. Prior to analysis, abundance data were log-transformed (Log_{10}) to normalize the distribution of copy numbers, which typically span several orders of magnitude. Comparisons were restricted to pathogens with sufficient positive detections (n > 10) to ensure statistical power and reliability. A significance threshold of alpha = 0.05 was applied. When comparing abundances between sites, *Ichthyophthirius multifiliis* was detected as a greater level at AhDiNa compared to Bollobokka, while *Yersinia ruckeri, Dermocystidium salmonis, Tetracapsuloides bryosalmonae, Myxobolus cerebralis,* and *Ceratonova shasta*, were detected at a greater level at Bollibokka. For the rest of the pathogens, the data is dominated by near-zero abundance, suggesting that these species are either absent or present below the detection limit in most samples from both sites.

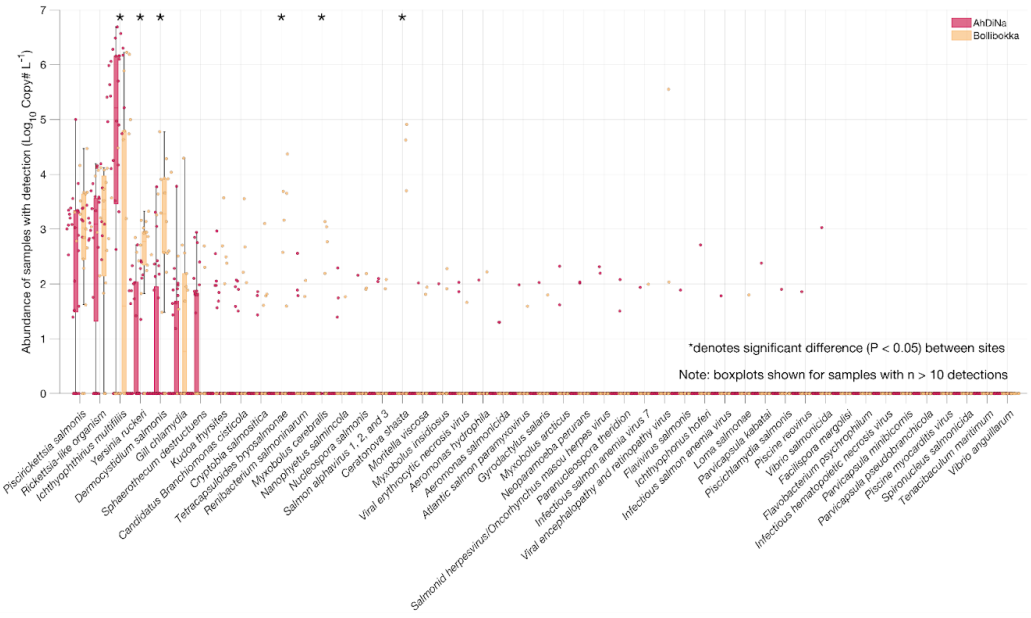

Figure 5.4. **Comparative Abundance of Pathogens in McCloud River Water Samples.** Pathogen abundance is quantified as Log_{10} Copy# L^{-1} from environmental surface water samples collected at the upstream AhDiNa site and downstream Bollibokka site. Individual jittered points represent the raw data for each positive detection, while boxplots summarize the distribution (median, quartiles, and range) for pathogens with n > 10 detections. Asterisks (*) denote a statistically significant difference in abundance between sites (P < 0.05) for a t-Test.

To further explore trends in the abundance of pathogens across sites as well as over time, we fit general-additive-models (GAMs). GAMs are useful to be able to detect

non-linear trends over time, such as our abundance time series data as well as flexible enough to also adjust for site (AhDiNa and Bollibooka) and year (2022 and 2023) effects. Specifically we fit GAMs that included predictor terms for site and year to assess if abundance differed by these terms and also included smoothing terms by day of year to identify any temporal trends in the abundance of pathogens and allowed this to vary by site and year. We fit separate models for the top six pathogens as identified by prevalence of detection in Figure 5.2 as these pathogens had enough detections to allow for assessments between space and time. Results for each pathogen are displayed in Figure 5.5 where observed data are shown as points and model fits with confidence intervals are shown as lines and shaded regions respectively. Additional text in Figure 5.5 shows the level of variance explained by the model (R^2), if mean abundance differed by site (Site Diff) or year (Year Diff), if the seasonal pattern in a given year is a predictor of abundance (DOY:Year2023 & DOY:Year2024), and if the seasonal trend was a significant predictor of abundance for a given site (DOY:AhDiNa & DOY:Bollibokka).

Predictive skill as assessed by R^2 varied from a low of 12% for *Ichthyophthirius multifiliis* to a high of 56% for *Dermocystidium salmonis.* Comparing site differences, abundances of *Ichthyophthirius multifiliis, Yersinia ruckeri, Dermocystidium salmonis,* and, *Gill chlamydia* were significantly different between AhDiNa and Bollibokka, with *Ichthyophthirius multifiliis* being higher at AhDiNa and the other pathogens being higher at Bollibokka. Across years, *Rickettsia-like-organism, Dermocystidium salmonis,* and *Gill chlamydia* had higher abundances in 2024 compared to 2023. Within years, pathogens that had a seasonal signal included *Piscirickettsia salmonis* in both 2023 and 2024, *Rickettsia-like-organism* in 2023.

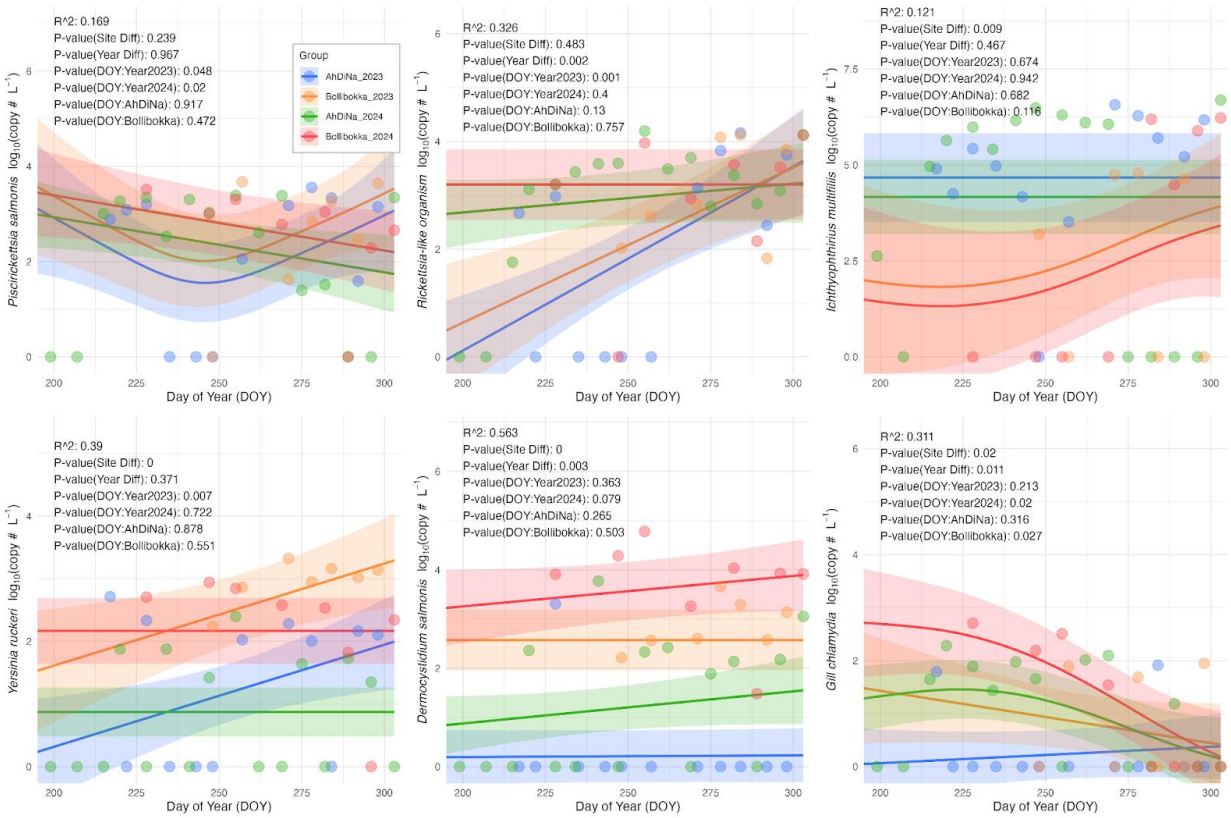

Figure 5.5. **General Additive Models (GAMs) of Pathogen Abundance Trends Across Space and Time.** Results of GAM fits for the top six pathogens by prevalence, displaying non-linear trends in genetic abundance (Log_{10} Copy# L^{-1}) across the Day of Year (DOY). Individual points represent raw observed data, while solid lines and shaded regions indicate model fits and 95% confidence intervals, respectively. Data are color-coded by site (AhDiNa in blue/green tones; Bollibokka in orange/red tones) and year (2023 vs. 2024). Accompanying text for each panel identifies predictive skill (R^2), significant differences between sites (Site Diff) and years (Year Diff), and the significance of seasonal patterns (DOY) by year and site.

By combining both prevalence and abundance data, we can get a clearer sense of what pathogens are relatively common in the environment and those that have greater levels of DNA/RNA detected. Figure 5.6 shows this relationship for both AhDiNa and Bollibokka. Note that only a subset of pathogens with a prevalence above 30% and abundance above 1 Log_{10} Copy# L^{-1} are annotated on this plot for visual purposes. This figure indicates that five pathogens are generally at the upper end of prevalence and abundance. These are *Ichthyophthirius multifiliis, Dermocystidium salmonis*is, *Rickettsia-like-organism, Piscirickettsia salmonis*, and *Yersinia ruckeri.* Additionally, the relationship between prevalence and abundance was found to follow a non-linear positive relationship, such that higher prevalence and abundance are correlated. A GAM was fit to this data to assess the association with the model fit being significant (P

< 0.05) and describing 92% of the variation in the data.

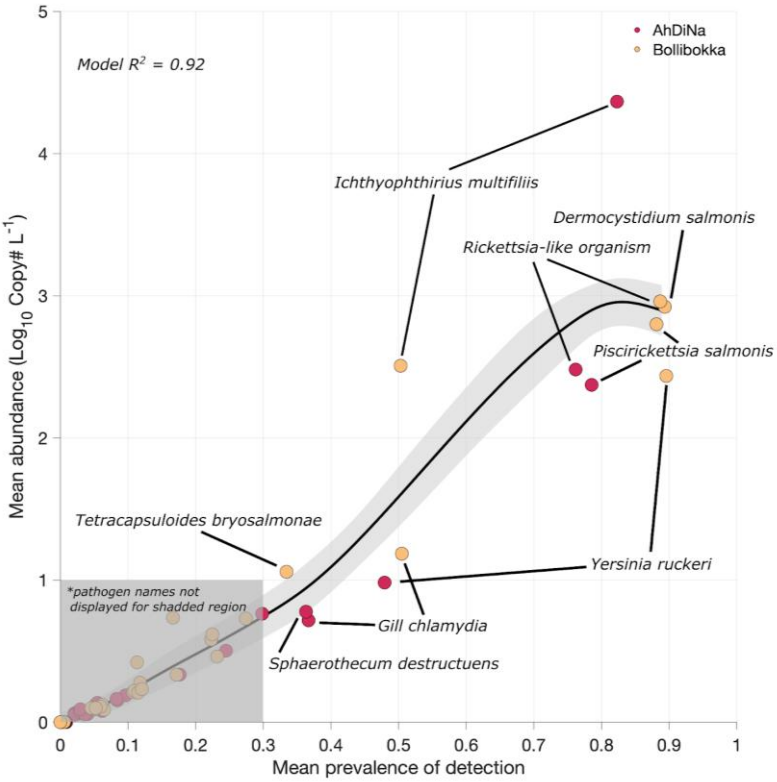

Figure 5.6. **Relationship Between Pathogen Prevalence and Mean Abundance in the McCloud River.** Scatterplot illustrating the non-linear positive correlation between the frequency of detection (Prevalence) and the concentration of genetic material (Log_{10} Copy# L^{-1}) for 47 screened pathogens. Data points represent observations from the upstream AhDiNa site and the downstream Bollibokka site. A General Additive Model (GAM) was fit to the data (solid line), showing a significant association ($P < 0.05$) that describes 92% of the total variation. Annotations highlight the five primary pathogens identified at the upper end of both prevalence and abundance scales: *Ichthyophthirius multifiliis*, *Dermocystidium salmonis*, *Rickettsia-like organism*, *Piscirickettsia salmonis*, and *Yersinia ruckeri*. Note: Only pathogens with prevalence >30% and abundance >1 Log_{10} Copy# L^{-1} are explicitly labeled for clarity.

Sentinel Studies

Sentinel studies occurred over two years in 2023 and 2024 with a focus on quantifying the prevalence and abundance of pathogens present in juvenile Chinook salmon. Sentinel studies involve deploying a population of assumed pathogen-free fish into a specific river location to monitor how they interact with the ambient environment over a measured period of time. This approach allows researchers to combine environmental water data with physical tissue analysis to identify the specific concentrations and

conditions under which pathogen exposure leads to actual infection and/or disease. In our studies, our primary outcome of interest was the detection of pathogens in fish tissues. Similar to water samples, sentinel samples were screened using molecular methods that detect both the presence (yes/no outcome) and abundance (quantitative outcome) of pathogen DNA and/or RNA.

In both years, juvenile salmon that were a part of feeding and/or behavioral studies were opportunistically enrolled in sentinel studies of pathogen exposure. Sentinel fish were sampled in October and consisted of collecting two to three tissue types from enrolled fish. More specifically, a sample of gill tissue was collected in 2023. Sampling the gill is a critical component of pathogen monitoring because the gills serve as a primary interface between the fish and its environment. In addition to a gill sample, we collected an internal body scrape, which consisted of sampling the internal body cavity of an individual. Originally, we planned on targeting specific organs in the body cavity, such as the intestine, as this can lead to a more targeted understanding of pathogen occurrence. However, due to the relatively small size of sentinel fish in our studies, we were not able to isolate specific organs and opted to sample the entire body cavity as a pooled sample (i.e., an internal body scrape which likely included the intestine, spleen, and kidney). In 2024, we collected gill and body scrape samples in addition to an external swab from a fish's skin to represent a mucus sample. Similar to the gill, the external mucus and skin can serve as a primary interface between the fish and its environment. Additionally, in 2023, we detected a high prevalence of the *Ichthyophthirius multifiliis* in water samples, which is a pathogen that first targets the mucus of fish to begin the infection process. Therefore, we wanted to assess if we could detect this pathogen at similar levels with a less-invasive mucus swab compared to a gill and internal tissue sample.

In both years sentinel studies occurred at the upstream site of AhDiNa. In 2023 we sampled 14 individual fish, while in 2024 we sampled 30 individual fish. In 2023, fish enrolled into the sentinel study were apart of a feeding study were fish were held in an enclosure in the McCloud River, while in 2024 fish enrolled into the sentinel study were apart of a behavioral study where fish were held in a circular tank on the side bank of the McCloud River. All fish used in the sentinel studies were taken from eggs reared by CDFW at AhDiNa.

Following deployment we sampled fish tissues for pathogens. Fish were placed in aerated 5-gallon buckets filled with water from the same area. We euthanized fish individually with 500 $mg \cdot L^{-1}$ Tricaine mesylate (MS-222; Syndel, Ferndale, WA, U.S.A) buffered by an equal concentration of sodium bicarbonate. Within five minutes of being euthanized, we collected the tissues with sterilized (bleach followed by ethanol) surgical

scissors and forceps, and placed tissues in separate 2 mL centrifuge tubes containing RNALater (QIAGEN Sciences, Germantown, MD, U.S.A.). Tissues were held at -80°C until DNA/RNA extraction and qPCR analysis using established protocols (Miller et al. 2016).

Overall, a total of 118 tissue samples were screened. Of those, 81% (96/118) were positive for at least one pathogen. The distribution of the number of different pathogens detected in a tissue sample is shown in Table 5.3 and ranged from zero to as many as seven pathogens detected in a single tissue sample. Prevalence of detection for each of the 47 pathogens screened for across all sites and separated by pathogen type (i.e. bacteria, parasite, virus, and fluke) are summarized in Figure 5.7. Similar to water samples, we are using a prevalence threshold of 10% to separate pathogens that are considered to be common (>= 10%) or rare (<10%). By pathogen type, one bacterial pathogen and two parasites had a prevalence of above 10%, while the prevalence of viruses and the fluke were all less than 10%. *Flavobacterium psychrophilum* was the most prevalent bacterial pathogen (12%), *Ichthyophthirius multifiliis* was the most prevalent parasite (71%), while *Salmonid herpesvirus/Oncorhynchus masou herpes virus* was the most prevalent virus at 6% and the fluke (*Nanophyetus salmincola*) had a prevalence of 5%.

Table 5.3. Frequency of different pathogens detected in tissue from sentinel samples.

Tissue type	Pathogen count	0	1	2	3	4	5	6	7
gill	**number of samples**	6	22	9	7				
gill	**percent**	13.63	50.00	20.45	15.90				
body scape	**number of samples**	6	15	11	3	4	3	1	1
body scape	**percent**	13.64	34.09	25.00	6.82	9.09	6.82	2.27	2.27
mucus swab	**number of samples**	10	16	4					
mucus swab	**percent**	33.33	53.33	13.33					
all	**number**	22	53	24	10	4	3	1	1

	of samples								
all	**percent**	18.64	44.92	20.34	8.47	3.39	2.54	0.85	0.85

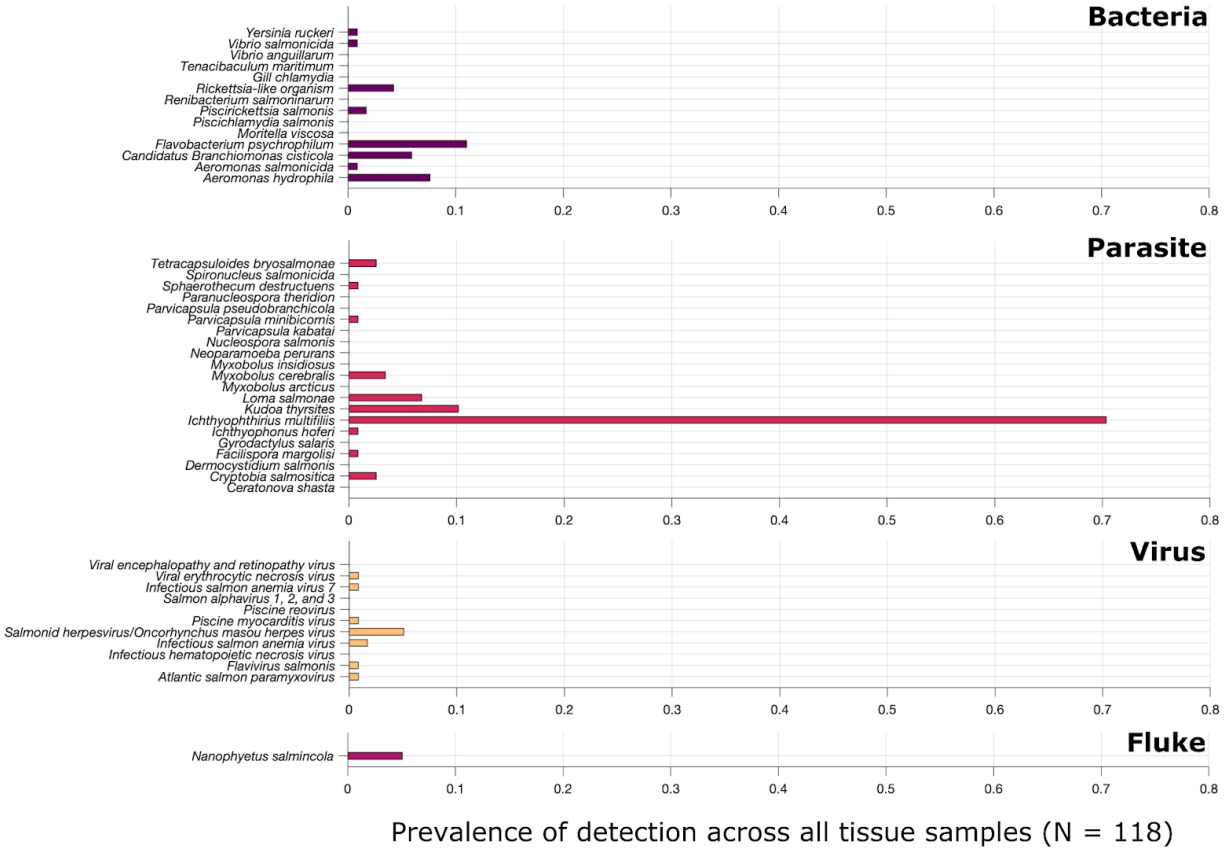

Figure 5.7. **Pathogen Detection Frequency in McCloud River Sentinel Samples.** Distribution of prevalence across four taxonomic groups (Bacteria, Parasite, Virus, and Fluke) screening for 47 total targets. Data represents the detection frequency (n/N) where N = 118. High prevalence was observed in *Ichthyophthirius multifiliis* (>70%).

Comparing prevalence across the three tissue types (gill, body, and mucus), we see a similar pattern of prevalence of detection across tissues as shown in Figure 5.8. Specifically, *Ichthyophthirius multifiliis* was frequently detected in all tissues types and at a much greater level than all other pathogens, in addition to two other pathogens that had a prevalence of detection above 10% across all tissues (*Flavobacterium psychrophilum* and *Kudoa thyrsites*). When comparing if the prevalence varied between tissues types, *Ichthyophthirius multifiliis* was not statistically more prevalent in any tissue, while *Flavobacterium psychrophilum* was more prevalent in the body compared

to gill and mucus, (21% vs. 4% and 7% respectively). The majority of tissue samples had pathogen prevalence below 10%.

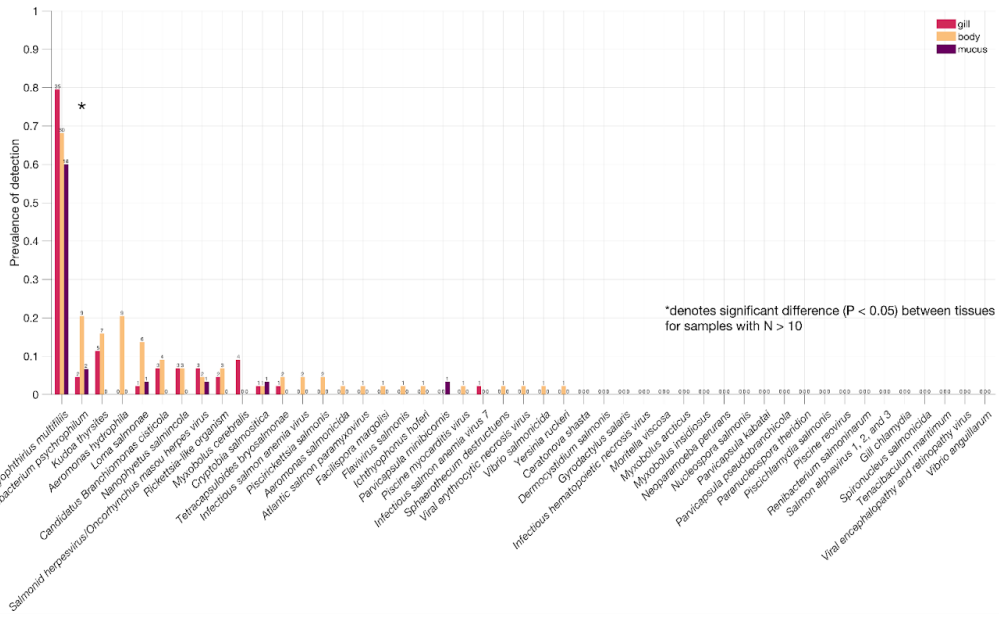

Figure 5.8. **Comparative Prevalence of Pathogens Across Tissues from Sentinels on the McCloud River.** Bars represent the frequency of detection for 47 pathogens across three tissues (gill, body, mucus) at the AhDiNa site. Asterisks (*) denote statistically significant differences ($P < 0.05$) between sites for pathogens with $N > 10$. Numbers above bars represent the number of positive samples.

To further explore differences in pathogens across tissues, pathogen abundance (Log_{10} Copy# ng^{-1}) for all three tissues types (gill, body, and mucus) in 2023 and 2024 are summarized in Figure 5.9. The abundance is shown as a heatmap, where individually sampled fish are shown on the x-axis and pathogens on the y-axis. Visually, Figure 5.9 shows that some pathogens are consistently detected at greater abundances (i.e., cells that are darkblue) over time at both sites, such as *Ichthyophthirius multifiliis*, while other pathogens are detected are lower abundances (i.e., cells that are light blue), such as *Kudoa thyrsites.* As with water samples, however, note that when comparing abundance data, it is most appropriate to compare similar pathogen types, such as parasites, to each other as parasites that are multicellular are expected to inherently have a great DNA abundance compared to unicellular bacteria. Additionally, even different parasites have different sizes and so a single *Ichthyophthirius multifiliis* would have a different abundance compared to a single *Kudoa thyrsites.* Therefore, hereafter, our statistical analysis is based on comparing the trends for the same species of pathogens.

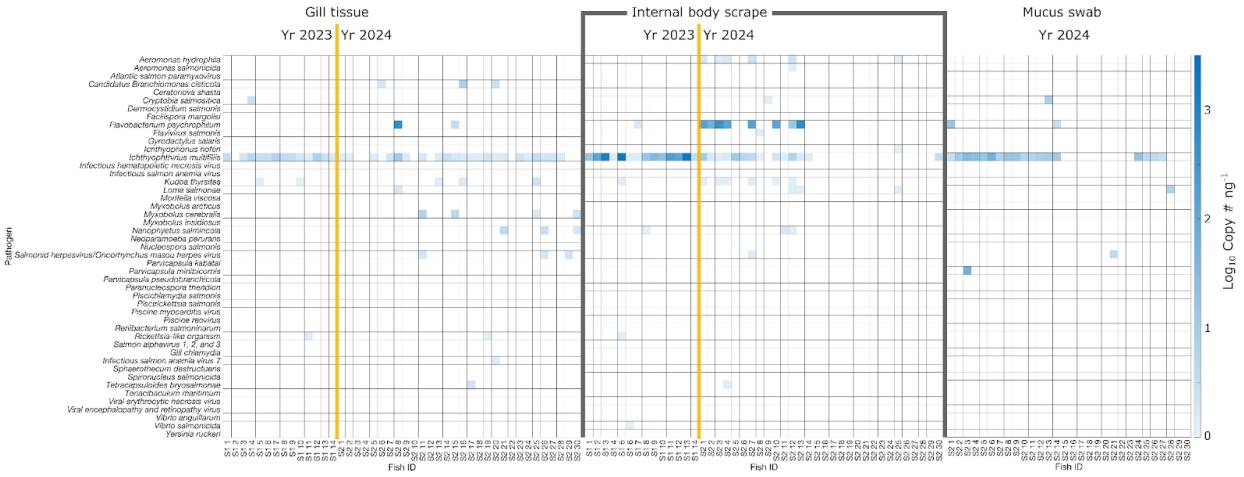

Figure 5.9. **Spatiotemporal Distribution and Relative Abundance of Pathogens in the McCloud River Sentinel Samples.** Heat map illustrating the detection and abundance of 47 pathogens in sentinel tissues of gill, body scrape, and mucus swab at the upstream AhDiNa sites across 2023 and 2024. Cell color density represents the relative abundance of pathogen genetic material, measured as Log_{10} Copy# ng^{-1}. The y-axis lists individual pathogen species, while the x-axis denotes individual fish. Pathogens such as *Ichthyophthirius multifiliis* demonstrate persistent signals across both years and tissues, whereas others show tissue or year pulses.

Isolating abundance data for gill, body, and mucus samples and displaying the distribution of abundance values is shown in Figure 5.10. To aid in visualization, box-plots are displayed when either site had more than 10 positive detection. To evaluate whether pathogen abundance varied significantly across different tissues, we compared the mean abundance (Log_{10} Copy# ng^{-1}) among the three sampled tissue types: gill, internal body scrape, and mucus swab. Because this comparison involved more than two groups, a One-Way Analysis of Variance (ANOVA) was employed to test the null hypothesis that mean pathogen abundance was equal across all tissue types. In instances where the global ANOVA model indicated a significant difference ($P < 0.05$), a Tukey's Honestly Significant Difference (HSD) post-hoc test was performed. This controlled for type I error while identifying which specific pairwise comparisons (e.g., Gill vs. Body Scrape) were statistically distinct. As with other abundance analyses, tests were only conducted for pathogens with sufficient positive detections ($n > 10$) to ensure statistical validity. When comparing abundances between tissues, *Ichthyophthirius multifiliis* was detected as a greater level in body and mucus samples compared to gill samples, while *Flavobacterium psychrophilum* and *Aeromonas hydrophila*, were detected at a greater level in body tissue samples compared to gill and mucus. For the

rest of the pathogens, the data is dominated by near-zero abundance, suggesting that these species are either absent or present below the detection limit in most samples from both sites.

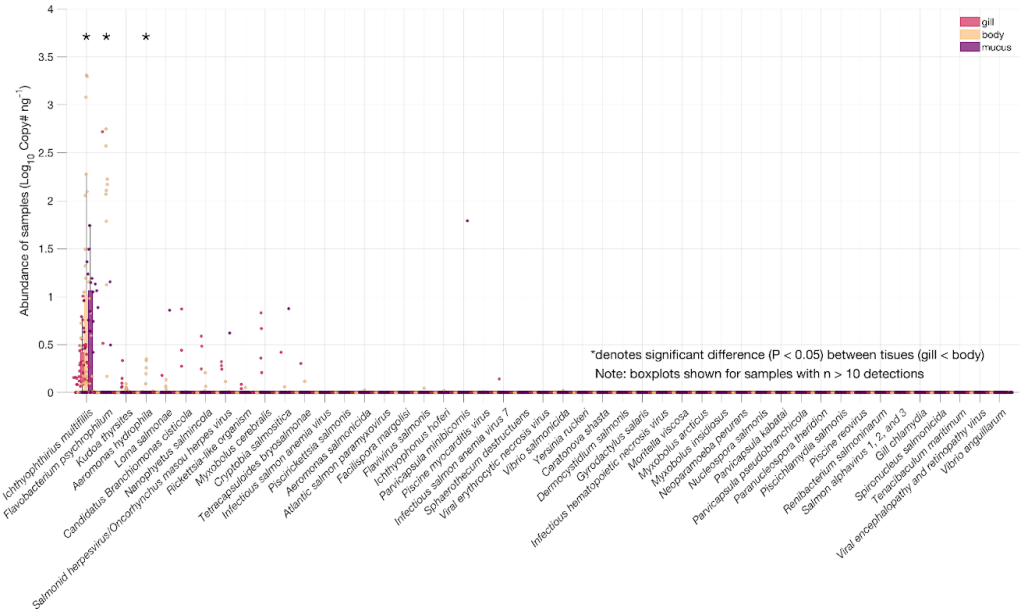

Figure 5.10. **Comparative Abundance of Pathogens in McCloud River Sentinel Samples.** Pathogen abundance is quantified as Log_{10} Copy# ng^{-1} from tissue samples (gill, body, mucus) samples collected at the upstream AhDiNa site. Individual jittered points represent the raw data for each positive detection, while boxplots summarize the distribution (median, quartiles, and range) for pathogens with n > 10 detections. Asterisks (*) denote a statistically significant difference in abundance between sites ($P < 0.05$) with an ANOVA.

As we had paired tissue samples from the same individual fish, we wanted to explore the level of agreement between tissue types and therefore assess the value of taking different tissues from our sentinel studies. For this assessment we used a Kappa test to statistically quantify the degree of agreement between pathogen detections in the gills, body, and mucus. This test allowed us to determine if the presence of a pathogen in one tissue type reliably predicted its presence in another, or if specific tissues were uniquely susceptible to certain pathogens. By evaluating whether the observed agreement exceeded what would be expected by chance alone, we could identify which tissue types provide the most comprehensive "signal" for monitoring and if sampling a single tissue (like the gill) is sufficient for a baseline assessment of fish health in the McCloud River. Overall, for the three pathogens we assessed Figure 5.11, only

Ichthyophthirius multifiliis showed slight agreement between tissues (Kappa = 0.05) with the gill tending to be the most sensitive tissue, i.e., Only two fish had positive detections of *Ichthyophthirius multifiliis* in a tissue besides the gill when the gill was observed to not have a *Ichthyophthirius multifiliis* detection. The other two pathogens assessed had systematic diss-agreement between tissues types, but also had relatively low prevalence of detection.

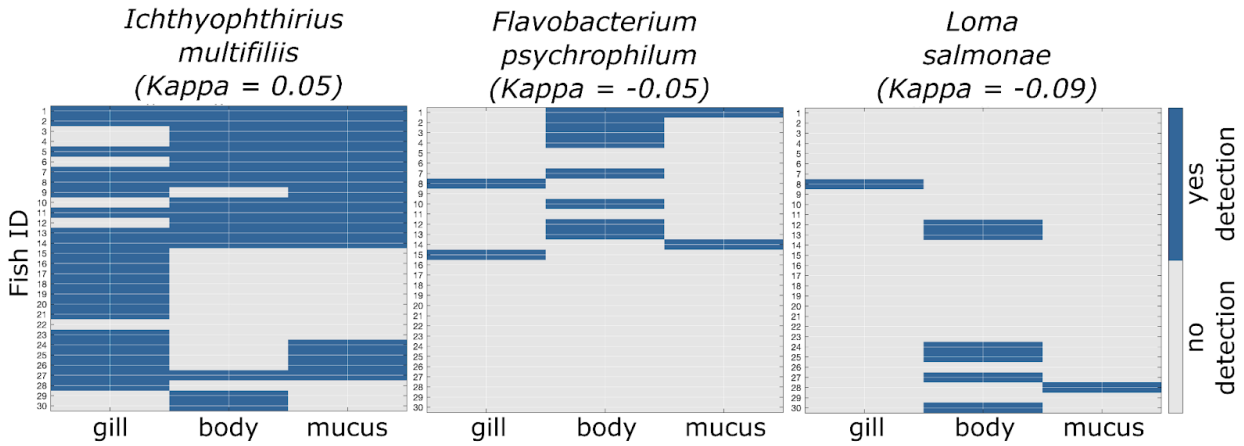

Figure 5.11. **Agreement of Pathogens in McCloud River Sentinel Samples.** Comparison of detection results for *Ichthyophthirius multifiliis*, *Flavobacterium psychrophilum*, and *Loma salmonae* across paired gill, body, and mucus samples (x-axis) for each individual fish (y-axis). IndThe Kappa coefficient (Kappa) quantifies the level of agreement beyond what would be expected by chance. Values for each pathogen are provided within the panels. Agreement is interpreted according to benchmarks: <0.20 (Slight), 0.21–0.40 (Fair), 0.41–0.60 (Moderate), 0.61–0.80 (Substantial), and >0.81 (Almost Perfect).

In addition to comparing agreement between tissue types, we wanted to assess any differences in detection across years. For this assessment we focused on comparing differences is *Ichthyophthirius multifiliis* across years and compared differences in the abundance (Log_{10} Copy# ng^{-1} using t-Test) as well as the prevalence of detection (% using a χ^2). Figure 5.12 below shows the results when comparing the two tissues (gill and body) types collected in both 2023 and 2024. In both gill and body tissues, there was a significantly higher abundance in 2023 compared to 2024. With regards to prevalence of detection, there was also a significantly higher prevalence in 2023 compared to 2024 in body tissues samples and a nearly significant (P = 0.135) higher prevalence in gill tissues. Overall, fish in 2023 appeared to have higher abundance and prevalence of *Ichthyophthirius multifiliis.*

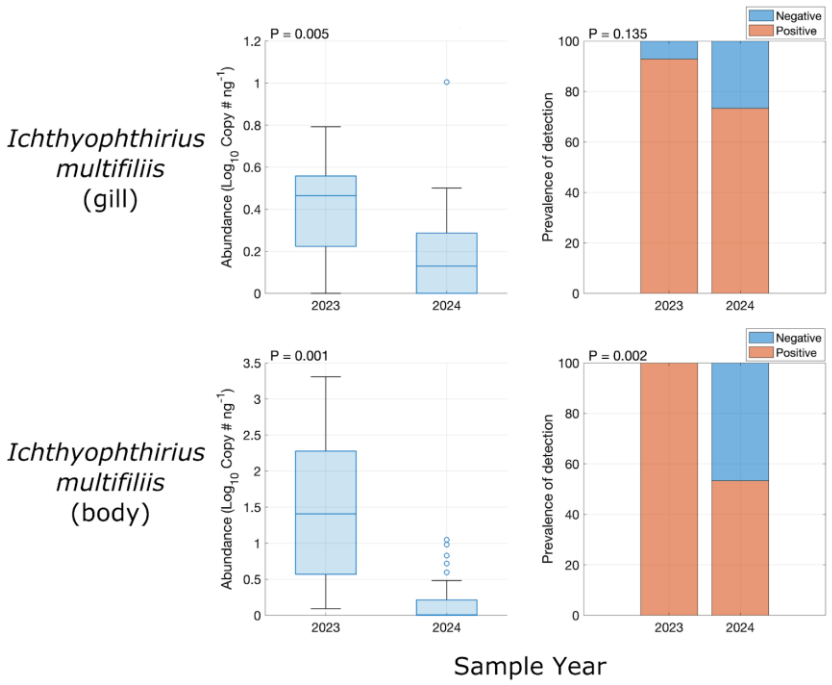

Figure 5.12. **Comparison of Abundance and Prevalence of *Ichthyophthirius multifiliis* by Year in McCloud River Sentinel Samples.** Comparison of the abundance (Log_{10} Copy# ng^{-1}) and prevalence of detection results for *Ichthyophthirius multifiliis* across 2023 and 2024 in two tissue types (gill and body). For each tissue, the abundance comparison is shown as a boxplot with year on the x-axis and abundance on the y-axis, while prevalence comparison is shown as a bar with year on the x-axis and prevalence on the y-axis. Results from statistical tests comparing differences between years are displayed as P-values for t-test and χ^2.

Hook-Line Studies

Hook-line sampling occurred 2024 with a focus on quantifying the prevalence and abundance of pathogens present in Rainbow and Brown Trout that would complement the sentinel studies of Chinook. Specifically, the hook-line studies involved targeting species that have similar susceptibility to many of the same pathogens as Chinook (i.e, Trout), but that have been in the system for a longer period of time and therefore represent a different exposure history. For example, while sentinel studies are useful in that you can control when and where fish are exposed, holding fish for long periods of time is often unfeasible. Therefore sentinel studies may represent more acute risk associated with pathogen exposure. To assess more chronic risks, we relied on sampling free-roaming fish in the system. In our studies, our primary outcome of interest was the detection of pathogens in fish tissues. Similar to water and sentinel samples, hook-line samples were screened using molecular methods that detect both the

presence (yes/no outcome) and abundance (quantitative outcome) of pathogen DNA and/or RNA.

In 2024, Rainbow and Brown Trout were captured in coordination Task 7 - Predation Risk. Specifically, anglers used hook-line methods to target these species to assess predation risk of Chinook. A sub-sample of fish collected for Task 7 were used for pathogen analysis. Specifically, this result shown here, gill and intestine tissues were collected for pathogen screening. Hook-line sampling occurred at the upstream site of AhDiNa and near the downstream of Bollibokka in October. Following collection, tissues were placed in separate 2 mL centrifuge tubes containing RNALater (QIAGEN Sciences, Germantown, MD, U.S.A.). Tissues were held at -80°C until DNA/RNA extraction and qPCR analysis using established protocols (Miller et al. 2016).

Overall, a total of 48 tissue samples were screened. Of those, 91% (44/48) were positive for at least one pathogen. The distribution of the number of different pathogens detected in a tissue sample is shown in Table 5.4 and ranged from zero to as many as six pathogens detected in a single tissue sample. Prevalence of detection for each of the 47 pathogens screened for across all sites and separated by pathogen type (i.e. bacteria, parasite, virus, and fluke) are summarized in Figure 5.13. Similar to water and sentinel samples, we are using a prevalence threshold of 10% to separate pathogens that are considered to be common (>= 10%) or rare (<10%). By pathogen type, one bacterial pathogen, one parasite, and one virus had a prevalence of above 10%, while the prevalence of the fluke was 0%. *Candidatus Branchiomonas cisticola* was the most prevalent bacterial pathogen (29%), *Ichthyophthirius multifiliis* was the most prevalent parasite (27%), and *Piscine myocarditis virus* was the most prevalent virus at 67%.

Table 5.4. Frequency of different pathogens detected in tissue samples from hook-line samples.

Tissue type	Pathogen count	0	1	2	3	4	5	6
gill	**number of samples**	1	4	9	6	2	1	1
gill	**percent**	4.17	16.67	37.50	25.00	8.33	4.17	4.17
intestine	**number of samples**	3	9	4	7	0	1	
intestine	**percent**	12.50	37.50	16.67	29.17	0.00	4.17	
all	**number of samples**	4	13	13	13	2	2	1

all	**percent**	8.33	27.08	27.08	27.08	4.17	4.17	2.08

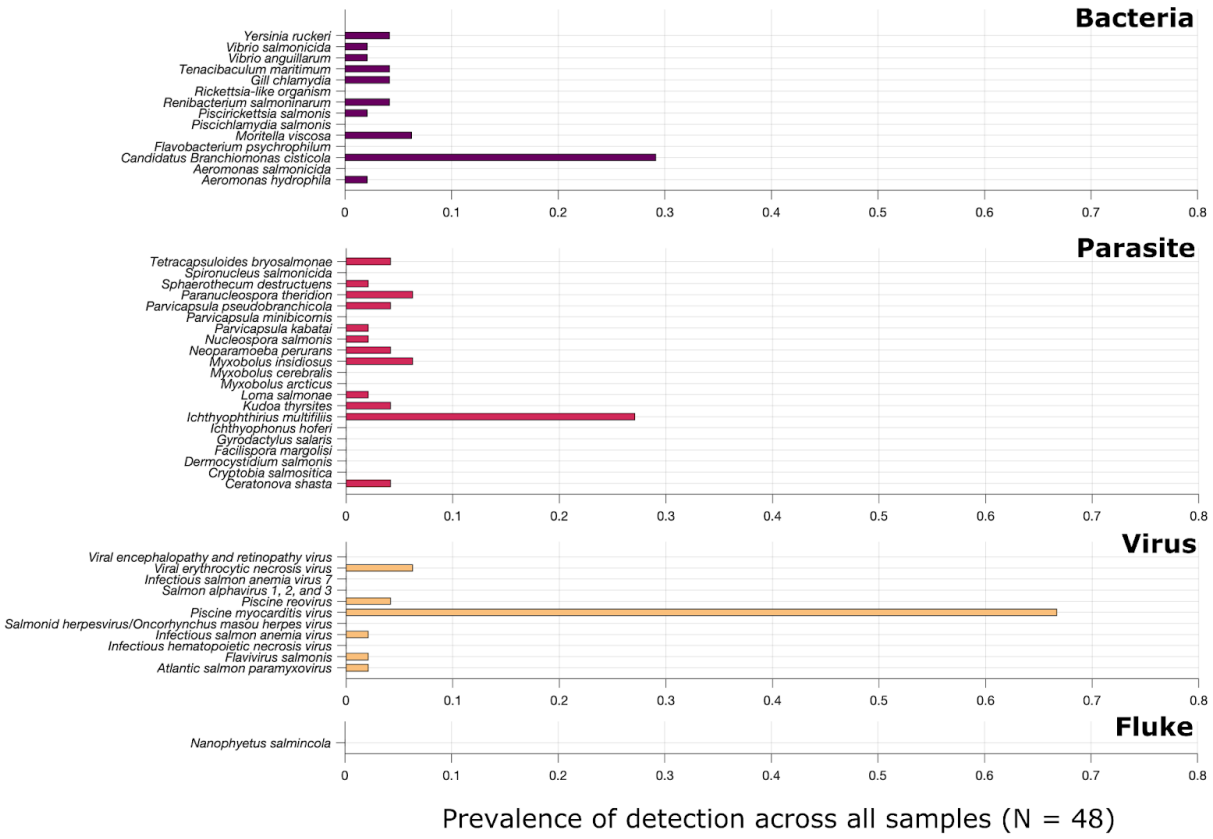

Figure 5.13. **Pathogen Detection Frequency in McCloud River Hook-Line Samples.** Distribution of prevalence across four taxonomic groups (Bacteria, Parasite, Virus, and Fluke) screening for 47 total targets. Data represents the detection frequency (n/N) where N = 48. High prevalence was observed for *Piscine myocarditis virus* (>60%).

Comparing prevalence across the two tissue types (gill and intestine), we see a similar pattern of prevalence of detection across tissues as shown in Figure 5.14. Specifically, *Piscine myocarditis virus* was frequently detected in both tissue types and at a much greater level than all other pathogens. When comparing if the prevalence (χ^2) varied between tissues types, *Candidatus Branchiomonas cisticola* was statistically more prevalent in the gill compared to the intestine. The majority of tissue samples had pathogen prevalence below 10%.

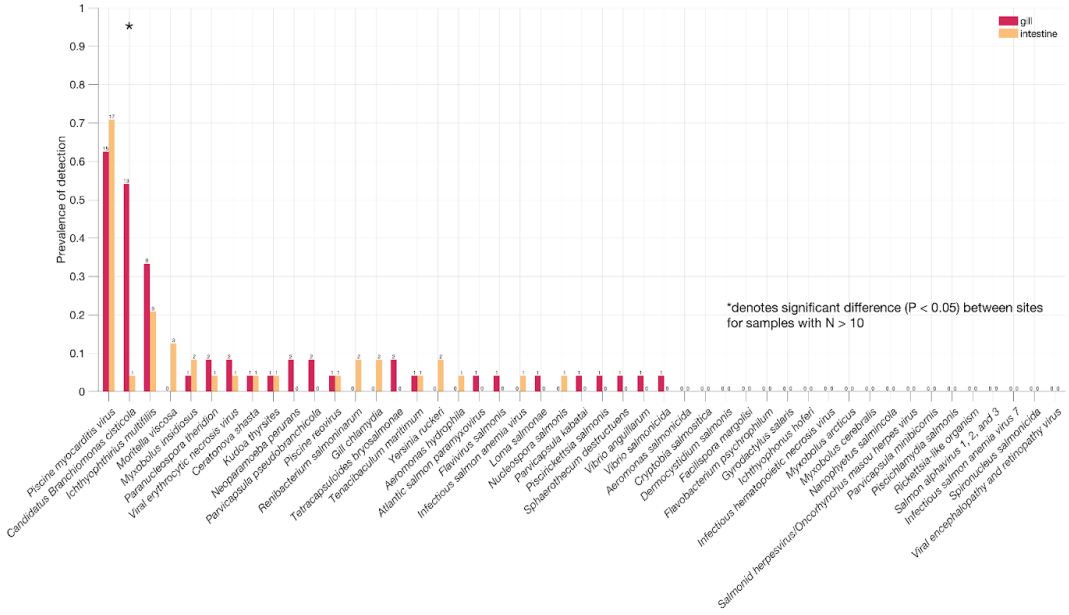

Figure 5.14. **Comparative Prevalence of Pathogens Across Tissues from Hook-Line Samples on the McCloud River.** bars represent the frequency of detection for 47 pathogens across two tissues (gill and intestine). Asterisks (*) denote statistically significant differences ($P < 0.05$; χ^2) between sites for pathogens with N > 10. Numbers above bars represent the number of positive samples.

To further explore differences in pathogens across tissues, pathogen abundance (Log_{10} Copy# ng^{-1}) for both tissues types (gill and intestine) 2024 are summarized in Figure 5.15. The abundance is shown as a heatmap, where individually sampled fish are shown on the x-axis and pathogens on the y-axis. Visually, Figure 5.15 shows that some pathogens are consistently detected at greater abundances (i.e., cells that are darkblue) over time at both sites, such as *Candidatus Branchiomonas cisticola*, while other pathogens are detected are lower abundances (i.e., cells that are light blue), such as *Piscine myocarditis virus.* As with water samples and sentinel samples, however, note that when comparing abundance data, it is most appropriate to compare similar pathogen types, such as parasites, to each other as parasites that are multicellular are expected to inherently have a great DNA abundance compared to unicellular bacteria. Therefore, hereafter, our statistical analysis is based on comparing the trends for the same species of pathogens.

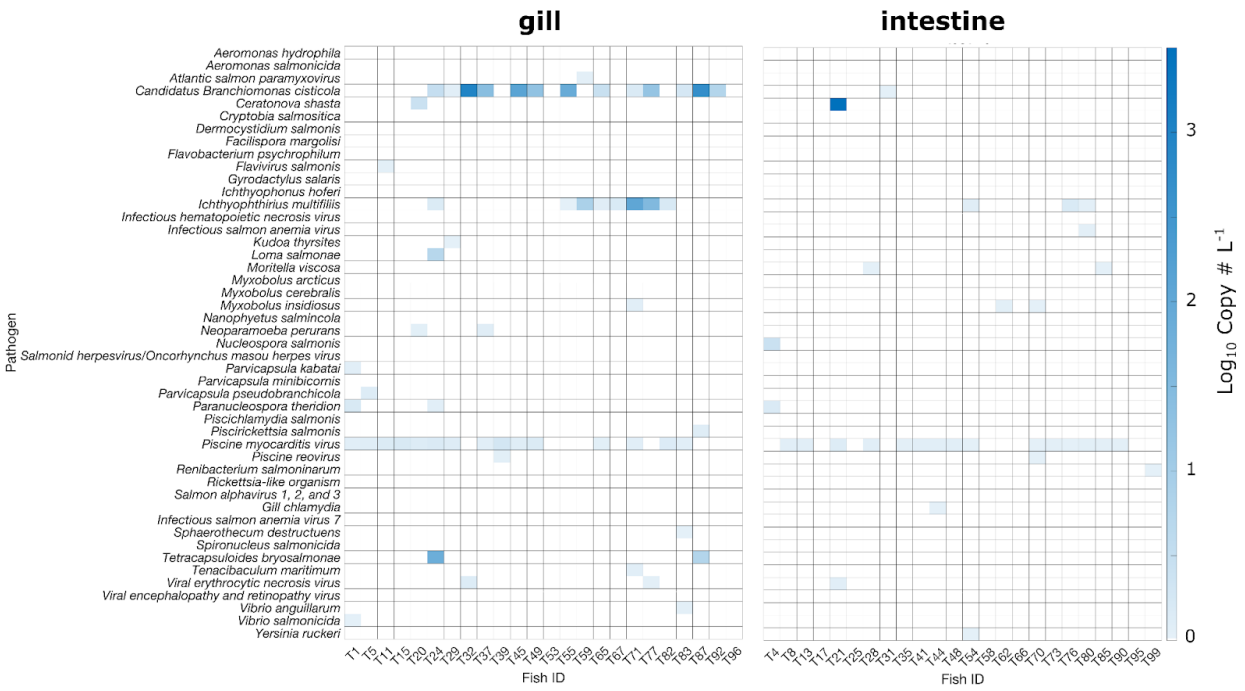

Figure 5.15. **Spatiotemporal Distribution and Relative Abundance of Pathogens in the McCloud River Hook-Line Samples.** Heat map illustrating the detection and abundance of 47 pathogens in Rainbow and Brown Trout tissues of gill and intestine in 2024. Cell color density represents the relative abundance of pathogen genetic material, measured as Log_{10} Copy# ng^{-1}. The y-axis lists individual pathogen species, while the x-axis denotes individual fish. Pathogens such as *Piscine myocarditis virus* demonstrate persistent signals across both tissues, whereas others show tissue or year pulses.

Isolating abundance data for gill and intestine samples and displaying the distribution of abundance values is shown in Figure 5.16. To aid in visualization, box-plots are displayed when either site had more than 10 positive detection. When comparing abundances between tissues (t-Test), no pathogen was detected as a greater level in gill or intestine samples. The majority of pathogens were dominated by near-zero abundance, suggesting that these species are either absent or present below the detection limit in most samples from both sites.

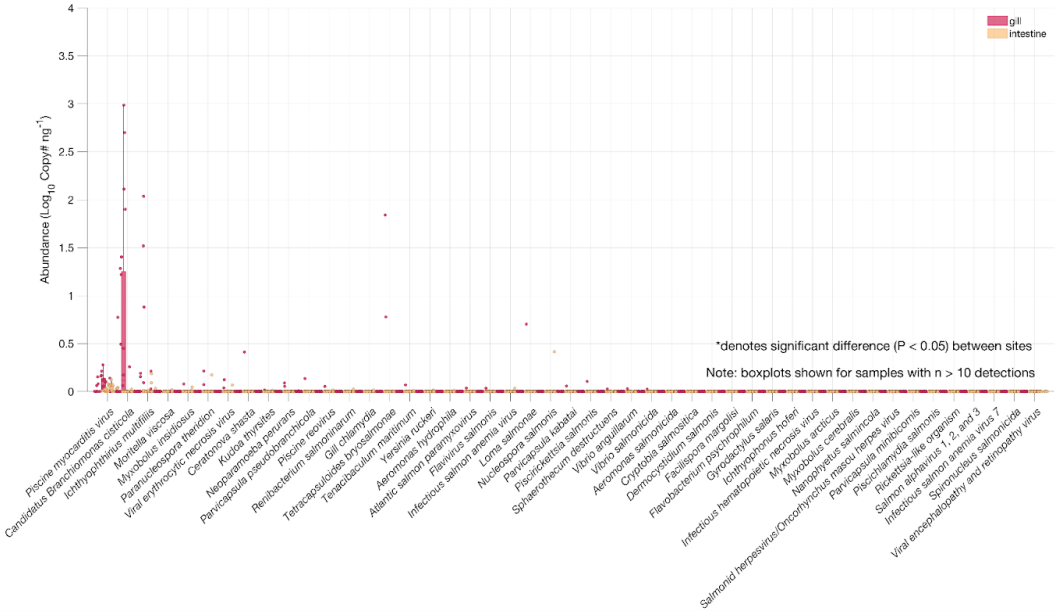

Figure 5.16. **Comparative Abundance of Pathogens in McCloud River Hook-Line Samples.** Pathogen abundance is quantified as Log_{10} Copy# ng^{-1} from tissue samples (gill and intestine). Individual jittered points represent the raw data for each positive detection, while boxplots summarize the distribution (median, quartiles, and range) for pathogens with n > 10 detections. Asterisks (*) denote a statistically significant difference in abundance between sites ($P < 0.05$) using a t-Test.

Discussion

The central objective of this task was to develop a baseline and shared understanding of how pathogens relate to the reintroduction potential of winter-run Chinook salmon on the McCloud River. To achieve this, we employed a multi-faceted monitoring approach that combined environmental surveillance with biological tissue screening across two years (2023–2024). This integrated strategy included the routine screening of environmental water samples to map pathogen distribution and abundance, sentinel exposure studies to quantify acute infection risks in juvenile salmon, and hook-line sampling of wild trout to identify chronic pathogen reservoirs within the resident fish community. By combining these distinct lines of evidence, we were able to move beyond simple detection to a more holistic understanding of what pathogens are in the environment as well as in fish. The following discussion synthesizes these findings to characterize the current pathogen landscape, identify primary disease risks, and evaluate the implications for the health and resilience of reintroduced salmon populations.

Synthesis of Key Findings

High Pathogen Diversity and Cumulative Exposure

The McCloud River environment contains a diverse array of salmonid pathogens, presenting a complex exposure landscape. Exposure risk, as assessed by prevalence, was generally high across the system, with 88% of water samples and 81% of sentinel tissue samples testing positive for at least one pathogen. Furthermore, reintroduced salmon are likely to face cumulative stressors; 45% of water samples contained three or more distinct pathogens, and single sentinel fish tissues contained up to seven different pathogens. While bacteria and parasites were the most commonly detected taxonomic groups, viral prevalence in environmental samples remained low (<5%), except in the case of hook-line samples where the prevalence of *Piscine myocarditis virus was* >60%.

Primary Pathogens of Concern

Out of 47 screened pathogens, five consistently appeared at the upper end of both prevalence and abundance scales, representing higher risk:

- ***Ichthyophthirius multifiliis*:** This parasite is the dominant in the system. It was the most prevalent pathogen in water (57%) and sentinel tissues (71%) .
- ***Rickettsia-like organisms* (RLO) and *Piscirickettsia salmonis*:** These bacteria demonstrated persistent, high-abundance signals in environmental water analysis.
- ***Yersinia ruckeri* and *Dermocystidium salmonis*:** These pathogens showed significant prevalence, particularly in downstream reaches.
- ***Piscine myocarditis virus:*** This pathogen was the most common detected in hook-line samples.

Analysis confirmed a non-linear positive relationship ($R^2 = 0.92$) between prevalence and abundance for these pathogens, indicating that as they become more frequent in the environment, the infectious pressure (dose) likely increases.

Spatiotemporal Variability in Risk

Exposure risk is not uniform across the river or across time. *Ichthyophthirius multifiliis* was statistically more prevalent at the upstream AhDiNa site (82%) compared to the downstream Bollibokka site (50%). Conversely, Yersinia ruckeri (89%) and Dermocystidium salmonis (89%) posed significantly greater risks at the downstream Bollibokka site. Across time, we observed significant inter-annual variation; sentinel fish in 2023 exhibited significantly higher abundance and prevalence of *Ichthyophthirius multifiliis* compared to 2024, suggesting that reintroduction success may vary based on

annual environmental conditions. General Additive Models (GAMs) further identified clear seasonal signals, with "Day of Year" explaining up to 56% of the variance in abundance for pathogens like *Dermocystidium salmonis*.

Hidden Reservoirs and Chronic Risk

The study highlights a critical distinction between "acute" exposure (measured by sentinels) and "chronic" exposure (measured by wild trout). While sentinel studies successfully identified immediate threats like *Ichthyophthirius multifiliis* and *Flavobacterium psychrophilum*, they missed other pathogens. Most notably, *Piscine myocarditis virus* was detected in 67% of wild Rainbow and Brown Trout tissues but was rare (<1%) in water samples and sentinel fish. This identifies the benefit of taking different types of samples (i.e., environmental water and fish tissues).

Implications of Tissue Specificity

Our evaluation of tissue agreement emphasizes that relying on a single tissue type for health screening is insufficient. Agreement between tissues was generally poor (Kappa < 0.20). While gill tissue was generally sensitive for *Ichthyophthirius multifiliis*, *Flavobacterium psychrophilum* was significantly more prevalent in internal body scrapes (21%) compared to gills (4%). Similarly, in wild trout, *Candidatus Branchiomonas cisticola* showed specific preferences for gill tissue over the intestine.

Limitations of Molecular Monitoring for Inferring Disease Risk

While molecular (PCR-based) screening provides a sensitive and high-throughput method for mapping pathogen distribution, it is important to acknowledge specific limitations when using these data to infer actual disease risk:

- **Detection of Genetic Material vs. Viable Pathogens:**
  PCR assays detect the presence and abundance of specific DNA or RNA sequences, which indicates the presence of the pathogen's genetic material but not necessarily viable or infectious organisms. Unlike culture or histology-based approaches, which confirm the presence of live "culturable" pathogens and active disease states (pathology), PCR can yield positive detections from non-viable organisms or just DNA persisting in the environment. Therefore, high environmental DNA (eDNA) copy numbers represent a potential for exposure rather than a confirmed rate of infectivity.
- **Challenges in Comparing Abundance Across Taxa:**
  Quantitative comparisons of pathogen abundance (Log10 Copy#) are confounded by biological differences between target organisms. Multicellular parasites, such as *Ichthyophthirius multifiliis*, inherently possess significantly greater genomic mass per individual compared to unicellular bacteria. Consequently, a single parasite may generate a much higher abundance signal

than a bacterium, making direct abundance comparisons across different pathogen types inappropriate. Abundance trends are most valid when comparing the same pathogen species over space and time as done in this report.

- **Resolution of Tissue Sampling:**
  In sentinel studies, physical constraints limited the resolution of internal tissue screening. Due to the small size of juvenile sentinel fish, specific organs such as the kidney, spleen, and intestine could not always be isolated individually and were instead pooled into a generic "internal body scrape". While this maximizes the likelihood of detection, it obscures organ-specific infection dynamics that might otherwise reveal the specific progression of a disease within the host.
- **Differentiating Infection from Surface Contamination:**
  For external samples, such as mucus swabs or gill clips, a positive PCR result indicates the pathogen is present on the fish but does not definitively prove that the pathogen has breached the host's physical barriers to cause an internal infection. This distinction is critical for pathogens like *Ichthyophthirius multifiliis*, which first target the mucus, versus systemic pathogens that require internal invasion to cause disease.
- **Detection Limits and Screening Scope:**
  Finally, it is important to interpret negative results with caution. The absence of a positive PCR detection does not definitively prove that a pathogen is entirely absent from the ecosystem; rather, it indicates that the pathogen's genetic material was not present above the assay's limit of detection within the specific volume of water or tissue analyzed. Pathogens may exhibit patchy distributions or exist at low densities that may fall below analytical thresholds. Furthermore, our monitoring was restricted to a targeted panel of 47 specific salmonid pathogens. Consequently, other disease-causing organisms, including novel viruses, unscreened bacteria, or emerging parasites not included in our specific assay design, may currently exist in the McCloud River but remain undetected by this study. Therefore, the results presented here should be viewed as a comprehensive baseline of *known* risks, rather than an exhaustive inventory of every biological agent present in the watershed.

Management Recommendations

Based on these findings, we propose the following recommendations to support the reintroduction of winter-run Chinook salmon:

1. **Commit to Long-Term Surveillance of Host-Pathogen-Environment Interactions:**
   Pathogen dynamics are not static; they fluctuate based on the complex interplay between the host, the pathogen, and the environmental conditions. This study has already demonstrated significant inter-annual variability, such as the sharp

decline in *Ichthyophthirius multifiliis* abundance and prevalence from 2023 to 2024. Furthermore, the act of reintroduction itself introduces new host densities that may fundamentally alter existing pathogen distributions and prevalence in the river. Therefore, continued monitoring is essential not merely to confirm current baselines, but to detect emerging shifts in disease risk as these ecological components—host density, environmental variability, and pathogen evolution—continue to interact and evolve over time.

2. **Maintain Multi-Method and Multi-Tissue Surveillance:**
   Future monitoring should retain the integrated approach of combining environmental water sampling with biological tissue screening, as water sampling maps distribution while tissue sampling captures infection dynamics. Crucially, sampling protocols would benefit from including multiple tissue types when sampling fish. Relying solely on gill tissue would have missed significant bacterial infections (e.g., *Flavobacterium psychrophilum*) in this study.
3. **Establish Quantitative Action Thresholds:**
   The strong correlation ($R^2 = 0.92$) between pathogen prevalence and genetic abundance allows for the development of quantitative warning thresholds. Rapid increases in DNA abundance (Log_{10} Copy L^{-1}) for high-risk pathogens like Ich could serve as a leading indicator, triggering adaptive management actions, such as altering flow regimes, before clinical disease outbreaks occur.

Ecological Context and Disease Causality

Finally, it is critical to contextualize these findings by recognizing that pathogens are inherent components of all natural aquatic ecosystems. The detection of various parasites, bacteria, and viruses is not inherently negative; rather, the complete absence of such organisms would be an ecological anomaly. The goal of this monitoring was not to observe a sterile environment, but to identify when natural background levels shift into states of high infectious pressure that exceed the ability of fish to mount an immune response and either defeat an infection or recover from a disease. Consequently, while this study has successfully mapped the presence and distribution of pathogens, further work is needed to definitively link these molecular detections to specific impacts on fish health. Moving forward, integrating molecular data with physiological assessments and histology will be key to distinguishing between benign pathogen exposure and active disease states that threaten population recovery.

References

Preece, ND, Abell SE, Grogan L, Wayne A, Skerratt LF, Van Oosterzee P, Shima AL, Daszak P, Field H, Reiss A, Berger L. 2017. A guide for ecologists: Detecting the role of disease in faunal declines and managing population recovery. Biological Conservation, 214, pp.136-146.

Pacioni C, Eden P, Reiss A, Ellis T, Knowles G, Wayne AF. 2015. Disease hazard identification and assessment associated with wildlife population declines. Ecological Management & Restoration, 16(2), pp.142-152.

Altizer S, Bartel R, Han BA. 2011. Animal migration and infectious disease risk. science, 331(6015), pp.296-302.

Chapman JM, Teffer AK, Bass AL, Hinch SG, Patterson DA, Miller KM, Cooke SJ. 2020. Handling, infectious agents and physiological condition influence survival and post-release behaviour in migratory adult coho salmon after experimental displacement. Conserv Physiol. 2020;8(1):coaa033. (doi:10.1093/conphys/coaa033)

Fujiwara M, Mohr MS, Greenberg A, Foott JS, Bartholomew JL. 2011. Effects of ceratomyxosis on population dynamics of Klamath fall-run Chinook salmon. Transactions of the American Fisheries Society 140:1380 –1391.

Foott JS, Stone R, Voss S, Nichols K. 2017. Ceratonova shasta and Parvicapsula minibicornis (Phylum Cnidaria: Myxosporea) infectivity for juvenile Chinook salmon (Oncorhynchus tshawytscha) in the upper Sacramento River: July–November 2016. Anderson (CA): US Fish and Wildlife Service California–Nevada Fish Health Center.

Miller, K.M., Gardner, I.A., Vanderstichel, R., Burnley, T., Schulze, A.D., Li, S., Tabata, A., Kaukinen, K.H., Ming, T.J., and N.G. Ginther. 2016. Report on the performance of the Fluidigm BioMark platform for high-throughput microbe monitoring in salmon. Fisheries and Oceans Canada, Ecosystems and Oceans Science.

Task 6: Chinook Outmigration Phenology

To assess the timing at which reintroduced Chinook salmon leave the McCloud River, particularly during periods when traps are not operating, we took advantage of emerging environmental DNA (eDNA) technologies. Chinook shed mucus, scales, and other cellular material into the water, and these particles contain DNA that can persist in the environment for approximately 24 hours. By collecting and filtering water, we can detect the presence or absence of Chinook and infer when and where fish have recently occupied different parts of the river. Our monitoring design combined manual, hand-collected samples to achieve high spatial resolution with automated sampling using MBARI “robot” autosamplers to obtain fine temporal resolution. Field collections were transferred to UCD for extraction of DNA from the Segarra Lab, then sent to the Baetscher Lab at NOAA in Alaska for qPCR amplification of Chinook DNA. Across the 3 years of the project, we iteratively calibrated, tested, and refined these methods, learning from each year’s results. Overall, we collected 743 hand samples over 300 sampling events (Figure 6.1), resulting in ~630 DNA and RNA extractions to date. The dataset accompanying this report includes metadata for each eDNA sample, including collection date, site, and extraction status. In addition, 132 ESP samples were collected in 2024 from a single autosampler at Bollibokka for outmigration detection, followed by 132 ESP samples from Bollibokka in 2025 and another 132 ESP samples from an autosampler at The Nature Conservancy (TNC) preserve, providing high-resolution records of Chinook movement further upstream. Ultimately, by examining year-round Chinook presence and expanding our sampling footprint, we began to delineate both the timing of outmigration and how reintroduced fish use habitats throughout the watershed.

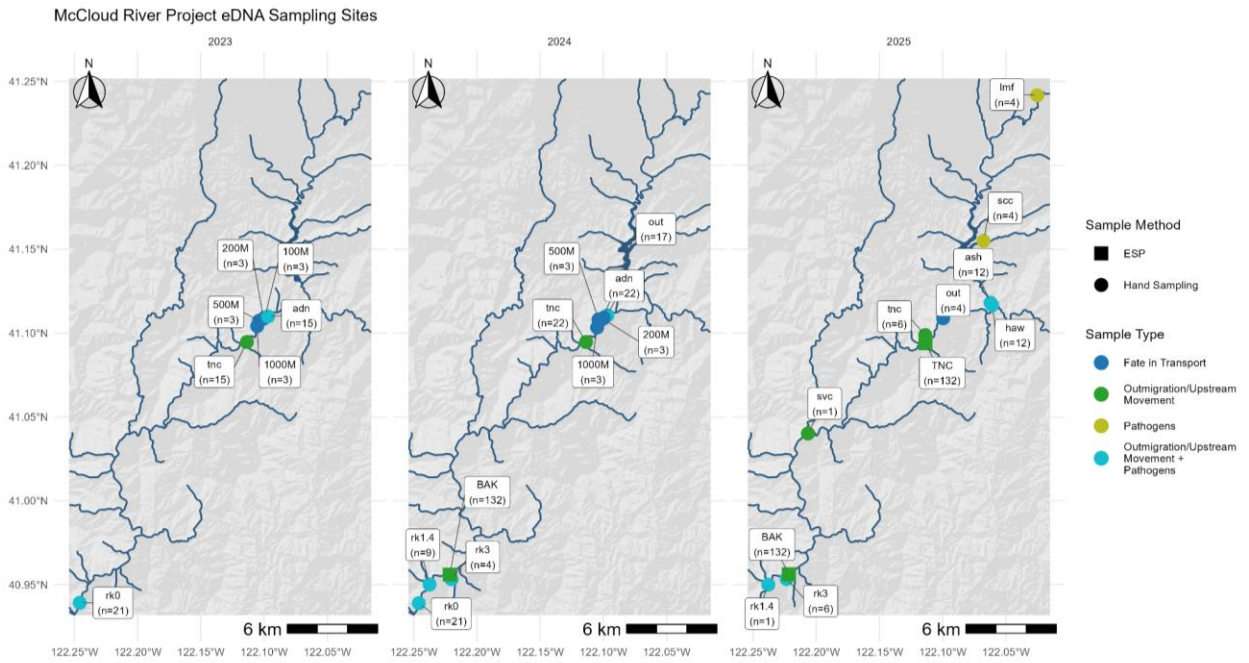

Figure 6.1. Summary map of eDNA sample collection sites on the McCloud River for 2023-2025. Samples are categorized by collection method (“ESP” for autosampler and “Hand Sampling”) and type. Some samples were collected for multiple purposes. Sites are labelled and the number of sampling events (i.e., dates) are summarized.

Fate in Transport

A key early step was to understand how far Chinook eDNA can be detected downstream, building on work such as a study by Spence et al. (2021) on detection of coho salmon in a coastal California stream. To establish a McCloud-specific baseline for eDNA transport and decay, we performed Fate-in-Transport experiments in which we used the high densities of Chinook at the Nur Nature Base as a source and sampled progressively downstream. While experiments initiated in 2023 could not be fully analyzed due to extraction challenges, 2024 sampling revealed that Chinook eDNA was no longer detectable approximately 200 m downstream of the outflow (Figure 6.2). Detections were highest at the outflow of the Nur Nature Base, where there was a high density of eggs and alevins (maximum ~60,000), but these detections dropped off at 200 m. Further downstream at 500 m and 1000 m detections were more variable, likely due to the presence of yearlings. The samples taken before egg delivery on 6/25/2024 also show many positive detections at 200 m downstream, indicating the presence of yearlings in the AhDiNa area from June to July. Although these trials were not controlled laboratory experiments and were subject to variable environmental conditions and did not control for density of different life stages, they provide a practical frame of reference

for interpreting eDNA detections along the mainstem. In 2025, we revisited this question by repeatedly sampling the Nur Nature Base outflow as egg and fry densities increased, with the goal of assessing differences in eDNA signal between life stages and determining whether increases in density translate into predictable increases in eDNA concentration (results pending).

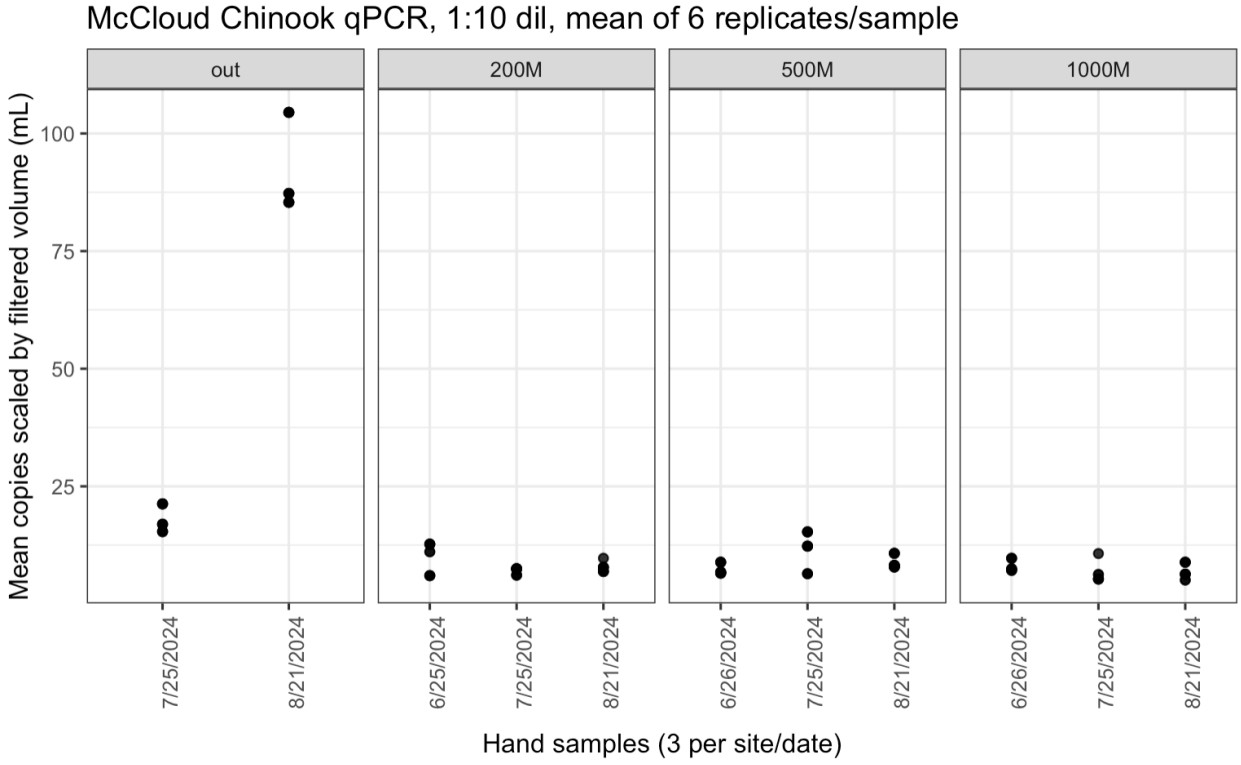

Figure 6.2. Mean copies of Chinook DNA, scaled by filtered volume, found in samples taken at the outflow of the Nur Nature Base (“out”) where eggs were incubating and hatching as of mid-July, then 200 m, 500 m, 1000 m downstream of the outflow site.

Detection of yearling presence

In 2023, our eDNA samples were collected at a limited set of mainstem sites, including AhDiNa (ADN), The Nature Conservancy preserve (TNC), and the Bollibokka area, to determine whether we could detect reintroduced Chinook presence in the river. We also extended sampling into the winter and early spring (November–March) at Bollibokka, although many of these samples were collected in the reservoir as the reservoir level rose, creating potential contamination from recreationally stocked Chinook. As a result, most winter–spring 2023 samples have not yet been analyzed. Lessons from 2023 informed a more comprehensive design in 2024. That year, we: (1) deployed a MBARI autosampler at Bollibokka to collect a March–October time series of Chinook eDNA and characterize outmigration at high temporal resolution; and (2) expanded our sampling

locations to include downstream of the rearing site (TNC), the rearing site outflow (OUT), and an upstream “control” site (ADN). While ADN was initially intended to represent a location with no Chinook, 2024 results showed clear eDNA detections upstream of the rearing site and before the delivery of eggs in July (Figure 6.3), indicating that that yearlings with extended in-river rearing were at AhDiNa, TNC, and Bollibokka. Detections at AhDiNa in the later summer period could also be fry from the Nur Nature Base leaving and moving upstream. Preliminary autosampler results for 2024 also suggest Chinook eDNA was present for most of the time series, with seasonal peaks in late spring and fall (Figure 6.4). Hand samples taken at the autosampler location in 2024 show agreement with the ESP findings (Figure 6.5), validating the ESP DNA preservation technique in this environment. These findings indicate that fish are present in the system year-round, with at least two potential outmigration peaks, and they underscore the importance of operating traps across an extended season to capture and transport fish to the ocean.

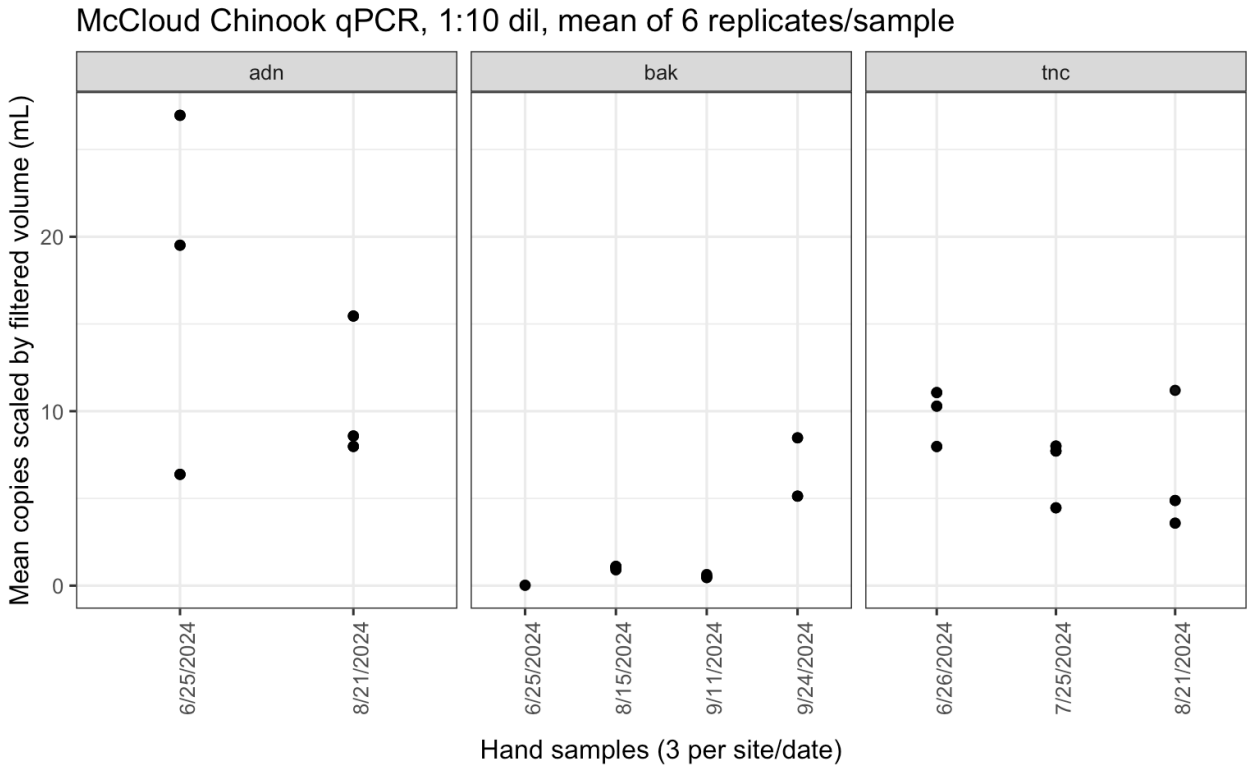

Figure 6.3. Mean copies of Chinook DNA, scaled by filtered volume, found in samples taken at various locations in the McCloud River across the summer and fall. AhDiNa (“adn”) is upstream of the streamside rearing areas. Bollibokka (“bak”) is the furthest downstream point, near McCloud Bridge and before fish enter the reservoir. The Nature Conservancy (“tnc”) is at the TNC Kerry-Landreth Preserve, downstream of AhDiNa. Eggs were not delivered at the incubation site at AhDiNa until mid-July.

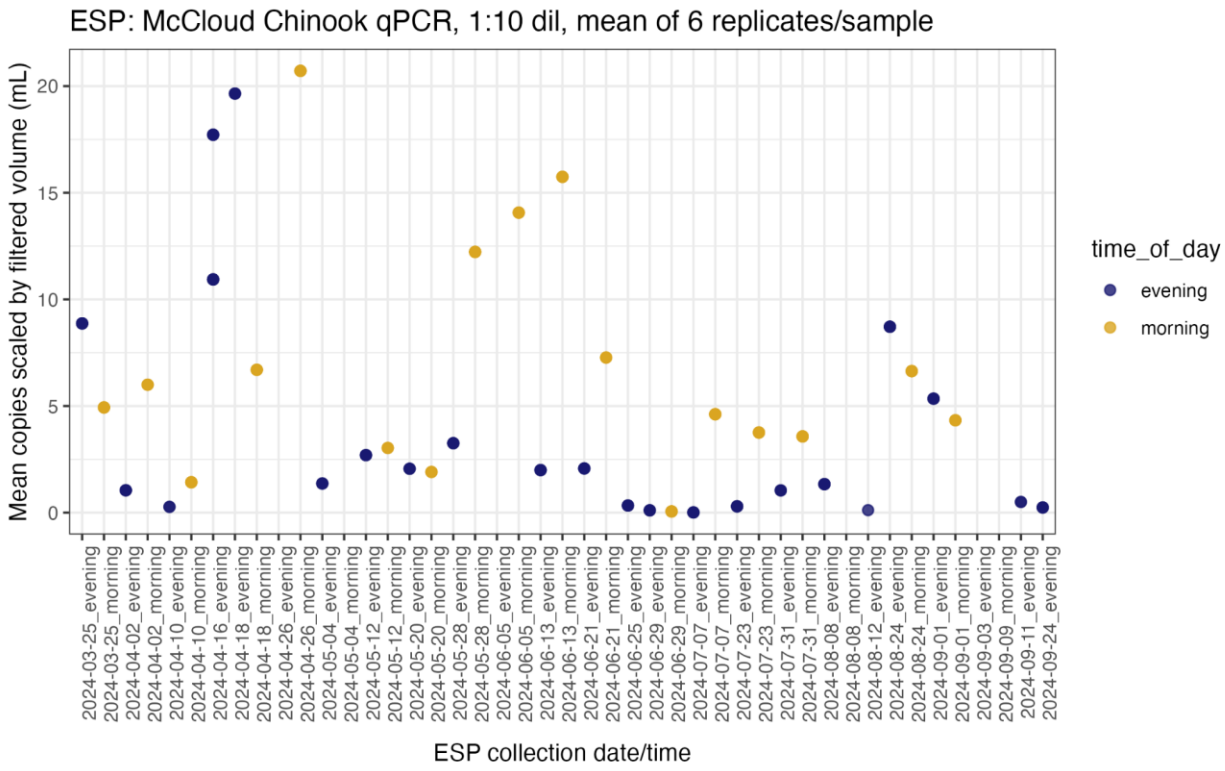

Figure 6.4. Mean copies of Chinook DNA, scaled by filtered volume, in water collected by the MBARI ESP stationed at Bollibokka. Evening represents samples collected at 8 pm, and morning is for samples collected at 8 am (local time).

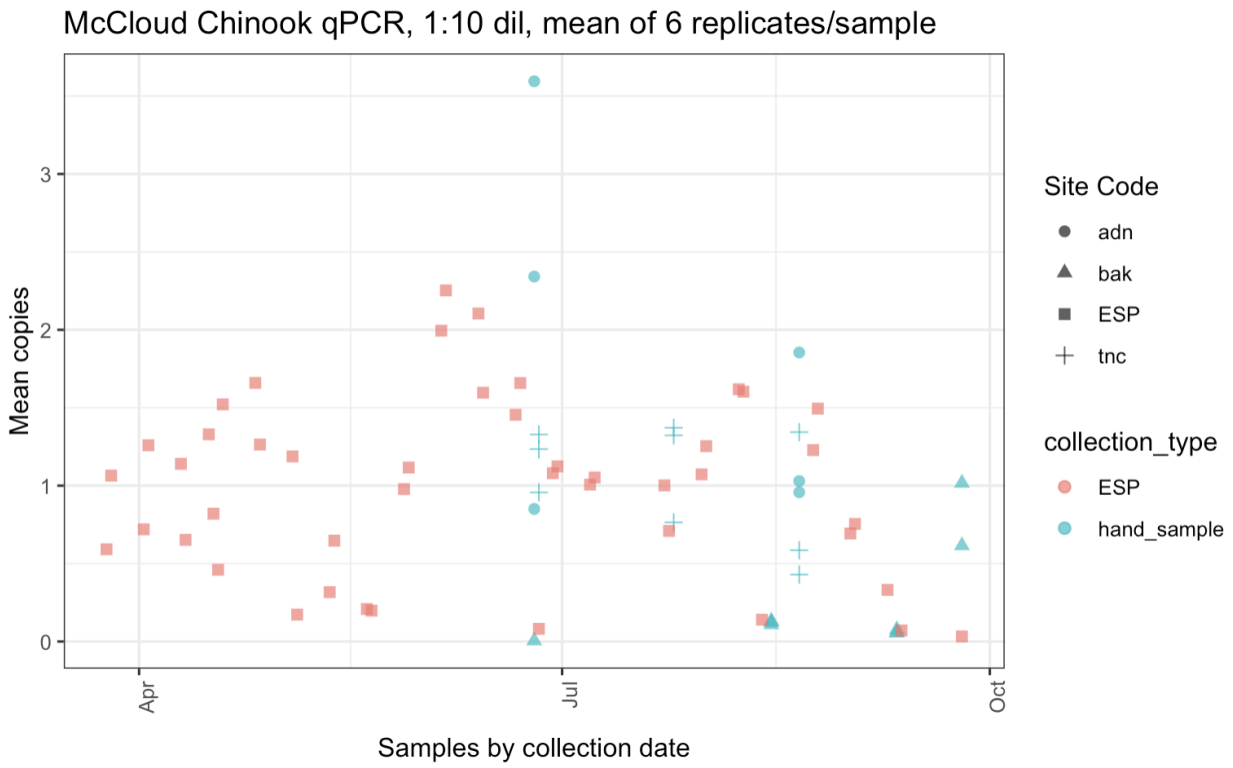

Figure 6.5. Mean copies of Chinook DNA found in autosampler samples (red) and hand samples (blue) in the 2024 field season. The blue triangles represent hand samples taken at the ESP site for cross-validation (n = 3). Note: the number of copies from qPCR are not scaled by water volume and DNA extraction volume.

Expanding understanding of upstream habitat use

We further extended our temporal coverage in 2024-2025 by collecting hand samples every two weeks at Bollibokka from November through May, during periods when the autosampler was not installed. Sampling locations were adjusted with reservoir level to ensure that samples remained in the river, thereby tracking winter and early spring outmigration while minimizing reservoir contamination. These samples are currently in the process of being analyzed. In 2025, we built on emerging patterns and ongoing conversations with Chief Sisk to further explore how far upstream fish travel and which habitats they use. Two new sites were added: one immediately below McCloud Dam at Ash Camp (ASH) and one in Hawkins Creek (HAW), a nearby tributary, with sampling from spring through October 2025. These sites, combined with the two autosamplers, provide our most comprehensive spatial and temporal coverage to date, capturing how Chinook move from the upper to lower accessible reaches. Analyses of these samples are ongoing.

From summer 2025 onward, eDNA signals are partially confounded by the return of adult salmon who remained in the river or returned from the reservoir, as we cannot distinguish between juvenile and adult Chinook DNA. Nonetheless, we can still examine peaks in eDNA concentration through time and across sites to infer periods of intense movement and tributary use. Sampling in Hawkins Creek will reveal if it is an important tributary habitat, and a single sample from Squaw Valley Creek during the spawning season was collected to test whether adults use this tributary as well. As monitoring continues and additional tributaries are incorporated, eDNA will help us understand how juveniles and adults collectively use the broader watershed.

References

Spence BC, Rundio DE, Demetras NJ, Sedoryk M. Efficacy of environmental DNA sampling to detect the occurrence of endangered coho salmon (*Oncorhynchus kisutch*) in Mediterranean-climate streams of California's central coast. *Environmental DNA*. 2021; 3: 727–744. https://doi.org/10.1002/edn3.175

Task 7: Predation Risk

Introduction

The success of the reintroduction program is dependent on the productivity and survival of juvenile salmon rearing and outmigrating from the McCloud River. If the McCloud River is a high predation risk environment for juvenile Chinook salmon, this could drastically reduce the benefits of reintroduction even if the viability of the egg life stage is improved compared to those reared on the valley floor. Little is known about the predator abundance, distribution, and consumption rates of salmon, for non-native (e.g., brown trout, spotted bass) and native (e.g. rainbow trout) predators in the McCloud River.

Over the course of late-Summer through Fall in 2023, 2024, and 2025, we employed a variety of methods to quantify the impact of predation on juvenile Chinook salmon as they rear and migrate between AhDiNa and Shasta Lake. In 2023, a pilot season, we collected stomach content samples from predators for molecular analysis to detect consumption of juvenile Chinook salmon.

We expanded these efforts in 2024, primarily in the upper McCloud near AhDiNa and the Nature Conservancy's Kerry Landreth Preserve, with limited sampling at the JSCS as well. In the upper McCloud we designated six reaches and performed a standardized hook-and-line, mark-recapture study to quantify predator abundance to extrapolate estimates of predation system-wide. In 2025 we began the field season with a hook-and-line predator sampling effort in the upper McCloud to identify year-over-year residency and movement rates. We also continued to collect predator diet samples at the McCloud Bridge and JSCS site.

Observations during 2024 suggested that predators (primarily, spotted bass and rainbow trout) were aggregating around the JSCS. In the 2025 season, we sought to better understand how this might relate to predation risk for juvenile salmon. To accomplish this, we designed and fabricated a novel version of the Predation Event Recorder (PER, Demetras et al. 2016) that was capable of sampling the shallow, fast-flowing river habitat found within the vicinity of the JSCS. These new PERs were fitted with GoPro cameras allowing us to visually confirm predation events. We deployed PERs weekly, beginning two weeks before JSCS installation and 3 weeks after JSCS installation. PERs were deployed both at the JSCS and McCloud Bridge, the latter of which we used as a "control" site (the JSCS site being the "impact" site, given that was where infrastructure to be tested was installed). This before-after control-impact (BACI)

study design allowed us to statistically evaluate the influence of the JSCS on predation risk.

Methods

Predator diet sampling

To assess potential predation on juvenile Chinook salmon in the McCloud River, predator diet samples were collected in 2023–2025. Diets were obtained via gastric lavage (Hafs et al. 2011). A low-pressure spray bottle filled with river water and fitted with a ~6-inch thin plastic nozzle was inserted into the fish's esophagus, and water was sprayed into the stomach while the fish was held slightly inverted (head down) over a 106 µm mesh sieve (Figure 7.1). Stomach contents were consolidated in the sieve and transferred to a 50 mL conical vial using a separate spray bottle containing 90% ethanol, then fully submerged in ethanol.

All tools and the sieve were disinfected with a 10% bleach solution, air-dried for at least 30 seconds, and rinsed with river water to remove residual bleach. Gastric lavage is a rapid (<1 min), typically non-lethal method; no mortality was observed. Samples were analyzed by Cramer Fish Sciences for Chinook salmon DNA using a species-specific quantitative PCR (qPCR) assay.

Figure 7.1. Gastric lavage sampling on the McCloud River. The photograph on the left shows the 2-person team processing potential predators that were captured and held in submerged hampers. The photograph on the right shows a rainbow trout being gastric lavaged over a sieve on the JSCS.

In 2023, diet sampling of potential predators took place from October 10, 2023 to December 4, 2023. A total of 45 stomach samples were collected from potential predators. Hook-and-line sampling took place in the upper McCloud River within the The Nature Conservancy's - Kerry Landreth Preserve (henceforth, "TNC"), approximately 7 river kilometers downstream from the juvenile winter-run chinook salmon reintroduction site (N=37 samples); and in the lower McCloud River near the incline plane and JSCS fish traps (N=8 samples). Additionally, stomach contents of potential predators were collected opportunistically from fish captured in the incline plane trap (IPT) in the lower McCloud River (N=18 samples). In 2023, gastric samples of all fish were sent to Cramer Fish Sciences for molecular analysis and detection of Chinook salmon DNA (N=45).

In 2024, predator diet sampling was performed in conjunction with a predator mark-recapture study (see "Predator mark recapture study" section below) from September 18, 2024 to November 8, 2024. In total, 546 potential predators were captured, of which 485 had stomach content samples collected. Hook-and-line sampling occurred in the upper McCloud River at five randomly selected 200m long sampling sites downstream of the juvenile winter-run chinook salmon reintroduction site near the AhDiNa and TNC areas (Figure 7.2; N=423 samples). Hook-and-line sampling also occurred in the lower McCloud River near the McCloud Bridge and JSCS (N=62 samples). In 2024, all gastric samples were sent to Cramer Fish Sciences for molecular analysis and detection of Chinook salmon DNA (N=481).

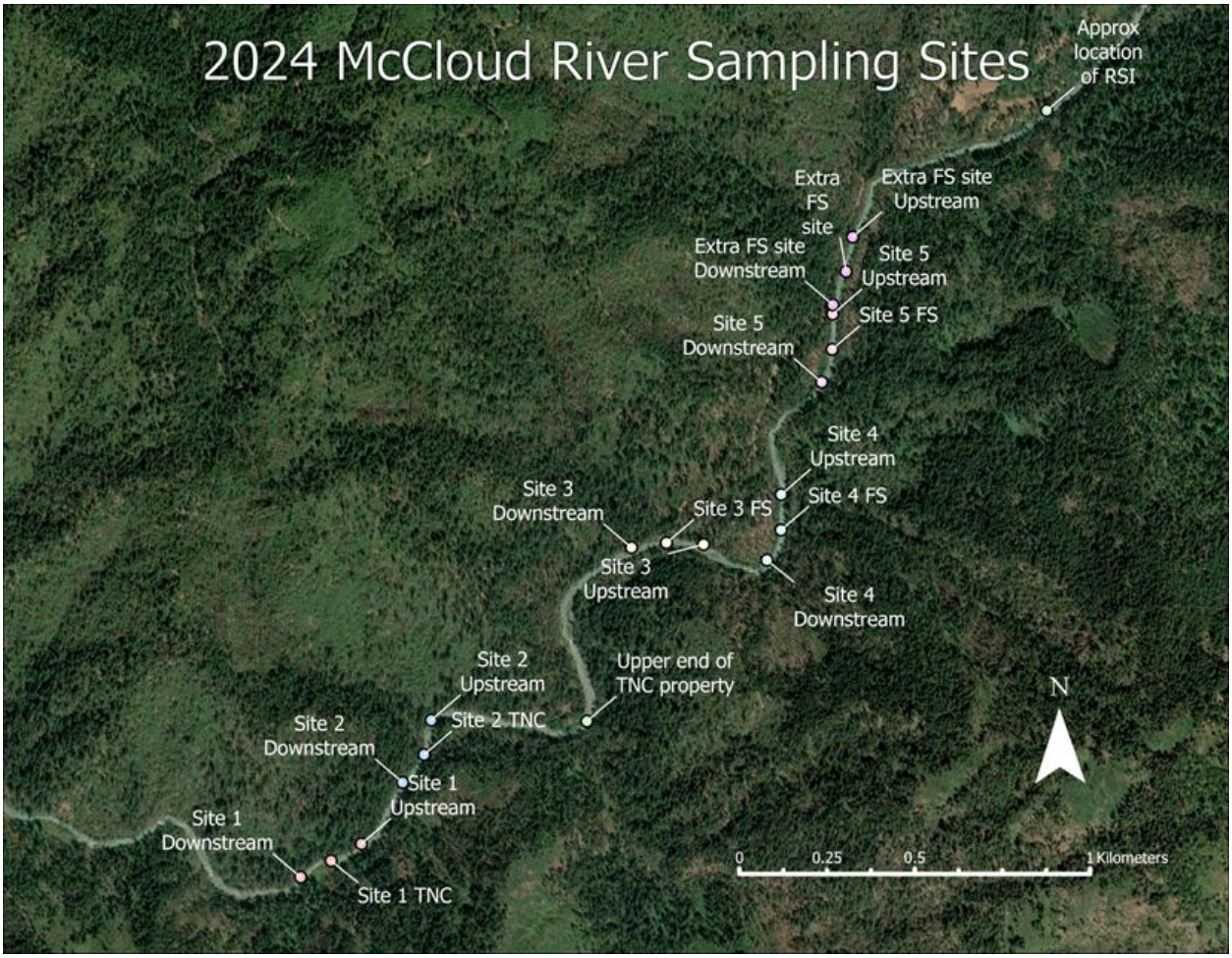

Figure 7.2. Upper McCloud River sampling sites. Colored dots denote upper, middle and lower portion of each 200m sampling site. “FS” denotes sites located on US Forest Service property, and “TNC” denotes sites located on The Nature Conservancy property.

In 2025, predator diet sampling focused on the lower McCloud River and took place near the McCloud Bridge (above the incline plane trap, IPT), downstream of the JSCS, and between the JSCS and the IPT (before installation of the JSCS in mid-September, the reaches upstream and downstream of the JSCS were treated as one continuous reach). Predator diet sampling took place over six weeks from September 1, 2025 to October 10, 2025. A total of 157 potential predators were sampled via gastric lavage. Due to limited molecular analysis capacity in 2025, only samples containing visible fish remains, apparent fish tissue, or otherwise substantial material were submitted to Cramer Fish Sciences (N=24).

Molecular analysis was conducted as follows. Conical vials were centrifuged at 3000 g for 10 min to pellet solids, and ethanol was decanted, leaving 2–3 mL covering the pellet. Pellets were incubated at 56 °C overnight to evaporate residual ethanol, then

resuspended in 2–5 mL of lysis buffer and vortexed for 30 s. A 200 µL aliquot from each sample was transferred to a labeled 1.5 mL microcentrifuge tube.

Aliquots were processed using the Qiagen Blood and Tissue Kit (Qiagen, Hilden, Germany) following manufacturer protocols for tissue DNA extraction. One or more extraction negative controls were included with each batch to ensure sample integrity. Potential PCR inhibitors were removed using the OneStep™ PCR Inhibitor Removal Kit (Zymo Research, USA) per manufacturer guidelines. Subsampled tissue was extracted using the Qiagen Blood and Tissue Kit following manufacturer protocols.

Chinook salmon DNA was initially screened using species-specific qPCR (Laramie et al. 2015) run in singlet. Positive samples were reanalyzed in triplicate with Chinook, Rainbow Trout, and Brown Trout assays (Brandl et al. 2015; Carim et al. 2016). Each 10 µL reaction contained 6 µL 2× TaqMan™ Environmental Master Mix 2.0 (Thermo Fisher Applied Biosystems®), 4 µL DNA template, and assay-specific primers and probe concentrations (Chinook: 0.9 µM primers, 0.2 µM probe; Rainbow Trout: 0.9 µM primers, 0.15 µM probe; Brown Trout: 0.6 µM forward, 0.3 µM reverse primers, 0.125 µM probe). Each plate included triplicate no-template controls and positive controls (voucher DNA). Quantification cycle (Cq) values were converted to relative concentration (ng/µL) using assay-specific standard curves derived from 10-fold serial dilutions of voucher DNA. Tissue resembling fish was tested using the same approach.

To screen for other prey items, a subset of samples was analyzed via metabarcoding using MiFish-U primers (Miya et al. 2015) following Keel et al. (2025). Sequences were processed with the METAWORKS pipeline (Porter and Hajibabaei 2022) and matched to reference sequences in NCBI GenBank using BLAST+ (Camacho et al. 2009). Field, extraction, and PCR controls were evaluated following Djurhuus et al. (2017).

Predator mark recapture study

In 2024, predator abundance was estimated at five randomly selected sites in the Upper McCloud River (AhDiNa and TNC areas). Site selection used a generalized random tessellation stratified (GRTS) selection protocol (Stevens and Olson 2004). At each 200 m site, two to three anglers sampled for three hours while maintaining, where practical, even spatial coverage across multiple habitat units (Figure 7.2).

Captured rainbow and brown trout were held in a submerged fish hamper (Figure 7.1) until processed (measured, gastric lavage, and PIT tag scan). Untagged fish were implanted with PIT tags in the body cavity using a syringe-style implanter; tagging occurred during all sampling weeks.

Although rainbow and brown trout can move long distances, individuals were assumed to remain near capture locations over short periods (1–2 weeks). Sampling was therefore conducted in three two-week blocks (mark week followed by recapture week; six weeks total) to approximate a robust design (Cooch 2008), which assumes no immigration or emigration during paired sampling events.

Recapture rates were lower than expected, suggesting a large population and/or broader movement than anticipated. Consequently, population density was estimated using simpler approaches, including the Petersen method with Chapman modification, where *N* is population size, *M* is fish marked, *n* is fish captured during recapture, and *m* is recaptures.

$$N = (M+1)*(n+1)/(m+1) -1$$

The Schnabel Index extends the Petersen method by providing a weighted average of population estimates across multiple sampling occasions. Here, Ct is the total number of individuals captured on occasion t, Mt is the number of individuals already marked in the population at that time, and Rt is the number of marked individuals recaptured on occasion t.

$$N = \sum(Ct * Mt) / \sum Rt$$

Both of these estimates should be interpreted with caution as they likely overestimate population sizes, especially given the low recapture rates. Nonetheless, these estimates fall within the range of density estimates from historical studies in nearby McCloud River reaches from 1998, 2013, and 2023 (Dege, 2023).

In 2025, a 600 m reach in the TNC reserve encompassing two sites from 2024 was sampled. The reach spanned from the downstream end of reach 1 to the upstream end of reach 2 (Figure 7.2). The reach was divided into two 300 m segments, with two 3-hour sampling blocks per day (one per segment) using five to six anglers. Captured fish were scanned for PIT tags and marked with a caudal fin clip prior to release.

Because sampling occurred over three consecutive days within a continuous reach (rather than weeks across discrete 200 m sites), assumptions differed slightly regarding trout movement (e.g., immigration/emigration) and catchability (e.g., limited time for fish to resume natural behavior before recapture).

While this effort aimed to obtain sufficient recaptures to support a robust population density model within the reach or across years, recapture rates remained low. As in 2024, we therefore used the Petersen estimate and Schnabel index for comparison.

Predation risk

PERs were designed and fabricated to evaluate predation risk in shallow, fast-flowing river environments (Figure 7.3). Each unit consisted of a PVC body with a waterproof cap and housed an internal battery, microcontroller (Adafruit Metro M4), GPS logger, and GPS antenna mounted in 3D-printed housing. The microcontroller used two reed switches to detect deployment status and predation events, logging a binary (0/1) signal based on magnet position to indicate when deployments began or ended and when a predation event occurred. GoPro cameras mounted externally provided visual confirmation of events and predator identification.

Fathead minnows (*Pimephales promelas*), similar in size to winter-run fry, were used as bait on PERs. Live minnows were tethered to the predation magnet with a monofilament leader using a loop knot threaded through the mouth and gills. This setup allowed the minnow to swim freely near the PER while enabling predators to remove it with sufficient force to dislodge the magnet. When predation occurred, the magnet detached, triggering the reed switch to log the time and location of the event.

PERs were released at the upstream end of each reach and allowed to drift downstream. If the tethered minnow remained alive and exhibited normal behavior upon recovery, it was reused for the next deployment. Minnows that were dead, missing, or showed signs of morbidity were replaced before redeployment.

To implement a BACI design, PER sampling alternated between two locations in the lower McCloud River: McCloud Bridge (control) and JSCS (impact). The McCloud Bridge site, located upstream of all trapping locations, consisted of a ~200 m run from the bridge to just above the IPT. The JSCS site, ~500 m downstream, included a fast riffle upstream of a log boom and slower water near and below the JSCS. Sampling occurred before and after installation to compare predation rates, spanning six weeks (9/2/2025–10/10/2025): two weeks pre-installation and three weeks post-installation (no sampling during installation), with four sampling days per week.

Both sites were sampled for approximately three hours each morning. Ten PERs were used, with each unit deployed 5–6 times per day. Prior to JSCS installation, a single continuous reach was sampled near the planned trap location. After installation, sampling consisted of three shorter drift segments: upstream of the log boom, from the log boom to the JSCS, and downstream of the JSCS, with PERs deployed directly behind the trap box.

During each second of a PER drift, a potential predation event could occur, making deployments suitable for time-to-event analysis, where shorter time to predation indicates higher risk. A Cox proportional hazards model, implemented in the R package *survival* (Therneau, 2021), was used to evaluate predation risk before and after JSCS installation. The response variable was time to predation (if an event occurred) or total deployment duration (if no event occurred), and predictors included two categorical fixed effects: site (JSCS or McCloud Bridge) and period (before or after installation). The model was then used to estimate predation risk at each site and period relative to the JSCS site before installation.

Predator species were identified for each predation event using GoPro footage. A predator was identified only when the entire fish was visible during the event. Events not captured on video were classified as unknown.

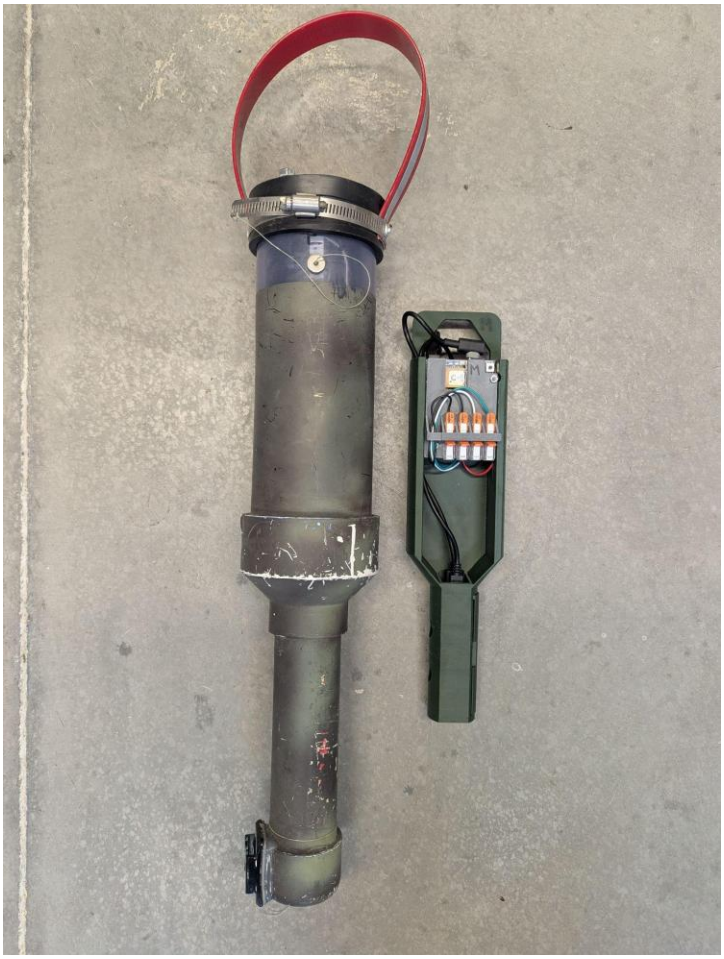

Figure 7.3. The PER housing (left) and the microcontroller and battery housing (right).

Predator abundance

To contextualize predation risk, predator abundance was quantified at both PER sampling sites (2025 only) using snorkel surveys. All visible predators were identified and counted. Surveys were conducted the day before each weekly PER sampling event (n = 7, including the week of JSCS installation) and consisted of two snorkelers drifting in parallel downstream, covering habitats likely to hold predators.

Snorkel surveys covered two reaches of the McCloud River: (1) from the UCD fry release location ~200 m upstream of McCloud Bridge to the IPT, and (2) from the IPT to the downstream end of the JSCS site. In addition to the PER sampling sites, these reaches included upstream habitats likely to hold predators and encompassed the portion of the lower river where most predator diet samples were collected.

Results

Predator diet sampling

Most diet samples were collected in 2024, reflecting intensive sampling at five sites near AhDiNa and the TNC preserve, totaling 484 processed samples (Table 7.1). In 2023 (pilot year), limited effort yielded 63 processed samples. In 2025, effort shifted toward PER work, and 156 diets were sampled, of which 24 (those with visible fish remains) were submitted for molecular analysis. Across all years, most samples were from rainbow trout, followed by brown trout and spotted bass (Figure 7.4).

In general, qPCR assays detected either no or only trace amounts of Chinook salmon DNA in predator diets. Only one diet—collected from a spotted bass caught in the IPT in 2023—contained a visually identifiable Chinook salmon. This was also the only sample with sufficient DNA for genotyping, which indicated a Livingston Stone Hatchery fish (sub-lot 138DT). Parentage-based assignment was not possible for other diets containing Chinook DNA.

All Chinook salmon detections with qPCR Cq <36 were considered positive, albeit most were at trace levels. However, a small number of additional samples contained more than trace levels. Using this threshold, 6.6% of all tested diets contained Chinook DNA (Table 7.1). Where sample sizes allowed comparisons among predator species (e.g., upper river in 2024 and lower river in 2025), detection rates were similar. Notably, Chinook DNA was more frequently detected in lower river diets than in upper river diets (20.6% vs. 3.7%; Table 7.1), despite the greater distance from the source of winter-run

fry at AhDiNa. Similarly, fish were more frequently found in predator diets in the lower river.

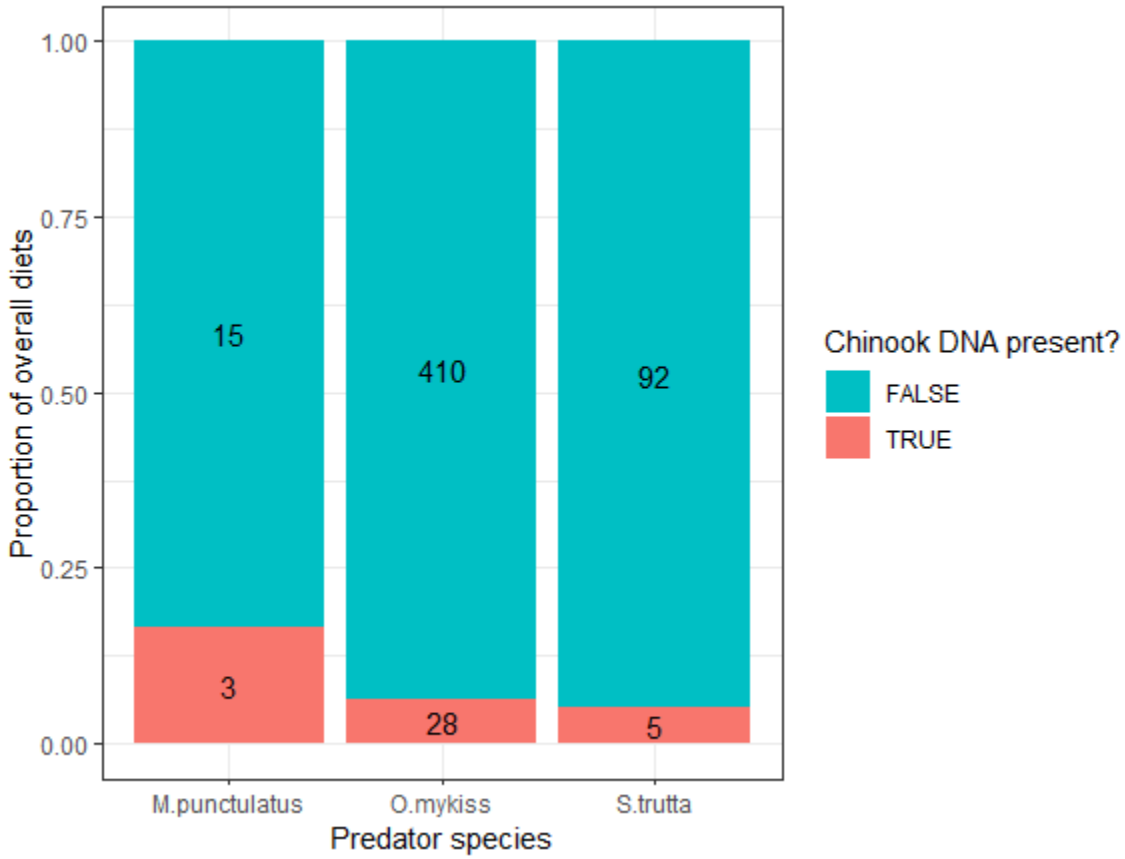

Figure 7.4. Proportion of overall diets containing Chinook salmon DNA from the three primary predator species, pooled across the upper and lower river and all three years of collections.

The trace levels of Chinook salmon DNA observed may reflect well-digested prey consumed several days prior. However, some cross-amplification of the qPCR assay with predator species—particularly rainbow and brown trout—cannot be ruled out. Although the assay was rigorously tested by Laramie et al. (2015) against these species, additional validation may be needed to distinguish these signals. Nonetheless, temporal patterns in Chinook DNA detections generally align with expected salmon presence in the river, and positive detections in centrarchid bass are not subject to this cross-amplification concern.

All 24 diet samples analyzed in 2025, along with a subsample from 2023 and 2024, were also metabarcoded using the MiFish primer set. Results indicated that sculpin and fathead dace were the primary prey items. Metabarcoding also allowed identification of predator species, and in some samples, only predator DNA was detected.

Table 7.1. Annual and Regional Summary of Predator Sampling Effort and Frequency of Chinook Salmon DNA Detection in Diet Samples (2023–2025). Positive occurrence of Chinook DNA in diet samples was defined as qPCR Cq values < 36.

Year	Region	Predator Species	# Diets Collected	# Diets Analyzed	# Visible Fish Parts	# Diets Positive for Chinook DNA	% Positive for Chinook DNA
2023	Upper	Rainbow trout	23	23	0	0	0.0
2023	Upper	Brown trout	14	14	0	2	14.3
2023	Lower	Rainbow trout	8	8	0	4	50.0
2023	Lower	Bass sp.	4	4	1	1	25.0
2024	Upper	Rainbow trout	342	342	1	13	3.8
2024	Upper	Brown trout	81	81	3	2	2.5
2024	Lower	Rainbow trout	58	57	0	9	15.8
2024	Lower	Brown trout	1	1	0	0	0.0
2024	Lower	Bass sp.	3	3	0	0	0.0
2025	Lower	Rainbow trout	86	8	4	2	25.0
2025	Lower	Brown trout	13	1	0	1	100.0
2025	Lower	Bass sp.	56	15	11	3	20.0
All Years	Upper	Rainbow trout	365	365	1	13	3.6
All Years	Upper	Brown trout	95	95	3	4	4.2
All Years	Lower	Rainbow trout	152	73	4	15	20.5
All Years	Lower	Brown trout	14	2	0	1	50.0
All Years	Lower	Bass sp.	59	22	12	4	18.2
All Years	Upper	All Species	460	460	4	17	3.7
All Years	Lower	All Species	226	97	16	20	20.6

All Years	**All Regions**	**All Species**	**686**	**557**	**20**	**37**	**6.6**

Negative field controls were collected during gastric lavage sampling in 2024 by following all processing steps without sampling a fish. Specifically, the sieve was sprayed with river water as if consolidating diet contents, then rinsed with 90% ethanol to transfer material into a conical vial. A total of 25 controls were collected, and all tested negative for Chinook salmon DNA, indicating no field cross-contamination. Although controls were not collected in 2023 or 2025, identical field protocols were used, suggesting cross-contamination was unlikely in those years as well.

2023

In 2023, genetic analysis of stomach contents showed that 6 of 45 fish (13%) contained low but detectable levels of Chinook salmon DNA. On October 10, 2 brown trout and 3 rainbow trout sampled from the upper TNC site tested positive; this occurred ~9 days after winter-run fry from the second heath tray stack were released at AhDiNa (7 rkm upstream). On October 19, 1 of 6 rainbow trout sampled below the CDFW trap tested positive. At the CDFW trap, 3 of 14 centrarchid bass contained Chinook DNA. It should be noted that predators collected from the trap may have consumed Chinook salmon within the trap box prior to processing.

2024

A total of 483 potential predators were captured from the upper McCloud River sampling sites, consisting of both rainbow trout (O. mykiss N=393, mean FL=9.5 inches) and brown trout (S. trutta N=90, mean FL=10.75 inches), resulting in 423 stomach samples. A total of 62 potential predators were captured from the lower McCloud River sampling site and the JSCS resulting in 61 stomach samples. Of those 61, 32 potential predators (30 rainbow trout, 1 brown trout, 1 Centrarchid bass) were captured and gastric lavaged from the lower river site on 5 separate occasions between 9/24 and 11/5, and 27 potential predators (25 rainbow trout, 2 Centrachid bass) were captured and gastric lavaged from directly upstream of the JSCS on 3 separate occasions between 9/24 and 10/15. A two sample t-test of mean fork length of predators sampled in the lower river versus the upper river found a significant difference in fork length of predators between the two reaches (upper river mean FL=9.5 inches SD=3.27, lower river mean FL=16.33 inches SD=2.94 inches t=14.65 p=<0.0001) (Figure 7.5).

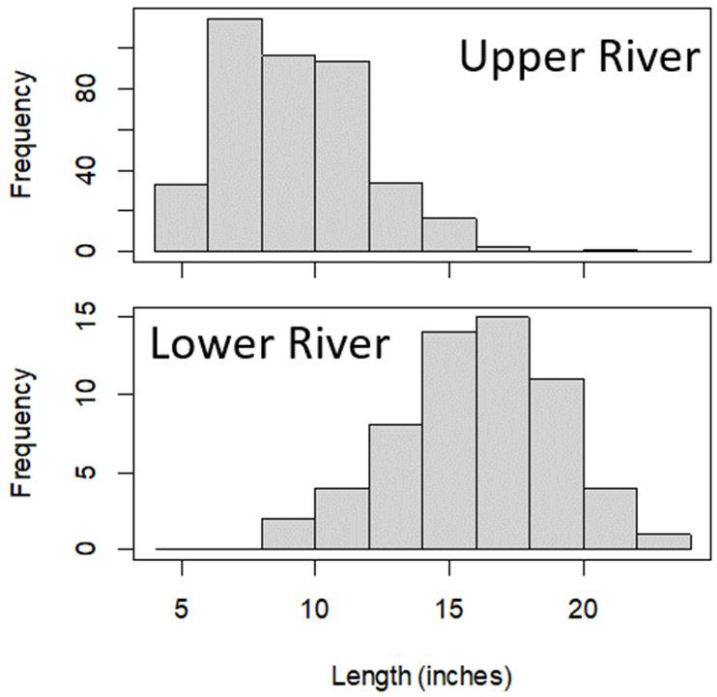

Figure 7.5. Histogram of sampled predator fork lengths from the upper river sampling sites (upper panel) vs. lower river sampling sites (lower panel).

A total of 484 gastric samples were analyzed by Cramer Fish Sciences in an attempt to identify the proportion of potential predators which had winter-run Chinook salmon DNA present in their diet. Visual assessment of gastric samples indicated that potential predators were largely feeding on invertebrate prey as well as algae. Only 4 out of the 484 samples (<1%) contained a visible but unidentifiable fish prey item (Fig. 7.6). Overall, genetic analysis of stomach contents revealed that 24 of the 484 (5.0%) gastric samples screened via the qPCR assay had detectable, albeit very low levels of Chinook salmon DNA present. Quantitative PCR Cq values for positive samples (Cq value <36) ranged from 35.987 to 26.597 with a mean value of 33.650. For the 4 visible fish prey items, flesh from the fish prey was subsampled and tested independently using the qPCR assay; all three of these samples tested negative for Chinook salmon DNA.

Figure 7.6. Photographs of two of the four visible fish prey items found in predator stomachs in 2024

Chinook salmon DNA was detected in upper river predator diets beginning in the first week of sampling, with two fish testing positive from sites 3 and 5 on 9/19 and 9/20, respectively (see Figure 7.2 for site locations). During the second week (9/26), two rainbow trout from site 3 and three from site 4 tested positive, along with one brown trout from site 5 on 9/27 (Figure 7.7). During week 3 (10/10), one rainbow trout each from sites 3 and 4 tested positive, and one rainbow trout from alternate site 7 tested positive on 10/11. In week 4 (10/16), two rainbow trout from site 3 and one brown trout from site 4 tested positive, followed by one rainbow trout from site 5 on 10/18. No fish from the upper river tested positive during the final two sampling weeks (10/30–11/1 and 11/6–11/8; Figure 7.7).

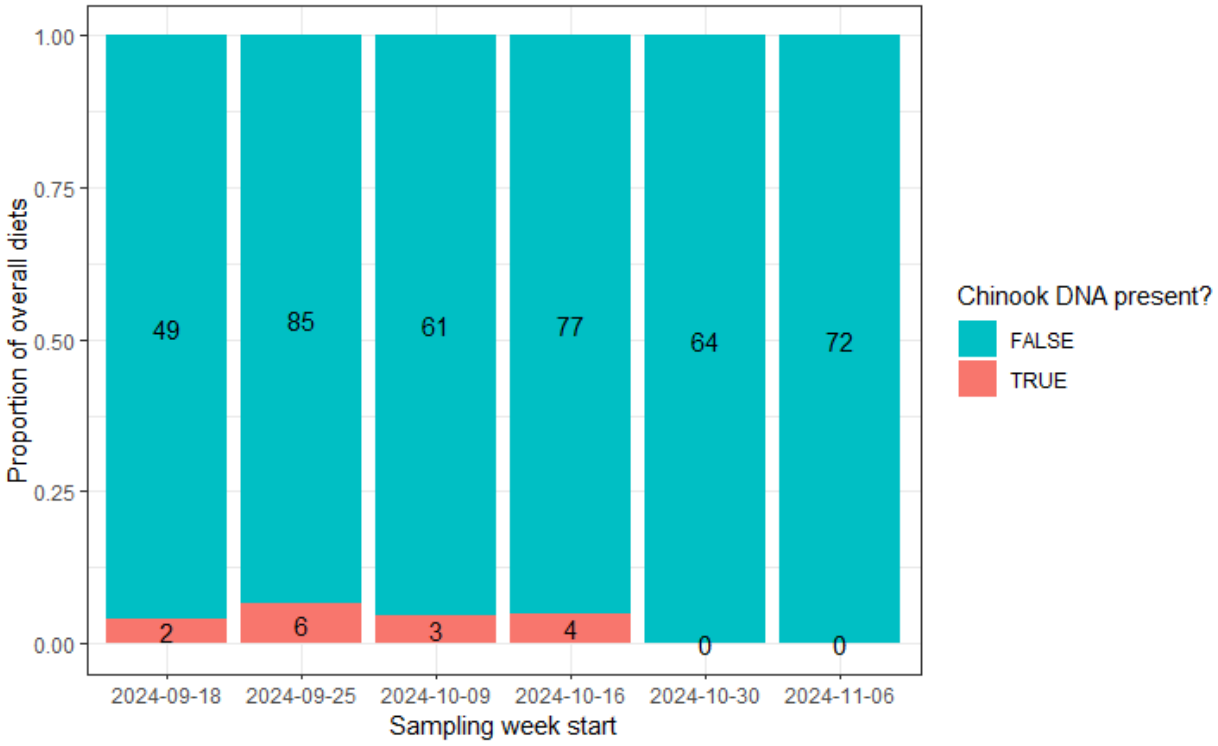

Figure 7.7. Proportion of overall diets containing Chinook salmon DNA from predators collected weekly in the upper river during the 2024 season.

No lower river diet samples tested positive for Chinook DNA during the first two sampling weeks. The first detection occurred on 10/8 during week 3, when a single rainbow trout collected at the JSCS tested positive at low levels. During sampling week 4 (10/15), four additional rainbow trout from the JSCS tested positive. Three additional rainbow trout tested positive during week 5 (10/29) from the McCloud Bridge site as well as a single rainbow trout during week six (11/5) the final week of sampling.

2025

Due to low or absent Chinook salmon DNA in diet samples lacking identifiable fish remains in previous years, only gastric lavage samples containing visible fish remains were tested for winter-run Chinook DNA in 2025. In total, 156 fish (min FL = 178 mm; max FL = 495 mm; mean FL = 336.8 mm) were sampled by hook and line, providing a broad representation of the predator assemblage in the study area.

Of these, 104 fish were collected at the McCloud Bridge site, including 42 rainbow trout (min FL = 7 in; max FL = 19.5 in; mean FL = 14 in), 6 brown trout (min FL = 10 in; max FL = 19 in; mean FL = 15.7 in), 2 kokanee (16 and 17 in), and 54 spotted bass (min FL = 9 in; max FL = 16 in; mean FL = 12.4 in). An additional 53 fish were sampled from the lower river near the JSCS, including 44 rainbow trout (min FL = 8 in; max FL = 19 in;

mean FL = 14.18 in), 7 brown trout (min FL = 7 in; max FL = 9 in; mean FL = 7.7 in), and 2 spotted bass (10.5 and 8 in).

Of the 156 fish, 24 samples (15%) contained identifiable fish remains and were selected for molecular analysis. Seventeen samples (3 rainbow trout, 1 brown trout, and 13 spotted bass) were from the McCloud Bridge site, and 7 samples (5 rainbow trout and 2 spotted bass) were from the lower river below the incline plane trap near the JSCS. This subset represents samples most likely to contain detectable prey DNA and therefore provides a more targeted assessment of predation.

Molecular analysis indicated that 6 of 24 samples (25%) contained detectable Chinook salmon DNA. Of these, 3 (50%) were from spotted bass at McCloud Bridge, 1 (17%) from a brown trout at McCloud Bridge, and 2 (33%) from rainbow trout at the lower river JSCS site. Although Chinook DNA was detected in these samples, none of the visible fish remains were morphologically identified as Chinook salmon, suggesting that prey items were highly digested and not visually distinguishable at the time of analysis.

Predator mark recapture study

2024 Season

By the sixth and final sampling week of the 2024 season, 310 rainbow trout and 71 brown trout had been PIT tagged (Table 7.2). An additional 60 trout were tagged during the final week (441 total) but were not available for recapture. Recaptures were rare until late in the study, and on only two occasions were more than one recaptured within a site on a given day. Rainbow trout were recaptured more frequently (n = 17) and at a slightly higher proportion of tagged individuals (5.5% vs. 2.8% for brown trout). Only two brown trout were recaptured, precluding a population estimate for that species.

2025 Season

A total of 323 trout were captured during the 2025 mark–recapture effort, including 289 rainbow trout and 34 brown trout. No brown trout were recaptured; therefore, population estimates were generated only for rainbow trout. A total of 126 rainbow trout were captured and marked on day 1, 105 on day 2, and 58 on day 3. Six rainbow trout with PIT tags from the 2024 season were recaptured, all within the same reach where they were originally tagged. These individuals ranged from 8.5–12 inches in 2024 and had grown 2–4 inches since the previous autumn. Although these fish exhibited limited movement, they were not included in population estimates because it could not be assumed that other tagged fish remained within the same reach or survived.

Three and four recaptures of newly marked fish occurred on days 2 and 3, respectively. Petersen and Schnabel estimates yielded similar, though higher, rainbow trout density estimates compared to 2024. However, the low number of recaptures precludes robust estimates of uncertainty. While useful for comparison with similar efforts over past decades, these estimates should be interpreted with caution.

Both estimates (Table 7.3) likely overestimate population size, particularly given the low recapture rates. Nonetheless, they fall within the range of trout density estimates reported from nearby McCloud River reaches in 1998, 2013, and 2023 (Dege, 2023).

Table 7.2. Summary of Rainbow and Brown Trout captures in 2024 in the five reaches in the Upper McCloud approximately between The Nature Conservancy and AhDiNa. Note that site 5 was not sampled during event 3 due to several anglers present in the site.

Site	Sampling Event	*O. mykiss*	Recaptures	*S. trutta*	Recaptures	Total Fish Caught	Total Recaptures
	1	13				13	0
	2	18		2		20	0
1	3	6		1		7	0
	4	16	1			16	1
	5	7		3		10	0
	6	14	1	4		18	1
	1	5				5	0
	2	19		3		22	0
2	3	15	1	5		20	1
	4	17		4		21	0
	5	12	1	4		16	1
	6	11	1	1		12	1
	1	15		1		16	0
	2	39				39	0
3	3	13		2		15	0
	4	14		3		17	0
	5	11	1	3		14	1
	6	19	7	4		23	7
	1	13		6		19	0
	2	20		3		23	0
4	3	7		2		9	0
	4	10		7		17	0
	5	3	1	5		8	1
	6	5	1	5	2	10	3
	1	9		1		10	0
	2	24	1	6		30	1
5	3	*n/a*	*n/a*	*n/a*	*n/a*	*n/a*	*n/a*
	4	5		5		10	0
	5	12	1	6		18	1
	6	10		1		11	0

Table 7.3. Rainbow Trout density estimates based on two methods for both 2024 and 2025, the Peterson method with Chapman Modification and the Schnabel index

Site	**Petersen Estimate** per 200m	**Schnabel Index** per 200m	**Fish per mile** Petersen estimate	**Fish per mile** Schnabel Index
2024				
1	412	1101	3323	8879
2	373	829	3008	6685
3	218	606	1754	4887
4	132	651	1060	5250
5	227	650	1831	5242
2025				
Lower (includes site 1)	539	1067	4347	8605
Upper (includes site 2)	1055	1464	8508	11806
Entire reach (includes sites 1 and 2)	1570	1268	12661	10226

Predation risk

A total of 868 PER deployments were conducted over the 2025 field season, with 354 before and 514 after JSCS installation. These deployments yielded 62.5 hours combined of data, including 25.1 hours pre-installation and 37.4 hours post-installation. Although more deployments occurred at the JSCS (impact) site, its faster water velocities and shorter reach resulted in fewer total sampling seconds compared to the McCloud Bridge (control) site (Table 7.4).

A total of 65 predation events were confirmed, including 11 attributed to rainbow trout, 3 to spotted bass, and 51 to unknown predators (Table 7.5). At the JSCS site, all identified predation events were attributed to rainbow trout, whereas at McCloud Bridge, events were attributed to both rainbow trout and spotted bass.

Following JSCS installation, predation risk increased 2.15-fold at the JSCS site relative to pre-installation levels (p = 0.01) (Figure 7.8). Predation risk at McCloud Bridge was 0.61-fold lower than at the JSCS site before installation (p = 0.05) and declined an additional 0.09-fold after installation (p = 0.005). Correspondingly, predation rates at the JSCS site increased from 1.65 to 4.36 events per hour, while rates at McCloud Bridge decreased from 0.48 to 0.07 events per hour over the same period (Table 7.4).

Most predation at the JSCS site occurred near the upstream end of the reach both before and after installation (Figure 7.9). In contrast, predation at McCloud Bridge was distributed more evenly throughout the reach (Figure 7.10).

Table 7.4. Summary of PER deployments

site	time	Sampling start	Sampling stop	# PER deploy	Sec of sampling	Confirmed preds	Preds per hour
JSCS	Before	9/3/25	9/11/25	190	30580	14	1.65
JSCS	After	9/23/25	10/9/25	321	33865	41	4.36
Bridge	Before	9/2/25	9/12/25	164	59848	8	0.48
Bridge	After	9/24/25	10/10/25	193	100803	2	0.07

Table 7.5. Predation events attributable to rainbow trout (RBT) and spotted bass (SPB) during each day of sampling in 2025.

date	site	Confirmed preds	RBT preds	SPB preds	# PER deployments	Sec of sampling
9/2/2025	bridge	1	0	0	38	16993
9/3/2025	jscs	3	0	0	44	7554
9/4/2025	bridge	3	0	1	44	13972
9/5/2025	jscs	2	0	0	73	13149
9/9/2025	jscs	6	0	0	41	5794

9/10/2025	bridge	4	0	2	48	15182
9/11/2025	jscs	3	0	0	32	4191
9/12/2025	bridge	0	0	0	34	11467
9/23/2025	jscs	7	2	0	58	6708
9/24/2025	bridge	1	0	0	25	14917
9/25/2025	jscs	2	0	0	33	4292
9/26/2025	bridge	0	0	0	8	5032
9/30/2025	jscs	4	0	0	63	7312
10/1/2025	bridge	0	0	0	39	18114
10/2/2025	jscs	3	0	0	61	6897
10/3/2025	bridge	0	0	0	46	19272
10/7/2025	jscs	12	3	0	66	5419
10/8/2025	bridge	1	0	0	32	17317
10/9/2025	jscs	13	8	0	40	3043
10/10/2025	bridge	0	0	0	43	25706

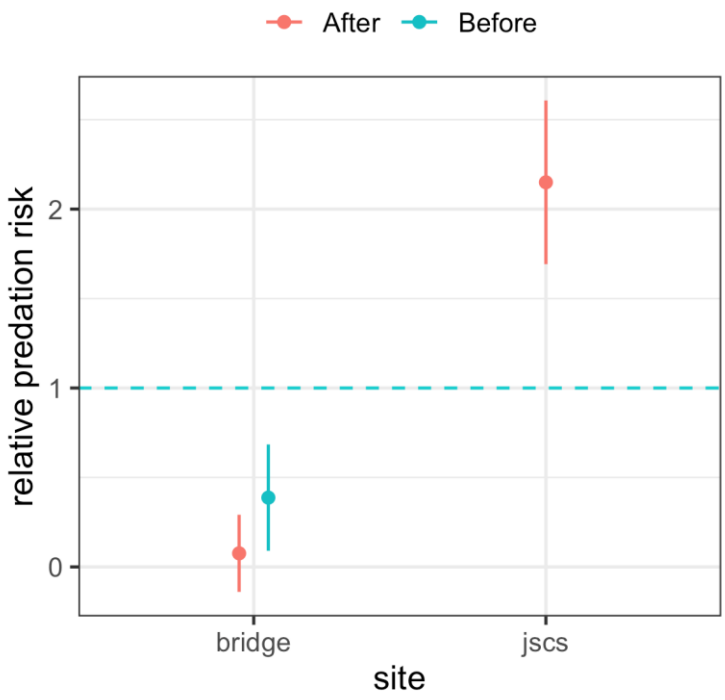

Figure 7.8. Change in predation risk attributable to JSCS installation. Predation risk at the JSCS site before the JSCS was installed is represented by the dashed horizontal line at y=1. This is not the actual value of predation risk at this site and time, but rather a frame of reference. Points show how predation risk at other sites and/or times differed from predation risk at the JSCS site before JSCS installation, while vertical lines show the standard error around each difference. Note that predation risk drastically increased at the JSCS site following JSCS installation while it decreased at the McCould bridge site.

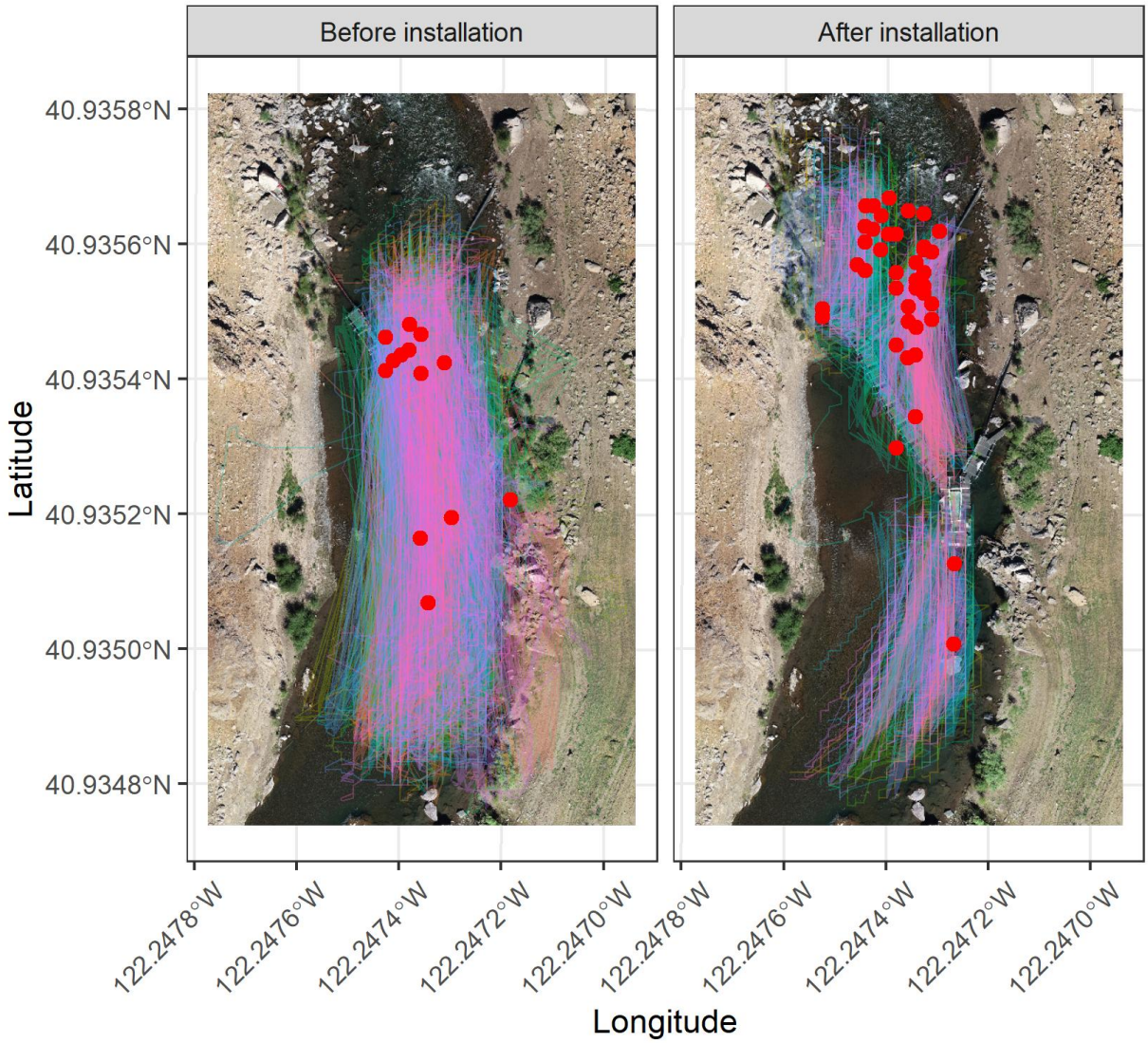

Figure 7.9. Spatial distribution of predation events at the JSCS site. Each line shows the GPS track of an individual PER deployment. Red dots show the location of predation events.

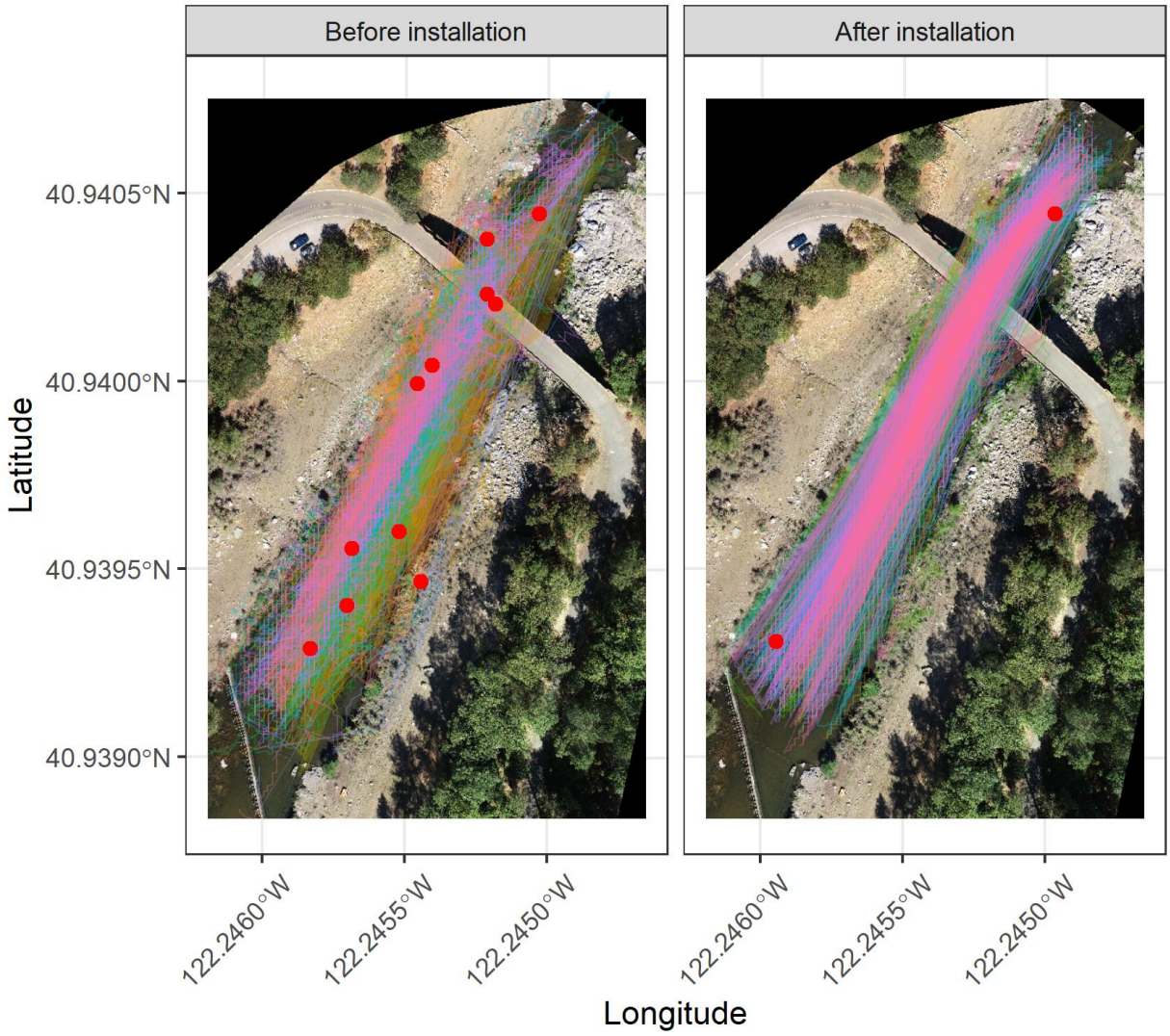

Figure 7.10. Spatial distribution of predation at the McCould bridge site. Each line shows the GPS track of an individual PER deployment. Red dots show the location of predation events.

Predator abundance

296 predators were counted during snorkel surveys in the lower McCould River, the vast majority being spotted bass observed within reach 1 (Figure 7.11). The number of spotted bass counted in reach 1 steadily increased throughout the study period before dropping to its lowest value during the last sampling event in early October. By contrast, very few spotted bass were observed in reach 2, which contained the JSCS. Instead, trout were the dominant predator observed there.

Three additional observations during snorkeling warrant inclusion here. First, spotted bass were observed to aggregate in a small channel directly in front of the IPT opening

during more than one snorkeling survey. Spawning kokanee were also observed in front of the IPT, but in the shallower flats in front of the IPT planes. Finally, an adult Chinook salmon was spotted between the IPT and JSCS during a snorkel survey at the beginning of the last week of PER sampling (10/6/25).

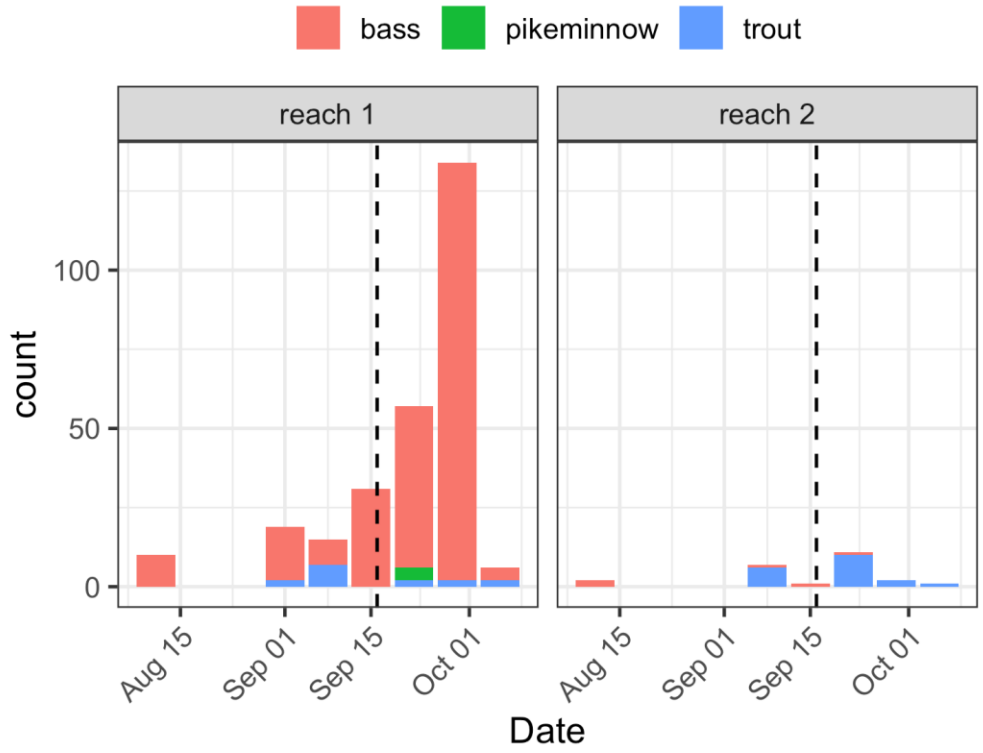

Figure 7.11. Counts of predators during snorkel surveys. Reach 1 was from the UCD fry release location ~200 meters upstream of the McCould Bridge to the IPT, and reach 2 was from the IPT to the downstream end of the JSCS site. The vertical dashed line represents the installation of the JSCS in reach 2.

Discussion

During the 2024 field season, predator aggregations were observed around the JSCS, leading to the hypothesis that these aggregations could increase predation risk for juvenile Chinook salmon. This hypothesis was tested in 2025 using PER deployments within a BACI study design. Predation risk at the control site (McCloud Bridge) declined over the study period, whereas risk at the impact site increased markedly following JSCS installation (Figure 7.9). Although this initially supported the hypothesis, predator abundance was higher at the control site than at the impact site after installation (Figure 7.11). This suggests that, rather than increasing predator abundance, the JSCS may have facilitated more efficient predation by fewer individuals.

At the JSCS site, predation primarily occurred upstream of the trap both before and after installation (Figure 7.9), an area characterized by suitable trout habitat. Most predators observed at the impact site were rainbow trout (Figure 7.11), consistent with observations from 2024 when the JSCS was located in the reservoir. Both stomach content analyses (Table 7.1) and PER GoPro footage (Table 7.4) identified rainbow trout as the primary predator of juvenile salmon (or PER-deployed minnows) in the lower McCloud River. This pattern suggests that JSCS installation may have increased foraging efficiency for rainbow trout. Alternatively, the timing of installation may have coincided with more favorable feeding conditions (e.g., cooler temperatures). It is also possible that PERs under-sampled deeper habitats at the control site or that predators were more cautious in slower water, potentially influencing detection rates. However, within a BACI framework, the relative change in predation risk before and after installation is more informative than absolute differences, and this change was substantially greater at the impact site.

As Lake Shasta recedes during summer, non-native spotted bass often persist in slower-moving river habitats within the reservoir footprint and were the most abundant predator observed in the lower McCloud River in 2025 (Figure 7.11). Despite this, both PER data (Table 7.4) and stomach content analyses (Table 7.1) suggest that spotted bass contribute less to predation on juvenile salmon than rainbow trout. This difference likely reflects contrasting physiological tolerances: bass are more active under warmer conditions, whereas salmon and trout are better adapted to cooler temperatures (McInturf et al. 2022; Burford et al. 2026). Under the cooler conditions typical of the McCloud River in early fall, both bass activity and salmon vulnerability to bass predation are reduced.

Nonetheless, spotted bass showed the highest incidence of visible fish remains in stomach contents and may exert broader ecological impacts. Large aggregations were observed at migration bottlenecks, such as near the IPT. Their preference for slower habitats may provide opportunities for targeted removal (e.g., hook and line, seining, or spearing). Seasonal patterns suggest that bass abundance increases near McCloud Bridge into early October, potentially reflecting downstream movement from upstream habitats, followed by a decline as fish either pass through the system or return to the reservoir with cooling temperatures and increased flow. This trend was consistent with both snorkel survey observations (Figure 7.11) and CDFW IPT data.

References

Brandl, S., G. Schumer, B. M. Schreier, J. L. Conrad, B. May, and M. R. Baerwald. 2015. Ten real-time PCR assays for detection of fish predation at the community level in the San Francisco Estuary–Delta. Molecular Ecology Resources 15(2):278–284.

Burford, B. P., Lehman, B. M., Zillig, K. W., Lo, V. K., McInturf, A. G., Kwan, G. T., ... & Michel, C. J. (2026). Linking aerobic scope to fitness in the wild reveals potential opportunities to help recover imperiled salmon populations. *Communications Biology*.

Camacho, C., G. Coulouris, V. Avagyan, N. Ma, J. Papadopoulos, K. Bealer, and T. L. Madden. 2009. BLAST+: architecture and applications. BMC Bioinformatics 10(1):421.

Carim, K. J., T. M. Wilcox, M. Anderson, D. J. Lawrence, M. K. Young, K. S. McKelvey, and M. K. Schwartz. 2016. An environmental DNA marker for detecting non-native brown trout (Salmo trutta). Conservation Genet Resour DOI 10.1007/s12686-016-0548-5

Dege, Michael. 2023. California Department of Fish and Wildlife Heritage and Wild Trout Field Report. 2023 McCloud Mark Recapture Study.

Demetras, N. J., D. D. Huff, C. J. Michel, J. M. Smith, G. R. Cutter, S. A. Hayes, and S. T. Lindley. 2016. Development of underwater recorders to quantify predation of juvenile Chinook salmon (Oncorhynchus tshawytscha) in a river environment. Fishery Bulletin:179-185.

Djurhuus, A., J. Port, C. J. Closek, K. M. Yamahara, O. Romero-Maraccini, K. R. Walz, D. B. Goldsmith, R. Michisaki, M. Breitbart, A. B. Boehm, and F. P. Chavez. 2017. Evaluation of Filtration and DNA Extraction Methods for Environmental DNA Biodiversity Assessments across Multiple Trophic Levels. Frontiers in Marine Science 4.

Hafs, A. W., J. M. Niles, and K. J. Hartman. 2011. Efficiency of Gastric Lavage on Age-0 Brook Trout and the Influence on Growth and Survival. North American Journal of Fisheries Management 31:530-534.

Keel, D.J., Karpenko, K., Blankenship, S.M., Schumer, G., O'Rourke, O., Ostberg, C.O., Chase, D.A., and J.J. Duda. 2025. A molecular specimen bank for contemporary and future study captures landscape-scale biodiversity baselines before Klamath River dam removal. Sci Rep 15, 20679. https://doi.org/10.1038/s41598-025-07042-1

Laramie, M. B., Pilliod, D. S., and Goldberg, C. S. 2015. Characterizing the distribution of an endangered salmonid using environmental DNA analysis. Biol. Conserv. 183, 29–37. doi: 10.1016/j.biocon.2014.11.025.

McInturf, A. G., Zillig, K. W., Cook, K., Fukumoto, J., Jones, A., Patterson, E., ... & Fangue, N. A. (2022). In hot water? Assessing the link between fundamental thermal physiology and predation of juvenile Chinook salmon. *Ecosphere*, *13*(11), e4264.

Miya, M., Sato, Y., Fukunaga, T., Sado, T., Poulsen, J. Y., Sato, K., Minamoto, T., Yamamoto, S., Yamanaka, H., Araki, H., Kondoh, M., Iwasaki, W. 2015. MiFish, a set of universal PCR primers for metabarcoding environmental DNA from fishes: detection of more than 230 subtropical marine species. Royal Society Open Science. 2: 150088. http://dx.doi.org/10.1098/rsos.150088

Porter, T. M., and M. Hajibabaei. 2022. MetaWorks: A flexible, scalable bioinformatic pipeline for high-throughput multi-marker biodiversity assessments. PLOS ONE 17(9):e0274260.

Stevens, D. L., and A. R. Olsen. 2004. Spatially balanced sampling of natural resources. Journal of the American Statistical Association 99:262-278.

Therneau T (2021). _A Package for Survival Analysis in R_. R package version 3.2-11, <URL:
https://CRAN.R-project.org/package=survival>.

Task 8: Parentage-Based Tagging

Parentage-based tagging (PBT) is a powerful genetic tool that links offspring to their breeding parents, effectively providing a “genetic mark” without requiring physical tags. In the broader winter-run Chinook program, genotyping of adult carcasses on the Sacramento River below Keswick Dam - primarily by Cramer Fish Sciences (CFS) - is paired with juvenile incidental mortalities at the Red Bluff rotary screw trap to infer which spawners produced successful offspring. At Livingston Stone National Fish Hatchery (LSNFH), all winter-run spawners are genotyped, and crosses are carefully planned to maximize genetic diversity, so each hatchery release has known parentage and can be tracked by PBT. Over the past three years, we have leveraged this infrastructure to track the fate of winter-run Chinook salmon reintroduced into the McCloud River in two main ways: (1) linking incidental juvenile mortalities collected at in-river traps to their parents, thereby gaining insight into rearing method and age; and (2) determining the success of McCloud-reared fish that survive the ocean phase and return as adults. Beginning in 2025, PBT also becomes critical for evaluating the success of in-river spawning.

For each year of reintroduction, the parent crosses associated with each egg delivery from LSNFH have been carefully documented by USFWS, providing a detailed record of which parents contributed to each batch of eggs. These “family groups” differ among egg deliveries and across rearing methods, including the Nur Nature Base (NNB), the Remote Site Incubator (RSI), and the Hatch Boxes. In the first year of the project (2023), we recognized the opportunity to take advantage of incidental mortalities collected by in-river trapping staff and test whether PBT could retrospectively link juvenile mortalities to their specific egg-delivery groups and rearing locations. Mortalities were transferred to UC Davis, dissected, and subject to an internal body scrape to maximize the probability of obtaining high-quality DNA, after which tissues were sent to CFS for parentage assignment. In total, 182 juvenile winter-run Chinook salmon mortalities were collected and dissected in 2023. Genotyping was successful for 179 of the 182 mortalities, and 166 fish were matched to parents and egg-delivery groups, resulting in 112 fish being assigned to a heath-tray rearing origin, and 54 assigned to NNB origin (Figure 8.1). Substantial data-quality issues in the field records meant that only 148 specimens had sufficient metadata (e.g., trap location, collection date, fork length) to support exploration of timing of mortalities. Of these, we found that heath-tray origin mortalities were concentrated in a 2-week window in October, following the release of fish from the RSI, in contrast to the extended window we found NNB mortalities, suggesting fish reared with volitional passage from the NNB may be outmigrating across a larger window of time (Figure 8.2). More work needs to be done to disentangle in-river growth based on spawn and collection dates for those fish that have the required data. Nonetheless, these efforts served as an important proof-of-

concept for PBT application in this system and informed improvements in subsequent years.

During years 2 and 3 (2024–2025 field seasons), we implemented a more rigorous collection protocol in collaboration with field staff at the Incline Plane Trap (IPT), Rotary Screw Trap (RST), and the Juvenile Salmon Collection System (JSCS). All trap mortalities were collected in separate, clearly labeled bags to avoid cross-contamination and were accompanied by standardized metadata. This improved protocol resulted in 159 mortalities collected and 140 of those dissected in 2024, and 418 collected and dissected in 2025. As in 2023, tissue samples from 2024 were sent to CFS for parentage assignment, while 2025 samples are prepared for transfer. PBT analyses for 2024 and 2025 are still pending, but they hold considerable promise for quantifying differences in outmigration timing across rearing methods, as well as estimating growth by combining fork length measurements with spawn dates to back-calculate growth in the river. In addition, the 2025 mortalities provide the opportunity to test whether any surviving offspring originated from in-river spawners observed in July 2025. This interest in in-river spawning success also led us to collect fin clips from the 2025 mortalities for submission to the Central Valley Tissue Archive (CVTA). In total, we delivered 406 fin clips to the CVTA on December 22, 2025, with 12 mortalities in too poor condition for retrieving a fin clip. A complete list of dissected samples from 2024-2025, including metadata, is provided in the data accompanying this final report.

Current use of PBT on juvenile winter-run is constrained by the need for trap mortalities and labor-intensive dissections to obtain genetic material. These limitations spurred new experiments aimed at extracting genotype from the water that live fish occupy, thereby reducing reliance on mortalities and minimizing fish handling. This concept forms the basis of a Master’s thesis by Jamie Ward, a Winnemem Wintu Tribe member, CSU Chico graduate student, and UC Davis field crew member. Jamie’s work builds on observations by CFS scientist Hilary Stark that mucus from dead salmon can yield successful genotypes. During the 2025 field season, Jamie conducted both a pilot and a full-scale experiment. The pilot study, using frozen fall-run Chinook juveniles, demonstrated that a genotype could be recovered from water in which a frozen fish had been placed for 5 minutes, but that DNA quickly degraded thereafter. This study also tested multiple DNA preservation methods. The subsequent full experiment used live winter-run salmon at LSNFH, holding fish in small volumes of water for 1, 3, 5, and 60 minutes to assess whether fish genotype could be reliably obtained from water samples. Results are not yet available, but this experiment forms the core of Jamie’s thesis and could ultimately enable PBT analyses on live fish, greatly expanding opportunities to assess which breeding groups are successful without removing fin tissue from individuals.

Finally, PBT has already proved crucial in documenting successful returns of McCloud-reared fish. During the 2025 spawning season, genotyping of returning adults identified two jack winter-run Chinook whose eggs had reared in the McCloud River in 2023. Analyses of adult carcasses from the mainstem Sacramento River are ongoing, so additional McCloud survivors may yet be identified. As more adults return in future years, PBT will remain our primary tool for determining McCloud-origin survivors.

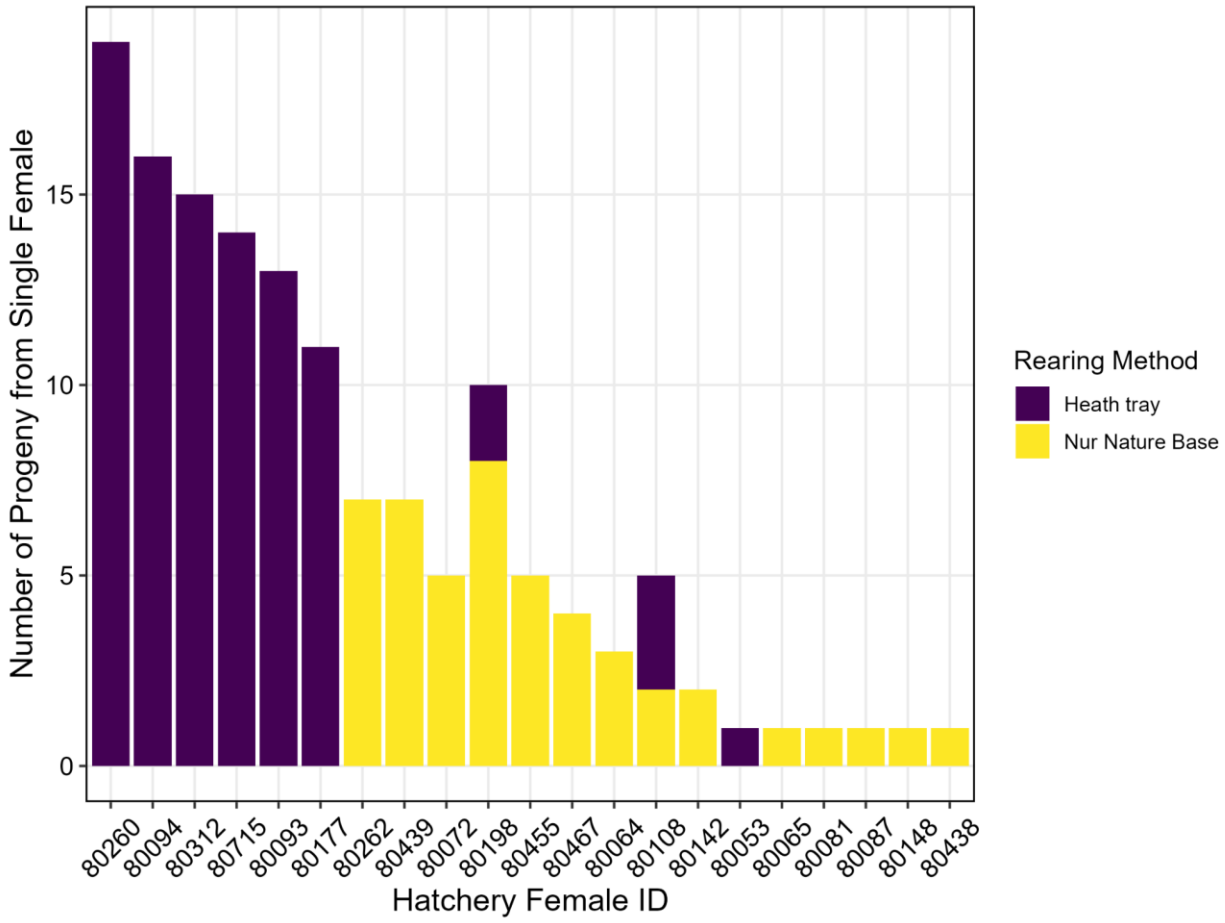

Figure 8.1. Number of juvenile salmon recovered as mortalities in the McCloud River with a positive parentage assignment linked to individual females spawned at Livingston Stone National Fish Hatchery in summer 2023.

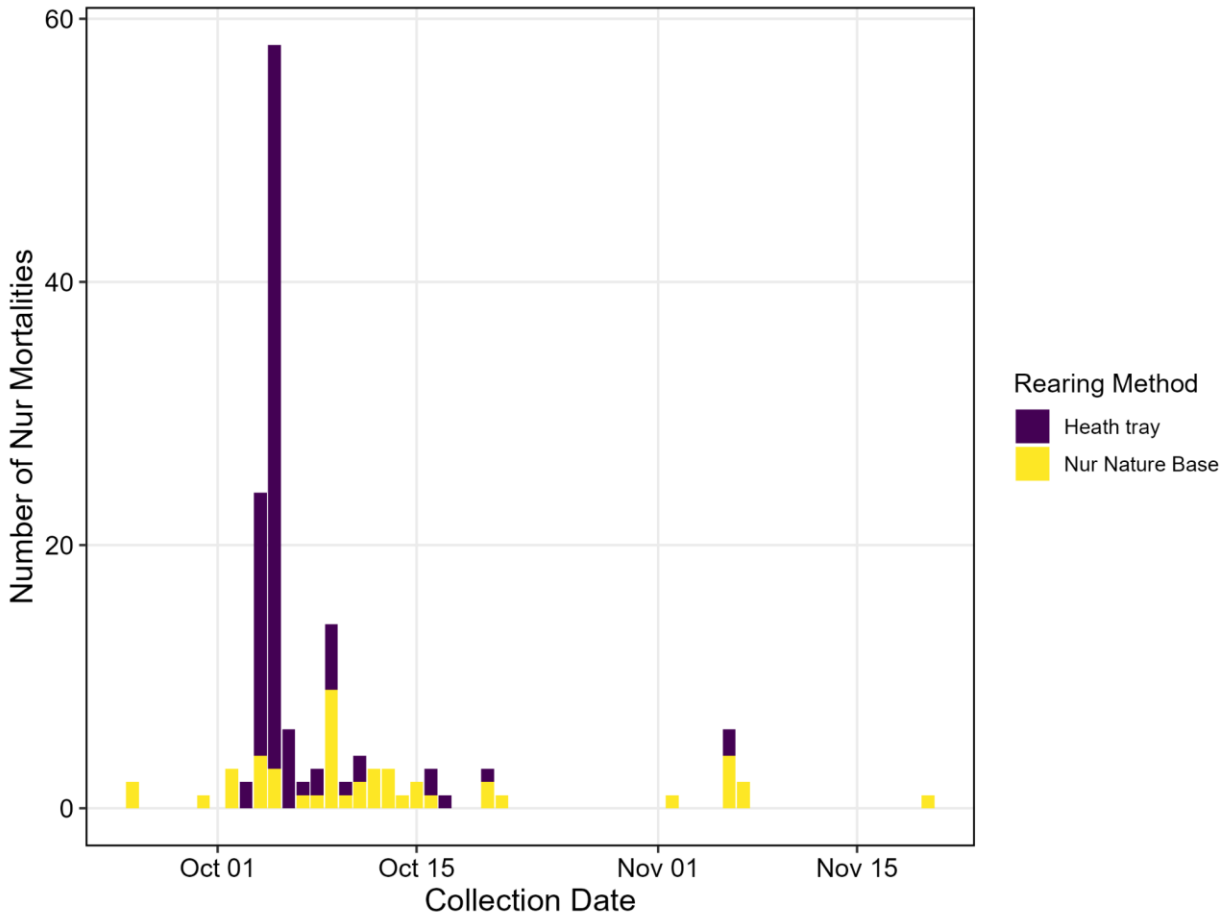

Figure 8.2. Collection date of juvenile mortalities in the McCloud River, colour-coded according to their rearing method. Rearing method was identified using parentage-based tagging techniques.

Products

Manuscripts

Drafts of manuscripts to be submitted to journals in 2026.

1. *Four years of joint learning towards bringing salmon home*
   Authors: Rachel Johnson (lead author) with all collaborators as co-authors
   Target Journal: Fisheries
   Abstract outline: Introduce the project starting from the call to action from both the Tribe and agencies after multi-year droughts left winter-run in peril. Discuss the process of jointly developed and aligned implementation, including alignment of scientific priorities. Present the parallel lines of evidence (scientific findings and traditional knowledge) and interpretation for how salmon have responded to reintroduction to their ancestral waters.

2. *Seeing the unseen: Leveraging cutting edge tools to characterize salmon life history upon return to ancestral waters*
   Authors: Rachael Ryan (lead author), Carson Jeffres, Amelie Segarra, Miles Daniel, Diana Baetscher, Jim Birch, Kevan Yamahara, Paloma Herrera-Thomas, Matthew Salvador, Abigail Ward, Jennie Hawkins, Matt Emmard, Jamie Ward, Caleen Sisk, Marine Sisk, Scott Blankenship, …, Rachel Johnson
   Abstract outline: Introduce the need for innovative tools to enhance the spatial and temporal extent of reintroduced winter-run Chinook salmon monitoring and inform the reintroduction trapping effort. Discuss the methods used (hand sampling, ESP) for collection, extraction technique, qPCR and detections. Results revealed seasonal patterns in outmigration phenology that differ from the valley floor populations, with detections year-round, highlighting the need for enhanced trapping efforts.

3. *Minimizing handling and maximizing data: Coproduction of a Salmon Viewer*
   Authors: Carson Jeffres (lead author), Jamie Ward, Caleen Sisk, Marine Sisk, Matthew Salvador, Brian Knight, Rachel Johnson
   Abstract outline: Discuss how working in alignment with the WWT led to the necessity to innovate how we measure fish to be less invasive. Work through the steps of co-development with the Tribe, UCD engineering students, and other collaborators and the process of receiving feedback and iterating on past designs. The benefits of this new approach went beyond reducing stress of fish by enabling automated data acquisition and giving researchers and monitors a way to get fish weight, in addition to fork length, providing more information on fish condition. Many avenues for future applications.

4. *Automated Morphometric and Weight Prediction of Juvenile Chinook Salmon*
   Authors: Brian Knight, Carson Jeffres
   Abstract: Minimizing handling of threatened and endangered fish has become increasingly important as populations have dwindled. To minimize handling in morphometric measurements, the HandsFreeFishing program has been developed for juvenile Chinook Salmon (*Oncorhynchus tshawytscha*). By segmenting a 2D image many morphometric measurements are able to be estimated; from these measurements a weight prediction model is built based on fish whose ground truthed weights were measured using a digital scale. While many segmentation methods may be used, here Meta's Segment Anything model (SAM) is employed to produce segmentation masks of raw images. This model is open source and easily used on any image (of any size) with good performance. In the proposed framework, the user supplies a bounding box around a target fish along with minimal orientation data (left or right facing, upside down or right-side up); the rest of the segmentation, feature extraction, and final weight prediction is completely automated. A main goal of the segmentation is to estimate the surface area of the side profile of the fish. Then, assuming an ellipsoidal shape, this surface area can be related to the volume of the fish, which is directly proportional to the weight. Even on a relatively small dataset of 149 (fork length 27-90mm) images our results confirm the predictive qualities of the morphometric features measured. The model achieved weight prediction with a mean absolute error of 0.16 g with a mean absolute percentage error of 12%, and an r-squared value of 0.99, on fish ranging from 0.31g - 7.74g. The raw images come from a variety of fish viewers, the design of which is relatively inexpensive and reproducible, and, in conjunction with the HandsFreeFishing program, allows for minimal handling compared to traditional length and weight measurement methods.

Presentations

1. Paloma Herrera-Thomas, Marine Sisk, Jamie Ward, Carson Jeffres, Rachel Johnson. "Hands-off! Innovative methods in fisheries sciences". International Society for River Science Symposium, October 2025. *Poster presentation*.
2. Rachael Ryan. "Reviving salmon population diversity through reintroduction to spring-fed habitat & Tribal-Western science partnership". International Society for River Science Symposium, October 2025. *Oral presentation.*
3. Jamie Ward, Scott Blankenship, Hilary Starks, Paloma Herrera Thomas, Marine Sisk, Cassandra Curl, Gabriel Ward, Arron Sisk, Nina Sisk, Carson Jeffres, Rachel Johnson. "Parentage Based Tagging of Migrating Juvenile Salmon". Bay-Delta Science Conference, October 2024. *Poster presentation*.

4. Rachel Johnson. “Two-eyed seeing creates new hope for California salmon”, February 2026. University of Essex. Translational Ecology Course. *Oral presentation*
5. Rachel Johnson. “Two-eyed seeing creates new hope for California salmon”, February 2026. Merced and Tuolumne Salmon Alliance. *Oral presentation.*
6. Rachel Johnson. “The reawakening of salmon life histories: listening to the past to conserve the future”. September 17, 2025. Sacramento River Science Partnership. *Oral presentation*
7. Rachel Johnson. “Evolutionary Mismatch: Life history of mountain climbers on a hot valley floor and their return to ancestral waters”. 2025. Tuolumne and Merced Salmonid Reintroduction Memorandum of Understanding meeting. *Oral presentation*
8. Rachel Johnson, Marine Sisk, Matt Johnson, Carson Jeffres. “Three years of joint learning in reuniting winter run Chinook salmon (Nur) to their ancestral waters”. 2024. Bay Delta Science Conference. Sacramento, CA. *Oral presentation*
9. Jesse Frey, Benjamin Atencio, Benjamin Burford, Nicholas Demetras, Brendan Lehman, Jeremy Notch, Rebecca Robinson, Lance Takata, Cyril Michel. Survival and capture efficiency of, and predation on, juvenile Chinook salmon (nur) in the McCloud River (Winnemem Waywaket). 2024. Bay Delta Science Conference. Sacramento, CA. *Oral presentation*
10. Rachel Johnson. “Evolutionary mismatch of the Endangered Winter Run Chinook salmon: life history of a mountain climber on a hot valley floor”. 2024. National Academy of Sciences Expert Panel on State and Federal Water Project Operations. Redding, CA.*Oral presentation*
11. Rachel Johnson. “Reconnecting Winter run Chinook salmon to ancestral waters: monitoring reintroduction to the McCloud River”. 2023. Sacramento River Science Partnership. Redding, CA. *Oral presentation*

Additional Products

1. General data dashboard for visualization of data collected 2022-2025: https://lookerstudio.google.com/s/lWjjDjaJbjw
2. Private dashboard for the Winnemem Wintu Tribe visualizing egg rearing data.
3. Masters thesis investigating the feasibility of non-invasive genotyping of juvenile salmon, Jamie Ward (California State University Chico, UC Davis, Winnemem Wintu Tribe) – *ongoing, two experiments completed*
4. Partnership Between Winnemem Wintu Tribe and State and Federal Agencies Revitalizes Salmon Spawning Hopes in the McCloud River
5. A promising new effort to save California’s salmon
6. New Hope for Saving Salmon

7. Chinook salmon return to California's far north- with a lot of human help
8. A lifeline for winter-run Chinook
9. Saving Salmon
10. Time to dance the salmon home
11. "We're praying that they remember these waters": supported by tribal ceremony, salmon eggs return to the McCloud River after 80years Absence
12. California's Salmon Society

Acknowledgements

We would like to first and foremost thank the Winnemem Wintu Tribe for their guidance, help, and collaboration with the research conducted on the Winnemem Waywaket (McCloud River), and their permission to conduct this research on their ancestral lands. We would also like to acknowledge our close collaborators and funders at the California Department of Fish and Wildlife. We thank The Nature Conservancy for permission to sample on the Kerry Landreth Preserve. We would like to thank all the field and lab support staff at UC Santa Cruz, UC Davis, NOAA, and MBARI. Finally, we are grateful for our partnerships and logistical support from California Department of Water Resources, California Department of Fish and Wildlife, NOAA's National Marine Fisheries Service, Pacific Northwest National Laboratory, and US Fish and Wildlife Service. We look forward to continuing to learn together with our partners in our joint efforts to return nur to the Winnemem Waywaket.